DESIGN, SIMULATION, OPTIMIZATION AND PERFORMANCE EVALUATION OF A NOISE-INDUCED HEARING LOSS INTERVENTION FOR THE 1500CC VARIABLE VALVE TIMING – WITH INTELLIGENCE (VVT-i) GASOLINE INTERNAL COMBUSTION ENGINE

DANIEL OMONDI ONYANGO

DOCTOR OF PHILOSOPHY

(Occupational Safety and Health)

JOMO KENYATTA UNIVERSITY

OF

AGRICULTURE AND TECHNOLOGY

2023

Design, Simulation, Optimization and Performance Evaluation of a Noise-Induced Hearing Loss Intervention for the 1500cc Variable Valve Timing – with Intelligence (VVT-i) Gasoline Internal Combustion Engine

Daniel Omondi Onyango

A Thesis Submitted in Partial Fulfilment of the Requirements for the Degree of Doctor of Philosophy in Occupational Safety and Health of the Jomo Kenyatta University of Agriculture and Technology

2023

DECLARATION

This thesis is my original work and has not been presented for a degree in any other University.

Signature: …… Date: ……

Daniel Omondi Onyango

This thesis has been submitted for examination with our approval as the university supervisors;

Signature: …….. Date: …….

Prof. Robert Kinyua, PhD.

JKUAT, Kenya

Signature: …….. Date: …….

Prof. (Eng.) Abel N. Mayaka, PhD.

Multimedia University, Kenya

DEDICATION

This work is dedicated to my spouse, Mrs. Roseline Atieno, my daughter Sharon Awino, and my two sons Rowland Oduor and Kelvin Ochieng.

ACKNOWLEDGEMENTS

I am heartily thankful to my supervisors, Prof. Robert Kinyua and Prof. (Eng.) Abel Mayaka, whose selfless time and care were sometimes all that kept me going.

Special thanks and appreciation also go to Japan International Cooperation Agency through the Africa-*ai*-Japan Project for the sponsorship and support provided, and to my family for their understanding and patience throughout the duration of my work.

TABLE OF CONTENTS

LIST OF TABLES

LIST OF FIGURES

LIST OF PLATES

LIST OF APPENDICES

LIST OF ABBREVIATIONS AND ACRONYMS

BEM	Boundary element method
BS	British Standards
CFD	Computational fluid dynamics
CIB	Continuous inclined barrier
dB	Decibel
dB(A)	Decibel measured on the A weighted scale
DALY's	Disability-adjusted life years
DOE	Design of experiments
DX	DesignXplorer
E.L.	Exposure limit
EMCA	Environmental Management and Co-ordination Act
FEM	Finite element method
Hz	Hertz
HDE	Hearing protective equipment
HDP	Hearing protective device
IL	Insertion Loss
ILO	International Labour Organization
ISO	International Organization for Standardization
JICA	Japanese International Cooperation Agency
JKUAT	Jomo Kenyatta University of Agriculture and Technology
KNBS	Kenya National Bureau of Statistics
KPLC	Kenya Power and Lighting Company
NIHL	Noise-induced Hearing Loss
ONIHL	Occupational noise-induced hearing loss
rpm	Revolutions per minute
RANS	Reynolds-average Navier-Stokes
SEC	Simple expansion chamber
SPL	Sound Power Level
TL	Transmission Loss

VVT-i	Variable valve timing with intelligence
WHO	World Health Organization

LIST OF SYMBOLS

c	Speed of sound
c_p	Specific heat at constant pressure
c_v	Specific heat at constant volume
d, r	Distance
f	Frequency
f_a	Friction factor
g	Acceleration due to gravity
g_x, g_y, g_z	Components of acceleration due to gravity
h	Height
k	Bulk modulus
k_{met}	Correction factor for metrology
k_t	Thermal conductivity
l	Length
p	Pressure
t	Time
x, y, z	Global Cartesian coordinates
ρ	Density
μ	Viscosity
μ_e	Effective viscosity
λ	Wavelength
ΔP	Pressure drop
D	Diameter
I	Sound intensity
Q	Mass source
R	Resistance
Rx, Ry, Rz	Distributed resistance
S	Cross sectional area
T	Temperature
W	Acoustic impedance

Z	Acoustic impedance mismatch

ABSTRACT

Noise pollution is a serious concern due to its adverse effects on safety and health. Prolonged exposure to excessive noise leads to noise-induced hearing loss. Effective solutions provide minimum layers of protection. This research investigated the performance of an active noise control method as a noise-induced hearing loss intervention for a 1500cc Variable Valve Timing with Intelligence (VVT-i) gasoline internal combustion engine. Autodesk Inventor and ANSYS were used for design, modelling and simulation of the prototype. Key design parameters included the length, diameter, and a continuous inclined barrier internal geometry configuration. Quantitative performance testing of insertion and transmission losses, and noise profile characteristics was done using an integrating sound level meter. Results obtained were used to evaluate the performance of the muffler design solution, quantification of residual noise hazards, and development of measures to address residual noise hazards. The engine noise characteristic was broadband, with noise levels in the lower frequencies exceeding 100dB(A) ($f=2.769$, $p=0.0088$). Critical frequencies affecting hearing occurred between 33.5 and 2,000 hertz. Unmuffed engine noise exceeded the upper action limit of 85 dB(A), making it unsuitable for operation in both industrial setups and silent zones. A 50mm pitch continuous inclined barrier in a simple expansion chamber design solution exhibited noise levels between 60 and 80 dB(A) ($f=23.713$, $p=6.5E-22$) with a maximum of 90dB(A) at 4kHz. Residual noise from the design solution may be addressed by locating the receiver at 10m from the source, or providing a low-grade hearing protective equipment rating of 20dB(A). The design can be used as a noise-induced hearing loss intervention where elimination of the hazard is not feasible. Further investigation should be done to establish the minimum design configuration that would provide the maximum sound attenuation. In addition, further research could be carried out to determine the performance of the continuous inclined barrier solution at the lower and higher frequencies respectively.

CHAPTER ONE

INTRODUCTION

1.1. Background of study

In this chapter, a general overview of the problem of noise in the society is presented. It includes a clear statement of the purpose of investigation, the background of noise attenuation including statutory provisions, and a brief outline of the structure of this report.

Sounds are generally audible to the human ear if their frequency lies between 20 and 20,000 vibrations per second (Ikechiamaka et al., 2017), but the range varies considerably with an individual's genetic predisposition. Sound waves with frequencies less than those of audible waves are called subsonic; those with frequencies above the audible range are called ultrasonic.

Hearing within the lower frequency range of 20 to 100 hertz (Hz) requires that the sound be perceived at levels higher than 20dB(A), with the lower frequency requiring up to 80 dB(A). At frequencies below 20 Hz., greater chances exist of exposure to noise levels beyond 80 decibels (Kuehler et al., 2015). At around 5,000Hz, the ear is very sensitive to noise. This sensitivity is used to evaluate hearing loss demonstrated by a notch in the hearing audiogram. Pure tone testing using pure tone audiometry presents tones across the speech spectrum, and this is used to evaluate hearing deficiencies (Walker et al., 2013). The existence of an audiometric notch confirms occupational noise-induced hearing loss (ONIHL). In order to effectively evaluate the impact of the proposed intervention to hearing, results should be obtained in terms of octave band profiles that detail the centre-frequency characteristics of individual elements of the sound throughout the hearing spectrum. This enables comparisons to be made of the noise of interest with threshold limit values and limits of safe levels.

According to a report by the World Health Organization, noise from road, rail, aircraft and industry is the second largest cause of health problems after fine particulate matter pollution. The report further estimates that more than one million health years (the estimated number of healthy years of life lost to illness, disability or early death) are lost annually from these health effects (European Environment Agency, 2020). One

common source of noise in industrial setups and workplaces is the internal combustion (IC) engine. Typically, the IC engine is used to provide auxiliary power to drive machinery, effect transport needs, and to generate electric power in off-grid areas or when electrical energy from other sources has been disrupted. High noise levels generated during the operation of the IC engines present a hazard to workers, especially where the occupier does not put in place noise reduction measures.

In small and medium-sized organizations, the 1500cc VVT-i internal combustion engine is used to provide electrical power requirements (Reitz, et al., 2020). The engine is also commonly used in personal cars and other off-grid activities including saw milling of timber, irrigation, and water reticulation (Gaidar et al., 2020). During operation of these engines, noise is generated in a number of ways including from the combustion process, rotating and moving parts, discharge of combustion products to the environment, and vibration of supporting structures.

The Occupational Safety and Health Act of 2007 is a statutory instrument whose major aim is the prevention of accidents, injuries, and ill health at the workplace. The Act mandates the occupier to carry out appropriate risk assessment with the aim of identifying situations and equipment that are likely to cause injury to health. Specific subsidiary legislations have also been developed and implemented to guide in the management and control of workplace hazards, and to specify relevant action levels and set safe limits above which exposure may result in adverse health effects.

Internal combustion engines are a common form of energy transfer that has been perfected since the first invention by Karl Benz and Gollieb Daimlar of Germany in 1885 and 1886 respectively (Cromer et al., 2018). Models exist that give higher torque performances per joule of fuel consumed irrespective of the size of the engine. For energy to be converted in this form, a number of actions take place including motion of parts, combustion of fuel-air mixture, friction, vibration of structures around the engine, and corresponding generation of heat energy. These are usually accompanied by pressure waves which if not controlled, adversely affects the safety and health of persons within boundaries of such arrangements.

The 1500cc VVT-i internal combustion engine is the most common mode of private transport in Kenya accounting for 9.7% of the gross domestic products (GDP) (KNBS, 2012). Further, statistics indicate that the number of cars in the category indicated above that were registered in Kenya in 2012 was 644,805 compared to the number of Lorries, trucks and heavy vehicles (108,110) registered in the same year (KNBS, 2013).

1.2 Statement of the Problem

As the world population increases, demand for goods and services to satisfy needs and wants also increases. This leads to increased pressure for mass production. Workplaces therefore have to adopt technologies that require high energy inputs to meet these demands, and in the process, result in environmental pollution. One of the notable industrial pollutants that affects workers is noise from production activities and energy generation sources.

Internal combustion engines are a common form of energy transfer used in off-grid workplaces, and to supplement grid power requirements in most industrial set-ups. The internal combustion engine has been perfected since the first invention by Karl Benz and Gollieb Daimlar of Germany in 1885 and 1886 respectively (Cromer et al., 2018). Models exist that give higher torque performances per joule of fuel consumed irrespective of the size of the engine. For energy to be converted in this form, a number of actions take place including motion of parts, combustion of fuel-air mixture, friction, vibration of structures around the engine, and corresponding generation of heat energy. These are usually accompanied by pressure waves which if not controlled, adversely affects the safety and health of persons within boundaries of such arrangements.

The 1500cc VVT-i internal combustion engine is the most common mode of private transport in Kenya accounting for 9.7% of the gross domestic products (GDP) (KNBS, 2012). Further, statistics indicate that the number of cars in the category indicated above that were registered in Kenya in 2012 was 644,805 compared to the number of Lorries, trucks and heavy vehicles (108,110) registered in the same year (KNBS, 2013). The driver's cabin as a workplace provides a conducive environment for noise

exposure for poorly muffled engines. The magnitude of the impact of noise-induced hearing loss arising from the use of internal combustion engines in Kenya is not well documented.

Prolonged exposure to excessive noise levels from the internal combustion engine leads to noise-induced hearing loss, communication difficulties, lack of sleep, and industrial accidents due to poor perception of acoustic cues. There is therefore need to develop innovative noise reduction solutions to minimize these adverse impacts on health and safety.

1.3 Rationale and Justification

Internal combustion engines produce noise, which, in areas inhibited by people, is assessed as excessive according to the health and safety regulations. If noise is being generated from an engine in a protected area, it is possible to ensure the necessary noise reduction by inserting a silencer. The silencer should not however place a disproportionately high constriction on the flow of the exhaust emissions, which may affect the engine performance. In essence, a silencer in the exhaust system is a channel or conduit placing resistance to noise transferal in order to achieve as close a value as possible to the background noise levels. When the difference between a noise source and the background noise levels is large, adverse health and safety impacts may occur (Basner, et al., 2014).

It is estimated by the World Health Organization (2011) that disability-adjusted life years (DALY's) lost from environmental noise in Western European countries are 61,000 years for ischemic heart disease (heart problems caused by narrowing of heart arteries), 45,000 years for cognitive impairment of children, 903,000 years for sleep disturbance, 22,000 years for tinnitus (perception of ringing sounds from the ear) and 587,000 years for annoyance. If all of these are considered together, the range of burden would be 1.0 – 1.6 million DALY's. This means that at least one million healthy life years are lost every year from traffic-related noise in the Western European countries, including the European Union member states. In Kenya, data on DALY's lost from noise-related activities is not available.

As the use of internal combustion engines for transport and secondary power supply continue to increase in Kenya, the level of noise pollution also increases proportionately. The Environmental Management and Coordination Act, 2015 and the Occupational Safety and Health Act 2007 specify recommended noise limits to the surrounding that must be met (EMCA, 2015). These are 45 dB(A) and 55 dB(A) during the night and day respectively. Installations of appropriate sound absorbers are commonly used to achieve this. However, certain conditions make attainment of noise limits difficult resulting in environmental pollution and noise-induced hearing loss.

The development of alternative configuration for noise control will enhance compliance with environmental and occupational regulations limiting the levels of noise to the environment. It will also be a useful development in automotive and stationery engine noise control, especially during retrofitting.

The findings of this study will generate useful information needed to formulate engineering control solutions to mitigate against internal combustion engine noise. The potential uses for control systems are in light and heavy commercial vehicles, as well as stationery plants. Once this is achieved, it will be possible to minimize costs associated with installation of secondary intervention measures to make learning institutions, hospitals, homes and other workplaces quieter, especially those next to the motorway or industrial setups.

1.4 Objectives

1.4.1 Main Objective

The main objective of this study was to model, develop, simulate, optimize, and evaluate the performance of an active noise-control method as a noise-induced hearing loss intervention for the 1500cc VVT-i internal combustion engine.

1.4.2 Specific Objectives

Specific objectives of the research were;

1. To characterize the 1500cc VVT-i internal combustion engine noise profiles.
2. To model, develop, simulate, optimize, and test the performance of a new design configuration of a continuous inclined barrier in a simple expansion chamber muffler.

3. To determine residual noise hazards arising from application of the developed muffler.
4. To propose measures for the management of residual noise hazards.

1.5 Research Questions

This research sought to answer the following questions based on the specific objectives listed above;

1. What features of the noise characteristics are important in the control of noise-induced hearing loss?
2. How effective is the use of the continuous inclined barrier in minimizing noise-induced hearing loss arising from exposure to noise from internal combustion engines?
3. What is the level of residual risk after implementation of the proposed engineering control strategy?
4. What additional measures can be employed to address residual noise-induced hearing loss risks after implementation of the proposed engineering control strategy?

1.6 Scope

This research only looked at the 1,500cc capacity VVT-i gasoline internal combustion engine and involved identification of key elements of an engineering solution to excessive noise control. Only the reactive muffler solution was considered. All noise evaluations were carried out at no-load conditions.

1.7 Limitations of the research

Particular emphasis was laid on combustion exhaust noise only, and therefore other noise contributing factors including vibrating structures, air intake noise, and rotating parts were considered out of scope. The solution was also limited to engineering interventions, and hearing protective devices to cater for residual noise risks.

1.8 Conceptual Framework

Management of occupational noise-induced hearing loss (ONIHL) requires a thorough understanding of causative factors and underlying conditions potentiating noise pollution and consequences thereof. Prevention methods are best designed around the

causative factors and supported by strong statutory guidelines. These are summarized in **Figure 1.1** that outlines the conceptual framework supporting the proposed strategy.

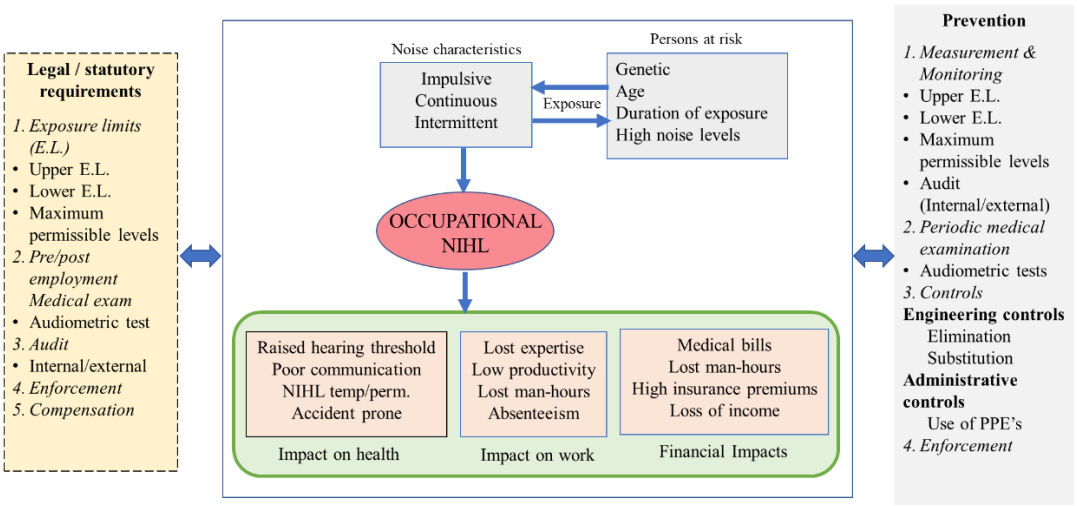

Figure 1.1: Conceptual framework for the development of a noise control strategy

Specific noise characteristics predispose workers to conditions beyond which the auditory system can withstand. These conditions may be accelerated by intrinsic factors specific to each individual. Consequences of damage to the auditory system include breakage of the hearing receptors within the external acoustic meatus. It is therefore necessary that solutions around a control strategy be designed to take into consideration intrinsic and extrinsic factors, as well as established evaluation and enforcement parameters.

CHAPTER TWO

LITERATURE REVIEW

2.1 Introduction

This chapter presents literature associated with developments in the noise control industry; that is, the global and local perspective. It highlights the historical development of noise control for internal combustion engine exhaust emissions.

2.2 Noise and Vibration

When sound perceived at a receiver location is higher than the background noise level and causes interference with or disrupts activities of the receiver, it is referred to as noise. Noise could also occur when sound is transmitted in a non-uniform or erratic manner as to be disruptive to the recipient. Sound is an invisible form of energy made by vibration. The vibrations that create sound must travel through a medium. This travelling vibration is referred to as a sound wave. When a sound wave travelling through the air encounters an obstacle, some of the energy of the sound wave gets absorbed, thus causing the vibration of the medium and eventually a decay of the energy results. The loudness of sound increases with the strength of the vibrations. The path of sound depends on the vibrating material and its size.

2.3 Mechanism of sound propagation

Sound propagates in air by compression and rarefaction of air molecules in the direction of travel. However, in solids, molecules can support vibrations in other directions, hence; a number of different types of sound waves are possible. Waves can be characterized in space by oscillatory patterns capable of maintaining their shape and propagating in a stable manner.

When sound travels through a medium, its intensity diminishes with distance. The intensity *(I)* of sound is inversely proportional to the square of the distance *(r)* from the source – that is, $I \alpha r^2$. In solids, sound travels under the influence of sound pressure. Since molecules or atoms of a solid are bound elastically to one another, the excess pressure results in a wave propagating through the solid. In idealized materials, sound pressure is only reduced by the spreading of the wave. Natural materials, however, all produce a noise reduction effect which further weakens the sound. This

further weakening results from scattering and absorption. The combined effects (attenuation) can be affected by properties and loading conditions of natural materials. Attenuation is generally proportional to the square of sound frequency and can be determined by evaluating the multiple back wall reflections.

Ultrasonic waves are reflected at boundaries where there is a difference (impedance mismatch) in acoustic impedances (Z) of the materials on each side of the boundary. The greater the impedance mismatch, the greater the percentage of energy that will be reflected at the interface or boundary between one medium and another.

The fraction of the incident wave intensity that is reflected can be derived because particle velocity and local particle pressures must be continuous across the boundary. When the acoustic impedances of the materials on both sides of the boundary are known, the fraction of the incident wave intensity that is reflected can be determined. Different materials may be selected or the material velocity and density may be altered to change the acoustic impedance of one or both materials.

2.4 The internal combustion engine, engine noise, and VVT-i technology

The IC engine provides the power required through combustion of a predefined air-fuel mixture in a well-designed vessel with a provision of the mixture inlet, ignition mechanism, and provision of combustion product outlet. The sequence of power generation involves the air-fuel mixture intake, compression of the mixture to a predetermined final volume, ignition of the mixture to obtain the power through a set of linkages to the final output shaft, and exhaust of the combustion products. This process is repeated as long as the engine is on. The process of power generation results in noise through the air-fuel intake as the mixture gushes in at the intake stroke, vibration of the engine and surrounding structures as the sequence of power generation takes place, and through the discharge of combustion products. Noise arising from the point can be higher if combustion is not complete and reaction is extended to the environment.

Noise directly from internal combustion (IC) engines may exceed 108 dB(A) (Gaikoumis et al., 2011) depending on the load and the speed of operation. This is much higher than recommendations from the World Health Organization's standards

that specifies at most 5 dB(A) above the prevailing background noise levels (WHO, 1999). In Kenya for example, studies by SGS (2014) and KPLC (2011) have shown that ambient noise levels during the day and on the outskirts of Nairobi ranges between 40 to 45 dB(A) while that within the industrial area recording 51.5 to 62.5 dB(A). There is therefore need to ensure that noise from such engines characteristic of the transport industry and industrial processes is controlled to minimize adverse health and environmental effects (Stansfeld et al., 2011).

IC engines are generally identified through specification of the total cylinder volume. Depending on the anticipated load requirements, an IC engine may have a single cylinder or a number of them. Arrangement of the cylinders may also vary depending on the manufacturer and space constraints. These arrangements include vertical, horizontal, or "V" configurations. The total volume specification, usually in cubic centimetres, is the total volume of the cylinders at the maximum extent of the piston. Thus, a 75cc IC engine is smaller in capacity than a 1500cc one. Consequently, the resultant power generated through combustion in the 1500cc engine would be higher than that of 75cc (Heywood, 2018).

Conventional engineering noise control designs for IC engines basically achieve noise reduction through two devices; the catalytic converter and the muffler or silencer. While the catalytic converter ensures that the combustion reaction process is complete, the muffler or silencer acts to reduce the magnitude of noise generated. Reactive or passive systems (mufflers or silencers) in which the exiting gases are either subjected to directional changes, sudden expansion, or gradual diameter change; all these coupled with or without passage through an absorptive medium in an effort to modify the wave form and consequently the exit sound levels. Computational fluid dynamics softwares have been developed to accelerate the design process of mufflers and predict their behaviour under working conditions.

In order to improve fuel economy, increase engine efficiency and reduce discharge of environmental pollutants, Toyota Motor Corporation developed the Variable Valve Timing with Intelligence (VVT-i) technology in 1995 to ensure that maximum power is derived from the combustion process, while at the same time ensuring that the

products of combustion are not harmful to the environment (Gaidar et al., 2020). In this technology, the air-fuel mixture drawn into the combustion chamber is dependent on the load requirements; the higher the load the richer the mixture. In addition, part of the exhaust gases is mixed with the inlet stream to maximize on the power derived from the combustion process.

2.5 Noise and human hearing

The anatomy of the human ear and the mechanism of hearing have been studied (Gada, 2017). The human ear is divided into three major parts as illustrated in **Plate 2.1** (Waugh & Grant, 2014)**.** The major parts include the outer, middle, and the inner ear. Sound is directed by the outer ear lobe, and propagates into the ear through the outer ear opening. The sound waves are detected by hair-like structures in the lower end of the outer ear (external acoustic meatus), and transmitted through a hydraulic system to the brain in form of pulses. On the other hand, sound may also be transmitted to the brain through the bone structure surrounding and above the ear opening, and onto the inner ear through which electrical signals are conveyed to the brain.

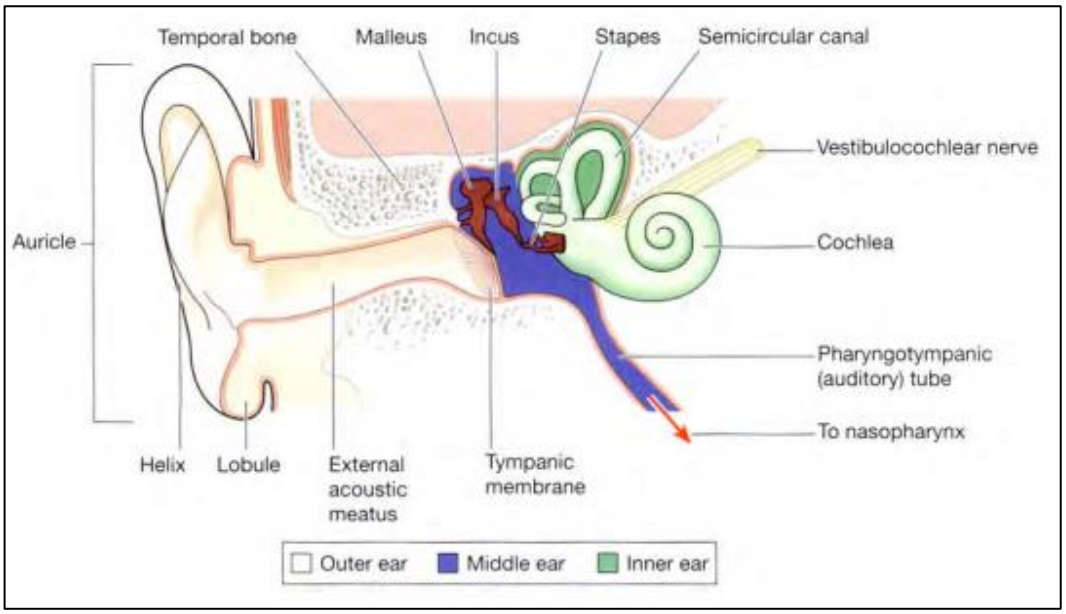

Plate 2.1: Anatomical structure of the Human Ear

(Waugh & Grant, 2014).

When the hair that acts as pressure sensors are damaged due to mechanical action (physical abrasion) or exposure to excessive noise levels, hearing impairment may

occur. The damage may be moderate, in which case the patient may survive and recover auditory ability to hear, or may be severe, in which case damage to hearing occurs.

Sensitivity of hearing at the various centre frequencies varies considerably. At lower centre frequencies of 20Hz, the threshold of hearing is the highest [>80 dB(A)] while at the middle hearing range of 500 to 1000Hz is the lowest [approaching 0 dB(A)]. The high threshold of hearing values at lower frequencies predisposes the individual to risks associated with exposure to high noise levels. At higher frequencies within the hearing range, the threshold of hearing becomes high. On the other hand, a maximum permissible noise level contour within the hearing range defines the upper values at which hearing is possible. This is known as the perception limit. In between the threshold limit value and the perception limit is the auditory field which includes a specific range that enables conversation to be perceived. This is presented in **Figure 2.1**.

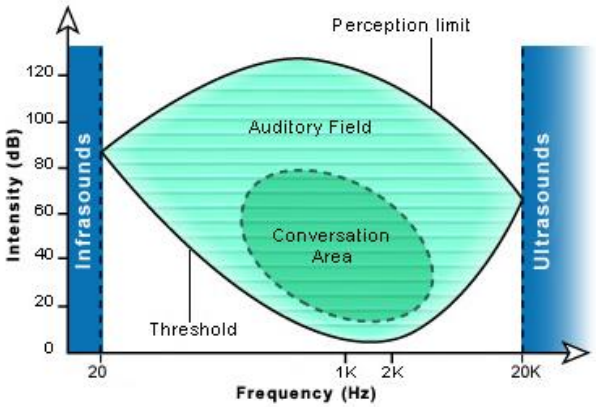

Figure 2.1: Audiometric curve indicating the range of human hearing

(Source: www.cochlea.org/en/)

2.6 Health effects of exposure to excessive noise and global interventions

Excessive noise is a global occupational health hazard with considerable social and physiological impacts (Stansfeld et al., 2011; WHO, 1999), including elevated blood pressure, reduced performance, sleeping difficulties, annoyance and stress, tinnitus, noise-induced hearing loss (NIHL) and temporary threshold shift (Basner et al., 2014). Of these, the most serious health effect is NIHL resulting from irreversible damage to

the delicate hearing mechanisms of the inner ear. NIHL typically involves the frequency range (pitch) of human voices, and thus interferes with spoken communications. Worldwide, 16% of the disabling hearing loss in adults [over 4 million disability-adjusted life years (DALYs)] is attributed to occupational noise, ranging from 7% to 21% in the various sub-regions. According to (Lie et al., 2016), the effects of the exposure to occupational noise are larger for males than females in all sub-regions and higher in the developing regions.

The World Health Organization (WHO) recommends that unprotected exposure to sound levels greater than 100 decibels (dB) should be limited in duration to four hours and frequency to four times a year. It further recommends that daytime exposure to environmental noise should not exceed 55 dB while night time values should not exceed 45 dB. The latter values are also specified in the International Labour Organization (ILO) Convention (Working Environment – Air Pollution, Noise and Vibration – Convention No. 148, 1977) and Recommendation (Working Environment – Air Pollution, Noise and Vibration – Recommendation No. 156 1977) which member states are expected to implement and enforce.

In accordance with the decision taken by the Governing Body of the ILO at its 271st Session (March 1998), a meeting of experts was convened in Geneva from 27th January to 2nd February 1999 to draw up a code of practice on ambient factors at the workplace. In response to technological developments, the code of practice was prepared with a view to updating the ILO's codes of practice on the protection of workers against noise and vibration in the working environment (Geneva, 1984). It was also intended to consolidate earlier documents on all types of air pollutants and other ambient factors in the working environment and to contribute to the practical implementation of the provisions contained in the Working Environment (Air Pollution, Noise and Vibration) Convention (No. 148), and Recommendation (No. 156), 1977, as well as other international standards.

2.7 Characteristics of Sound Waves

Sound waves are compressional oscillatory disturbances that propagate in a fluid. The waves involve molecules of the fluid moving back and forth in the direction of

propagation (with no net flow), accompanied by changes in the pressure, density and temperature. The sound pressure, that is, the difference between the instantaneous value of the total pressure and the static pressure, is the quantity we hear. It is also much easier to measure the sound pressure than, say, the density or temperature fluctuations.

In most cases the oscillatory changes undergone by the fluid are extremely small. These small oscillatory changes are sufficient to cause variations in air corresponding to a sound pressure level of 120 dB, which is a very high sound pressure level, close to the threshold of pain. At this level the fractional pressure variations are about 2×10^4, the fractional changes of the density are close to 1.4×10^4, the oscillatory changes may be considered adiabatic, and the particle velocity is about $50 mm.s^{-1}$, which at 1000 hertz (Hz) corresponds to a particle displacement of less than $8\mu m$.

Sound waves exhibit a number of phenomena that are characteristics of waves as shown in **Figure 2.2**. Waves propagating in different directions interfere; waves will be reflected by a rigid surface and more or less absorbed by a soft one; they will be scattered by small obstacles; because of diffraction there will only partly be shadow behind a screen; and if the medium is inhomogeneous for instance because of temperature gradients the waves will be refracted, which means that they change direction as they propagate. The speed with which sound waves propagate in fluids is independent of the frequency, but other waves of interest in acoustics, bending waves on plates and beams, for example, are dispersive, implying that the speed of such waves depends on the frequency content of the waveform.

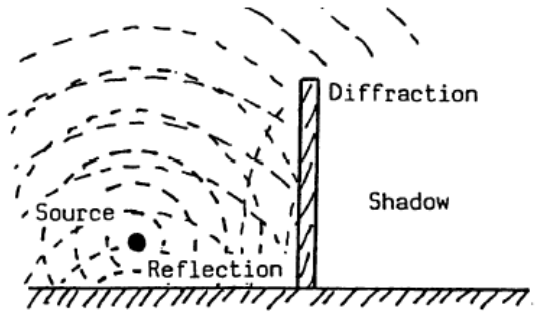

Figure 2.2: Various wave phenomena

(Jacobsen et. al., 2011)

2.7.1. Adiabatic compression

Since the process of sound propagation is adiabatic, the fractional pressure variations in a small cavity driven by a vibrating piston equals the product of fractional density variations and the ratio of specific heats. The physical explanation for the 'additional' pressure is that the pressure increase/decrease caused by the reduced/expanded volume of the cavity is accompanied by an increase/decrease of the temperature, which increases/reduces the pressure even further. The fractional variations in the density are identical with the fractional change of the volume (except for the sign).

For internal combustion engines, sound is produced during air intake, combustion, vibration or movement of parts that constitute the engine assembly, and exhaust discharge through the exhaust system. When an intake or exhaust valve is opened for example, pressure wave is created. The wave propagates through the fluid in the pipe at the speed of sound. When this wave encounters a change in cross-sections area such as the end of the pipe, a rarefaction wave of opposite sign will be reflected from the end of the pipe. This phenomenon can either act to enhance the resulting sound wave or reduce its magnitude.

2.7.2. Sound attenuation

The attenuation or dissipation of acoustic energy as a sound wave moves through a medium may be attributed to three basic mechanisms;

i. Viscous effects resulting in thermodynamically irreversible propagation of sound
ii. Heat conduction effects which result in non-adiabatic propagation of the sound
iii. Internal molecular energy interchanges which result in a time lag between changes in translational kinetic energy and the energy associated with rotation and vibration of the molecules.

The viscous energy dissipation effects result from the relative motion between different portions of the fluid during compression and expansion that occurs when a sound wave moves through the fluid. For a Newtonian fluid, the magnitude of this effect is proportional to the viscosity μ of the fluid.

As the fluid is compressed and expanded during the transmission of the sound wave, changes in temperature occur in different portions of the fluid. There is a tendency for energy to be conducted from regions of compression where the temperature is elevated, to regions of expansion or rarefaction, where the temperature is reduced. The heat transfer effect tends to reduce the amplitude of the pressure wave and dissipate energy as the wave moves through the medium. The magnitude of this effect is proportional to the thermal conductivity k_t of the fluid and inversely proportional to the specific heat c_p or the thermal energy storage capacity of the medium.

2.8 Acoustics

Acoustics involves the application of the Navier-Stokes equations of fluid momentum and the flow continuity equation (Gilles & Rieusset, 2016).

From the law of conservation of mass, the continuity equation can be derived:

$$\frac{\partial \rho}{\partial t} + \frac{\partial(\rho v_x)}{\partial_x} + \frac{\partial(\rho v_y)}{\partial_y} + \frac{\partial(\rho v_z)}{\partial_z} = 0 \quad (1)$$

where

v_x, v_y, and v_z = components of the velocity vector in the x, y and z directions respectively,

ρ = density

x, y, z = global Cartesian coordinates

t = time

The Navier-Stokes equations are as follows;

$$\frac{\partial \rho v_x}{\partial t} + \frac{\partial(\rho v_x v_x)}{\partial x} + \frac{\partial(\rho v_y v_x)}{\partial y} + \frac{\partial(\rho v_z v_x)}{\partial z} = \partial f_x - \frac{\partial P}{\partial x} + R_x + \frac{\partial}{\partial x}\left(\mu_e \frac{\partial v_x}{\partial x}\right) + \frac{\partial}{\partial y}\left(\mu_e \frac{\partial v_x}{\partial y}\right) + \frac{\partial}{\partial z}\left(\mu_e \frac{\partial v_x}{\partial z}\right) + S_x \quad (2)$$

$$\frac{\partial \rho v_y}{\partial t} + \frac{\partial(\rho v_x v_y)}{\partial x} + \frac{\partial(\rho v_y v_y)}{\partial y} + \frac{\partial(\rho v_z v_y)}{\partial z} = \partial f_y - \frac{\partial P}{\partial y} + R_y + \frac{\partial}{\partial x}\left(\mu_e \frac{\partial v_y}{\partial x}\right) + \frac{\partial}{\partial y}\left(\mu_e \frac{\partial v_y}{\partial y}\right) + \frac{\partial}{\partial z}\left(\mu_e \frac{\partial v_y}{\partial z}\right) + S_y \quad (3)$$

$$\frac{\partial \rho v_z}{\partial t} + \frac{\partial(\rho v_x v_z)}{\partial x} + \frac{\partial(\rho v_y v_z)}{\partial y} + \frac{\partial(\rho v_z v_z)}{\partial z} = \partial f_z - \frac{\partial P}{\partial z} + R_x + \frac{\partial}{\partial x}\left(\mu_e \frac{\partial v_z}{\partial x}\right) + \frac{\partial}{\partial y}\left(\mu_e \frac{\partial v_z}{\partial y}\right) + \frac{\partial}{\partial z}\left(\mu_e \frac{\partial v_z}{\partial z}\right) + S_z \quad (4)$$

where

f_x, f_y, f_z = Components of acceleration due to gravity

ρ = density

μ_e = effective viscosity

R_x, R_y, R_z = distributed resistances

S_x, S_y, S_z = viscous loss terms

The fluid momentum (Navier-stokes) equation and the continuity equations are simplified to get the continuity equation using the following assumptions;

1. The fluid is compressible (density changes due to pressure variations)
2. There is no mean flow of the fluid

The acoustic wave equation is given by;

$$\nabla.\left(\frac{1}{\rho_0}\nabla p\right) - \frac{1}{\rho_0 c^2}\frac{\partial^2 p}{\partial t^2} + \nabla.\left[\frac{4\mu}{3\rho_0}\nabla\left(\frac{1}{\rho_0 c^2}\frac{\partial p}{\partial t}\right)\right] = -\frac{\partial}{\partial t}\left(\frac{Q}{\rho_0}\right) + \nabla.\left[\frac{4\mu}{3\rho_0}\nabla\left(\frac{Q}{\rho_0}\right)\right] \quad (5)$$

where

c = speed of sound $\left(\sqrt{k/\rho_0}\right)$ in fluid medium

ρ_0 = mean flow density

k = bulk modulus of fluid

μ = dynamic viscosity

p = static pressure [$p(x, y, z, t)$]

Q = mass source in the continuity equation

t = time

The Navier-Stokes equation provides a mathematical model of the motion of a fluid.

2.9 Noise Management

The goal of noise management is to maintain low noise exposures, such that human health and well-being are protected. The specific objectives of noise management are to develop criteria for the maximum safe noise exposure levels, and to promote noise assessment and control as part of environmental health programmes. This is not always easy to achieve. The United Nations' Agenda 21 (UNCED, 1992), as well as the European Charter on Transport, Environment and Health, both support a number of environmental management principles on which government policies, including noise management policies, can be based.

These include:

a. **The precautionary principle**. In all cases, noise should be reduced to the lowest level achievable in a particular situation. Where there is a reasonable possibility that public health will be damaged, action should be taken to protect public health without awaiting full scientific proof.
b. **The polluter pays principle**. The full costs associated with noise pollution (including monitoring, management, lowering levels and supervision) should be met by those responsible for the source of noise.
c. **The prevention principle**. Action should be taken where possible to reduce noise at the source. Land-use planning should be guided by an environmental health impact assessment that considers noise as well as other pollutants.

The government policy framework is the basis of noise management. Without an adequate policy framework and adequate legislation, it is difficult to maintain an active or successful noise management programme. A policy framework refers to transport, energy, planning, development and environmental policies. The goals are more readily achieved if the interconnected government policies are compatible, and if issues which cross different areas of government policy are coordinated.

Some of the legislations in Kenya governing the levels of noise include; the Occupational Safety and Health Act 2007 and its subsidiary legislation – Noise Control Rules, and the Environmental Management and Coordination Act 2015 and its subsidiary Legislation – Noise and Excessive Vibration Pollution (Control) Regulations 2009.

2.10 Noise Control

Complete elimination of unwanted noise is not possible and attempts to do so may be too expensive. Hence, minimum acceptable levels of noise must be formulated, and these levels constitute the criteria for acceptability. Criteria for acceptability are generally established with reference to appropriate regulations for the workplace and community. In addition, for community noise, it is advisable that at worst, any facility should not increase background noise levels in a community by more than 5 decibels

[dB(A)] over existing levels without the facility, irrespective of what local regulations may allow (WHO, 1999).

Although noise control legislation exists in several countries, there are challenges in enforcement especially in developing countries (Ganiyu & Ogunsote, 2010). Noise control begins with education, public awareness and the appropriate use of media in highlighting the effects of noise. Three strategies have been devised for noise control (Bies et al., 2017). They are control at the source, control along the path and control at the receiving end.

Along the sound path, barriers can be used to control noise. There are three kinds of barriers available, namely, space absorbers made out of porous material, resonant absorbers and panel absorbers. Engineers, for example, use silencers or mufflers to control noise from internal combustion engines. Functions of silencers include;

1. reduction of pressure gradient associated with the exhaust
2. reduction of shear in the mixing region between exhausting gases and ambient or slowly moving air in the neighbourhood of the exhaust system, and
3. stabilize and reduce the magnitude of any shock waves developed in the exhaust.

The predominant sources of engine noise, listed in order of magnitude, are that of exhaust, intake and casing (Bi et al., 2015). The cooling fan may also contribute some noise. Exhaust noise includes the various noise sources of the exhaust system (expansion joint, piping and exhaust). Intake noise includes all noise sources within the intake system (air filter, ducting or piping and the air intake itself). Casing noise is the result of mechanical and structural propagation of radiated noise. Fuel combustion, engine timing and the extent of component wear also contribute to the casing noise.

Silencers can be divided, according to the principle of their function, into resonator-type silencers (Martins et al., 2018) and absorption-type silencers (Karthikeyan et al., 2017). The principal difference between these silencers is the aspect of disseminating the acoustic energy through the duct system. Where a resonator-type silencer is installed, it reflects the acoustic energy back to the source. This means that the

acoustic energy is not converted into heat energy but partial standing waves are created in the duct system between the silencer and the noise source, which can decrease the machine's efficiency. A typical example of using resonator-type silencers are piston combustion engines whose silencers must be tuned so that the removal of exhausts from the machine's combustion centre is not seriously affected.

These types of silencers have been researched on and different configurations developed. **Figure 2.3** and **Figure 2.4** illustrate the absorptive and reactive type silencers respectively as reported by Masa'id et al., (2021).

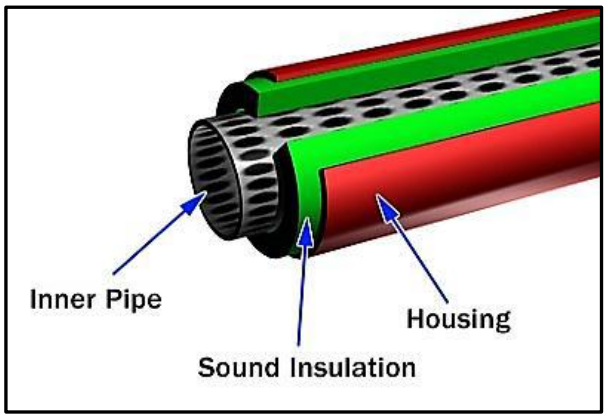

Figure 2.3: Absorptive Silencer

(Source: Masa'id et al., (2021))

The reduction of sound energy using absorptive materials is achieved by transferring the acoustical pressure (wave motion) into material motion. This mechanical motion is converted into heat (energy loss) by material damping and friction. The more effective the sound wave penetrates the material the more effective the attenuation. Each baffle assembly consists of "compartments" and the basic theory is each compartment is locally reacting where the acoustic sound wave "pumps in and out" through the material as well as through the perforated facing sheet or pack material retainer. The perforation pattern adds damping and frictional losses to the aero-acoustic wave oscillating through the holes; the smaller the holes and more perforations, the more attenuation. The packing consists of absorptive material that is principally fibrous materials or open cell foams that allow the wave energy to penetrate, induce material motion, and be attenuated.

The wavelength of sound is a major factor in sound reduction as well since the absorptive material only starts to become effective when its thickness is at least one-tenth the wavelength, implying that very low frequencies are not well attenuated. The effective depth of a baffle is one-half its thickness as acoustic energy is propagating into the baffle from both sides.

Figure 2.4: Reactive Silencer

(Source: Masa'id et al., (2021))

Reactive silencers are basically chamber and tube type units that may include some packing materials for middle and high frequency performance. These types of silencers are principally used on reciprocating engines (pistons) or other equipment having significant impulse type sound energy. The chamber and tubes are designed (tuned) to the principal impulsive frequencies that need to be attenuated. The attenuation is caused by the chambers and tubes that create internal reflective sound fields that reduce the sound energy. Because these units are tuned for each application, any changes will affect performance and includes connecting ducts, especially tail pipes. **Figure 2.4** shows a reactive silencer without any absorptive material. Note the internal pass tubes and chambers.

Reactive silencers are generally the preferred method for passive attenuation of low frequency sound from reciprocating engines. They are usually designed for fixed known frequencies and may not be appropriate for other engine models or specifications.

2.11 Silencer Design

Silencers may be designed based on design parameters and functional requirements such as those outlined by Sherekar & Dhamangaonkar (2014). These parameters vary depending on the type of silencer (reactive or absorptive) and engine specifications. Some of these are listed below;

2.11.1 Adequate Insertion Loss (IL)

An effective muffler will reduce the sound pressure of the noise source to the required level. In the case of an automotive muffler the noise in the exhaust system, generated by the engine, is to be reduced. A muffler's performance or attenuating capability is generally defined in terms of insertion loss or transmission loss. IL is the difference between the acoustic power (the rate at which sound energy is emitted, reflected, transmitted or received, per unit time) radiated without and with a muffler fitted and is a common measure of acoustic performance that represents the change in sound pressure level (dB) for the surroundings due to the insertion of noise reduction materials. This is expressed mathematically as;

$$IL = 10log_{10}\left(\frac{W_1}{W_2}\right) \quad (6)$$

where

W_1 = acoustic power (watts) without muffler

W_2 = acoustic power with muffler

The transmission loss (**TL**) is the difference (in decibels) between the sound power incident at the entry to the muffler to that transmitted by the muffler. The muffler designer must determine the required insertion loss so that a suitable type of muffler can be designed for the automotive application (Biswas & Mandal, 2013). For a simple expansion chamber, TL may be expressed as;

$$TL = 10log_{10}\left(\frac{1}{4}\left|coskl + j\frac{S_1}{S_2}sinkl + j\frac{S_2}{S_1}sinkl + coskl\right|^2\right) \quad (7)$$

where;

S_1 = cross sectional area at inlet

S_2, = cross sectional area at outlet

l = length of expansion chamber,

k = the wave number

$= w/c$

$= 2\pi/\lambda$

$= 2\pi f/c$

f = frequency

c = speed of sound

λ = wave length

It is worth noting that transmission loss is zero when l is a multiple of half of a wavelength, and peaks when frequency is $(c/4l) + n(c/2l)$; where n = 1, 3, 5,…. This is only valid for low-frequency range since at low frequencies, the sound wave can be treated as plane waves.

Transmission loss calculation starts losing its accuracy when the frequency goes above the cut-off frequency, which can be calculated as;

$$f_c = 1.84 \frac{c}{\pi D} \quad (8)$$

where

c = speed of sound

D = diameter of the largest pipe in the structure

Coherence, a measure of the degree of linear dependence between two signals as a function of frequency used to check validity of the frequency response measurement. It is used in the calculation of signal to noise ratio as a function of frequency. If random noise is present in either $x(t)$ or $y(t)$ then the value of the coherence would diminish. Causes of diminished coherence include undamping relationship between $x(t)$ and $y(t)$, insufficient frequency resolution in the frequency spectrum, poor choice of window function, and a time delay of the same order as the length of the record between $x(t)$ and $y(t)$.

IL curves are similar to TL curves. The significant difference between the two is that at very low frequencies of about 50 hertz, the IL curve is characterised by a dip at which the IL value is negative. At around this frequency, the mufflers sound pressure level would exceed the unmuffled value. Therefore, design should be done so as to ensure that the dip occurs at a frequency much lower than the firing frequency of the

engine. Area ratio can be used to increase the TL characteristics of a muffler. The higher the value of TL the better the muffler. The TL depends on the frequency: at resonance frequencies the TL is zero, corresponding to the lower peaks. TL is independent of the applied pressure or velocity at the input.

Phase change occurs in sound when sound waves exhibit 180^0 change in phase when reflected from a region with lower acoustic impedance, for example sudden opening.

2.11.3 Selection of size

The proper selection and sizing of the silencer is of utmost importance to ensure that pressure drop, acoustical performance and other specific design criteria are met. The selection of the correct type of engine exhaust silencer is determined by the type of engine, the end use of the engine and the degree of silencing required. Also, the silencer size selected must accommodate the specified volume of exhaust gas flow keeping the back pressure within the limits specified. The available space has a great influence on the size and therefore type of muffler that may be used. A muffler may have its geometry designed for optimum attenuation (Mohamad et al, 2019); however, if it does not meet the space constraints, this may not serve the intended purpose.

2.11.3 Backpressure

Backpressure represents the extra static pressure exerted by the muffler on the engine through the restriction in flow of exhaust gasses. Generally, the better a muffler is at attenuating sound the more backpressure is generated. In a reactive muffler where good attenuation is achieved, the exhaust gasses are forced to pass through numerous geometry changes and a fair amount of backpressure may be generated, which reduces the power output of the engine. Backpressure should be kept to a minimum to avoid power losses especially for better performance of vehicle (Reddy & Reddy, 2012).

Introduction of muffling systems in a duct imposes a pressure drop. The total pressure drop of a muffling system is a combination of friction and dynamic losses through the system. Frictional losses are proportional to the length of travel along tubes or ducts, while dynamic losses occur at duct discontinuities (e.g., contractions, expansions and bends). For laminar flow, frictional losses depend on the Reynolds Number and are

small. However, when Reynolds Number is greater than 2000 the flow will be turbulent and the pressure drop will be independent of Reynolds Number.

Expected pressure drop for flow through a duct may be estimated using the expression;

$$\Delta P = f_m \left(\frac{LP_D}{4s}\right)\left(\frac{\rho u^2}{2}\right) \quad (9)$$

where

f_m = friction factor

$\Delta P_{(Pa)}$ = pressure drop

$u_{(ms\text{^-}1)}$ = mean flow speed through duct

$s_{(m\text{^}2)}$ = duct cross sectional area

$P_{D(m)}$ = duct cross sectional perimeter

$L_{(m)}$ - length of duct

2.11.4 Cost and Weight

Generally, the larger a muffler is, the more it weighs and the more it costs to manufacture. For a performance vehicle every gram saved is crucial to its performance. Effectively supporting a muffler is always a design issue and the larger a muffler is the more difficult it is to support. A Muffler's mounting system not only needs to support the mufflers weight but it also needs to provide vibration isolation so that the vibration of the exhaust system is not transferred to the chassis and then to the passenger cabin. This vibration isolation is usually achieved with the use of hard rubber inserts and brackets that isolate or dampen vibration from the muffler to the chassis. Therefore, small light weight muffler is desirable (Chaudhari & Patel, 2014). Several researchers have come up with design methodologies for reactive silencers. Shah et al. (2010) proposed a seven-step methodology involving; setting targets and benchmarking, calculation of target frequencies, muffler volume calculations, internal configuration and concept design, virtual simulation, prototype manufacture and eventually experimental testing and design finalization for prototype. Suganesawaran et al. (2014) also used a methodology similar to the previous one. In the latter case, design targets included engine performance and targeted acoustic performance parameters. These two feds into information for the development of the base model which was used to develop design alternatives. Here, structural and flow analysis were

used as information to feed into the finalized alternative. Resulting best alternative is validated before prototyping and testing to obtain the final product.

2.12 Silencer Modelling

Modelling is a powerful tool for the interpolation, prediction and optimization of engineering noise control strategies. However, models need to be validated by monitoring data. One advantage of using models is that they enable examination and comparison of the consequences for noise exposure of the implementation of the various options for improving noise. It is worth noting that the accuracy of the various models available depends on many factors, including the accuracy of the source emissions data and details of the product being evaluated.

Zhu and Ji (2016) developed a computational technique for flow-noise prediction. In this work, a computational fluid dynamics (CFD) approach is developed and used to predict muffler characteristics in terms of major performance parameters incuding sound transmission loss. Computational techniques for flow-generated sound can be classified into two broad categories: direct computation and indirect, or hybrid, computation. The direct approach computes the sound together with its fluid dynamic source field by solving the compressible flow equations. It is also possible to use unsteady Reynolds-average Nevier-Stokes (RANS) methods (Holmberg et al., 2015) to compute the noise of the largest flow features.

The simulation domain must be sufficiently large to include all the sound sources of interest and at least part of the acoustic near field. Provided that a wave equation is satisfied at the edge of the simulation domain, an analytical solution to the wave equation using the Kirchoff-integral (Been & Moon, 2019) can be readily employed. Numerical means of solution extension typically involve solving simplified equations, such as the linearized Euler equations or wave equation in a larger domain external to the domain of the direct simulation (Ward, 2016).

Since it avoids any modelling approximations, the direct computation method using DNS provides a tool for studying sound-generation mechanism and generating database for developing and evaluating sound prediction models. However, because

of its high computational costs, its use is limited to simple flow configurations at low to moderate Reynolds number.

There are a number of distinct challenges posed by the computation of flow noise relative to general computational dynamics as investigated by Wang et al., (2017) and Balakumar et al., (2018). First, the noise generating flow is interestingly unsteady, which renders steady RANS method alone unsuitable and unsteady RANS calculations generally insufficient except when the flow is dominated by simple large-scale oscillations. Secondly, difficulty is the vast disparity in the magnitudes of the fluid dynamic and acoustic disturbances with the exception of high-speed flows involving shock waves only a small fraction of flow energy radiates to the far field (Guo et al., 2017).

Tutunea et al. (2013) used Computational Fluid Dynamics (CFD) method to explore aerodynamic performance of a resistance muffler (silencer). Resistance muffler research relates with the fields of acoustics, fluid dynamics, heat transfer and mechanism design. The author simulated the field by numerical method with Cosmos Flow and analyzed the effect which the internal flow had on the performance of the muffler, which may be a credible guidance of the muffler structural design. With this method, the pressure distribution in the muffler was simulated and the pressure loss predicted for the structure modification. The experimental results by Tutunea et al., (2013) verified that the assembly performance of the muffler was better than the original muffler.

According to Bashir & Carley (2020), boundary Element Method (BEM) results in faster initial prototypes and smaller computational models. The BEM technique only involves discretizing the boundary of an enclosed space or boundary of a noise radiating structure. Finite Element Method (FEM) on the other hand involves discritizing enclosed volume of interior noise inner and exterior problem, and a large space around a noise radiating structure for external problems (Fu et al., 2019).

2.13 Optimization for Improved Performance

In order to save on design times, costs and to achieve improved performance, algorithms that explore the design space have been used (Ranjbar & Kermani, 2016;

Praveen et al., 2018). These programmes establish the relationships between input and output parameters and their influence on the desired performance.

Ranjbar and Kermani (2016) used a generic algorithm and controlled random search method to maximize Transmission Loss of a Simple Expansion Chamber based on geometric parameters of the muffler. They found out that the diameter of the muffler should be at least three times more than other part of the SEC muffler. No experimental verification of the results were done. In addition, they did not look at the influence of other non-geometric parameters on the TL.

Praveen et al. (2018) also analysed the effects of a SEC muffler TL by varying the geometrical parameters using the generalized matrix method and Taguchi method for optimization. They established that while increasing the length of the chamber, the peak TL remained constant but the attenuating effects increased. In these two cases, the optimization of the SEC geometry by itself only serves to inform decisions on which more complex geometries may be evaluated, but the results obtained are not of any practical use since noise attenuation is insignificantly low for practical applications.

Several simulation and analysis programs have been developed with appropriate algorithms, and these have been used (Nazirkar et al., 2014; Ranjbar & Kermani, 2016; Praveen et al., 2018) to study performance of optimized muffler geometries. These include among others MATLAB, ANSYS, and COMSOL.

One of the most advanced optimization software used in the design and evaluation of noise attenuation systems is ANSYS. DesignXplorer (DX) is a tool in ANSYS that uses response surfaces and direct optimization to efficiently explore the solution space. Unique characteristics of this tool includes capabilities to explore and understand the performance at other design or operating conditions; find the conditions which give the best performance; determine the key parameters influencing the design; and explore the robustness of the design.

Mufflers and silencers are said to perform well when they are capable of reducing the noise levels from the source. Two major methods are used to evaluate performance of mufflers and silencers. One method in insertion loss (Liu et al., 2021), which

determines how much the device reduced the noise level by comparing the noise level before and after the installation of the device. A second method is the Transmission loss method (Kashikar et al., 2021), which is intrinsic to the design, and can be determined mathematically during the design process. Transmission loss method provides detailed information about the sound wave as it passes through the device. This allows for adjustments to be made in the geometry in order to achieve a given noise profile.

2.14 Additional layers of control of noise

When the primary control strategy is not sufficiently effective in reducing noise levels from a source, additional control layers should be implemented. These configurations are designed to operate at locations between the source and receiver such that the path of travel of the sound wave is obstructed. This results in reduction in the levels of sound energy reaching the ear. The most common configurations developed by researchers are discussed in the following sub sections.

2.14.1 Noise reduction by distance

The worker can be protected against the effects of excessive noise exposure through distance. In this case, sufficient distance is maintained between the worker and the noise source. A typical arrangement of noise reduction by distance is illustrated in **Figure 2.5**.

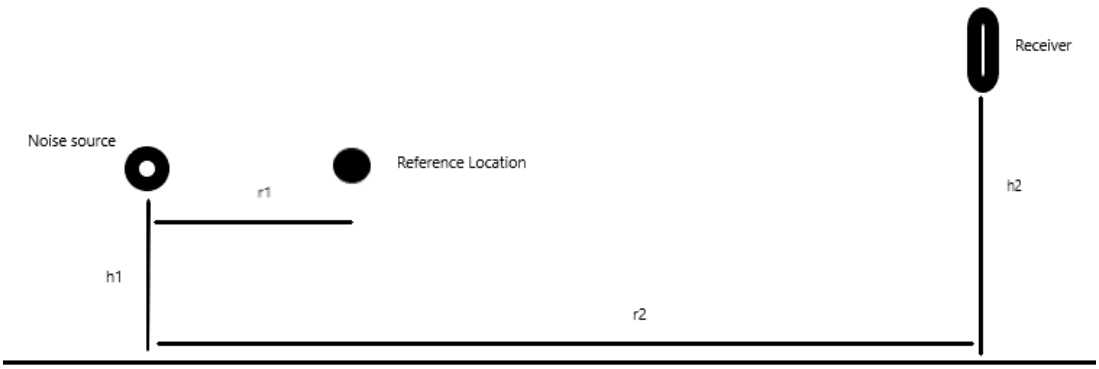

Figure 2.5: Configuration of noise control by distance

The nature of sound wave propagation in a free field is that sound pressure decreases inversely with distance. The spreading loss (A_s) in decibels between two positions at distances r1 and r2 from an acoustic source is defined by Hansen & Hansen (2021) as;

$$A_s = 20g \times log\left(\frac{r_2}{r_1}\right) \quad (10)$$

Where the value of $\boldsymbol{g}$ is 0 for plane wave propagation in uniform pipes, ½ for cylindrical propagation from a line source, and 1 for spherical wave propagation from point source. Parameters $\boldsymbol{r_1}$ and $\boldsymbol{r_2}$ represent distances between the acoustic centres of the source and the receiver respectively. The reduction in sound occurs when the complex 3D wave propagation results in loss of energy due to absorption, reflection, cancellation and retardation in the process.

Investigation into the effects of environmental conditions on outdoor sound propagation by Caviedes-Nozal et al., (2019) showed that up to 8ms^1 wind speed and temperature range between -2 and 6^{0}C results in variations in sound propagation over distances of around 300m. In this investigation, transfer functions between two subwoofers and four pairs of microphones separated by 170m to 300m of flat grassy meadow were measured every 30 minutes. Monitoring of wind direction, speed and temperature was also done at five strategic locations, with an additional temperature and humidity sensor located at 2m above the ground. However, the authors did not test the accuracy of the use of this method on sound propagation estimation.

The use of distance to address residual noise hazard to ensure that the worker is not exposed to dangerous noise levels is one of the cheapest solutions available. This is due to the fact that, as long as space is available, no hardware is required to achieve noise reduction. The ample space would be sufficient enough to potentiate loss in energy of the sound wave as it propagates through the medium (in this case, air). Under normal conditions, the wavelength of sound varies with frequency as presented in **Figure *2.6***.

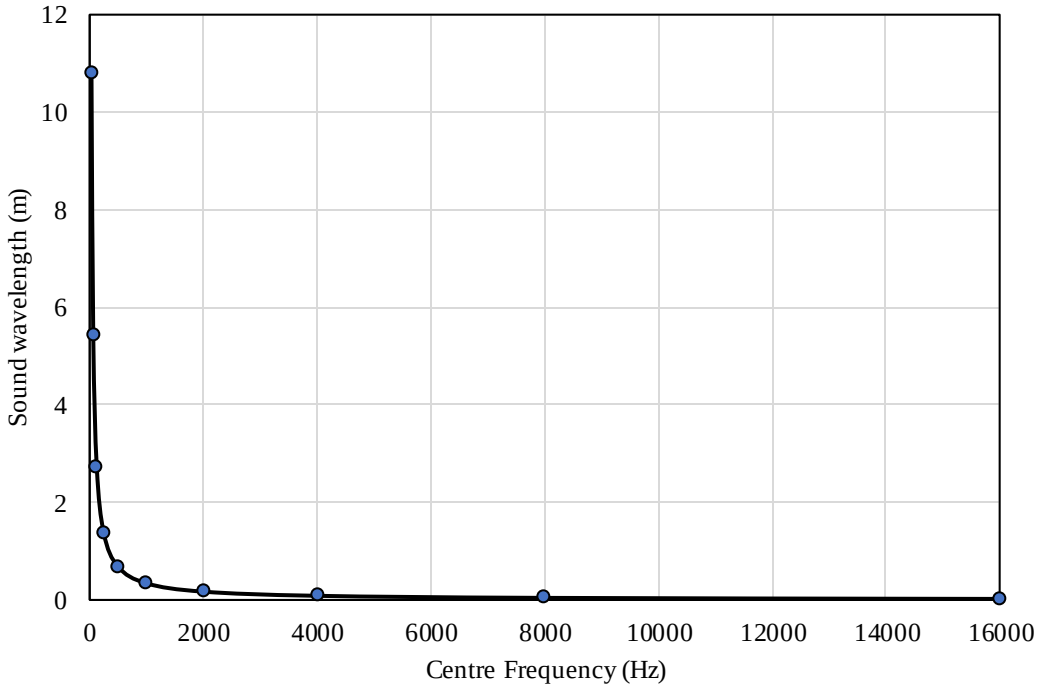

Figure 2.6: Variation of sound wavelength with frequency

Sound waves that fall within the hearing range of 0 to 2,000Hz have wavelengths that vary from 17m at 20 Hz to 17mm at 2000Hz. This relationship, derived from equation 19, shows that the highest risk to hearing occurs more at lower frequencies. Any action to control noise affecting hearing should therefore aim at influencing acoustic wave propagation by altering the wavelengths in this range. It is therefore important to ensure that within the hearing range, the worker is safe and able to perceive all the acoustic cues associated with his work. Use of distance in a free field allows air to create adequate retardation to the sound propagation, thereby altering the wavelength and hence a reduction in sound levels.

A relationship between the noise level at a varying receiver location and geometric sound wave decay is presented in **Figure 2.7**.

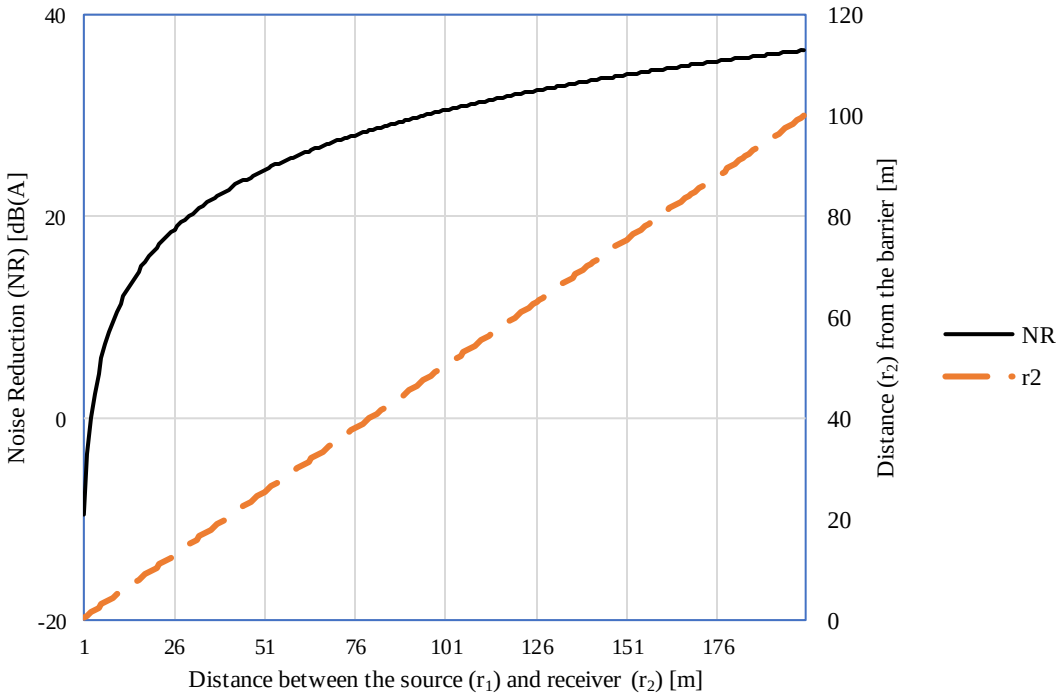

Figure 2.7: Variation of noise level with distance

From equation 15, the level of noise reduction depends on the ratio between location r_2 and r_1. As the distance between the source (r_1, which is held constant at 1.5m from the source) and receiver (r_2) increases, the sound level at the receiver location inversely increases and tends to approach a fixed noise value on the Y-axis. This implies that the noise level approaches the fixed value that is equivalent to the background noise level as one moves away from the source, thereby minimizing the impacts from the source. It is worth noting that when the distance from the source to the receiver is shorter than that between the source and the reference location r_1, the noise reduction is negative. This implies that there is sound amplification and therefore higher values are experienced. This indicates that equation 15 is only valid for $r_2 > r_1$.

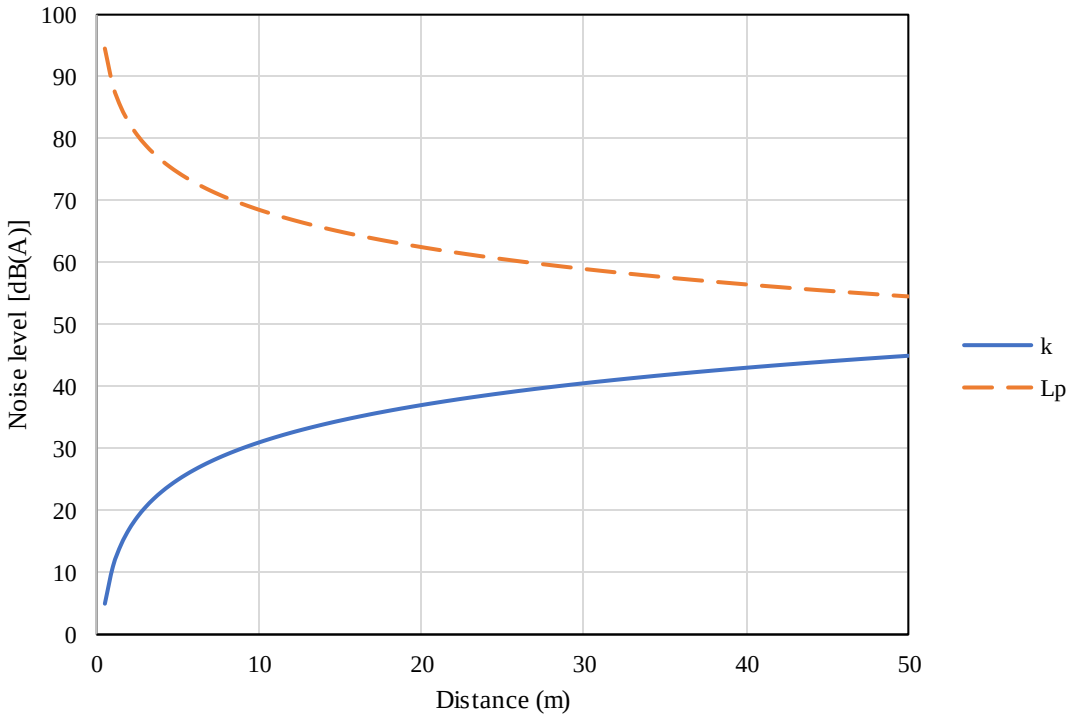

Figure 2.8: Relationship between geometric spread factor (k) and receiver noise level (Lp)

As the distance between the source and receiver increases, the receiver sound level decreases inversely, while the amount of noise reduction increases as depicted by the geometric spread factor (k). Safe and suitable location of the worker depending on the space available can then be selected from **Figure 2.8**.

2.14.2 Acoustic barriers in free field

When a noise source is present in a free field or an open area, the worker may be protected by the use of a barrier that separates him from the noise source. The location of the barrier and the barrier characteristics determines the amount of noise attenuation, and consequently, the effective noise level reaching the receiver. An illustration of acoustic barrier in free field configuration is as shown in **Figure 2.9**. Labels on the illustration has the following connotations;

h1 = height of the noise source from the ground

h2 = height of the receiver from the ground

dss = distance from the noise source to the top of the acoustic barrier

dsr = distance from top of the acoustic barrier to the receiver

d = the direct distance measured from the noise source to the receiver

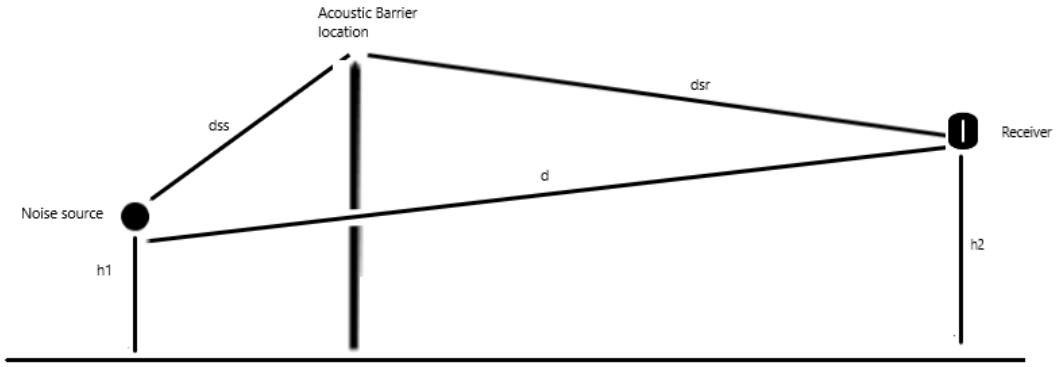

Figure 2.9: Configuration of acoustic barrier in free field

In this setup, the level of attenuation depends on the height and width of the barrier and the location of the receiver from the barrier. Barrier attenuation for each octave band (D_z) may be determined using the expression;

$$D_z = 10log_{10}\left[3 + \left(\frac{C_2}{\lambda}\right) C_3\, z\, k_{met}\right] \text{dB} \qquad (11)$$

Where $C_3 = 1$ for single diffraction

$C_2 = 20$, and includes the effects of ground reflections

z = difference between the path lengths of diffracted and direct sound as calculated by Equation 12.

λ = wavelength of sound at the normal mid-band frequency of the octave band in meters

k_{met} = correction factor for meteorological effects [k = 1 for $z \leq 0$]

$$z = [(d_{ss} + d_{sr})^2 + d^2] - d \qquad (12)$$

Where dss = distance from the source to the diffraction edge (m)

dss = distance from the diffraction edge to the receiver (m)

dsr = distance from top of the acoustic barrier to the receiver (m)

d = the distance parallel to the barrier edge between source and receiver (m)

Several acoustic barrier materials have been researched on and found to be effective in use in a free field environment. These include vegetation (Onder & Akay, 2015),

earth heaps, walls, and specially designed acoustic barriers for targeted noise characteristics (Lacasta et al., 2016).

According to a review by Ruiz-Garcia Cosola et al., (2022), attenuation due to forests and foliage (a form of acoustic barrier) provides varying levels of attenuation depending on the density of the vegetation; the denser it is the more attenuation is achieved. Hosseini et al., (2016) and dos Reis et al., (2022) established five factors that determine the level of noise reduction provided by vegetation. These include visibility, height and width of trees, height of receiver and noise source, and the distance between the noise source and receiver. A study by Akay & Onder (2022), on the use of plants to mitigate traffic noise established that the highest reduction of noise of up to 4.6 dB(A) can be achieved when when the distance between the sound source and plants is reduced. This is possible with the right combination of plant groups and hedge plants.

Using an acoustic barrier in a free field yields another form of solution to the problem of exposure to excessive noise. With the configurations and assumptions defined in the materials and methods section, result of the key parameter z (equation 12) is presented in **Figure 2.10**Error! Reference source not found..

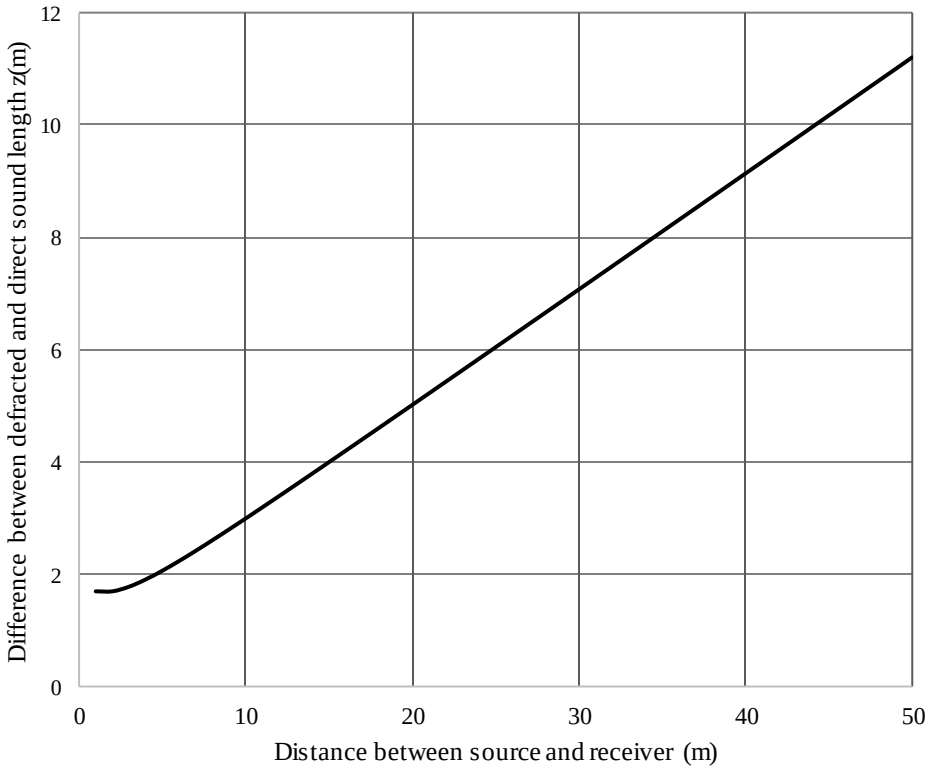

Figure 2.10: Variation of path length of diffracted and direct sound

This indicates that for a given set of basic parameters (height of noise source from the ground, distance of noise source to the barrier, height of the barrier, and height of receiver from the ground), the value of z increases with increase in distance between the source and the receiver. This influences the value of barrier attenuation especially in the frequency range between 32.5 and 2000Hz. In addition, the non-linear relationship at the start of the curve in **Figure 2.10** indicates that when the difference between the diffracted and direct sound length is less than two meters, sound attenuation in a free field is not significant.

Across the hearing frequency range, barrier attenuation is presented in **Figure 2.11**.

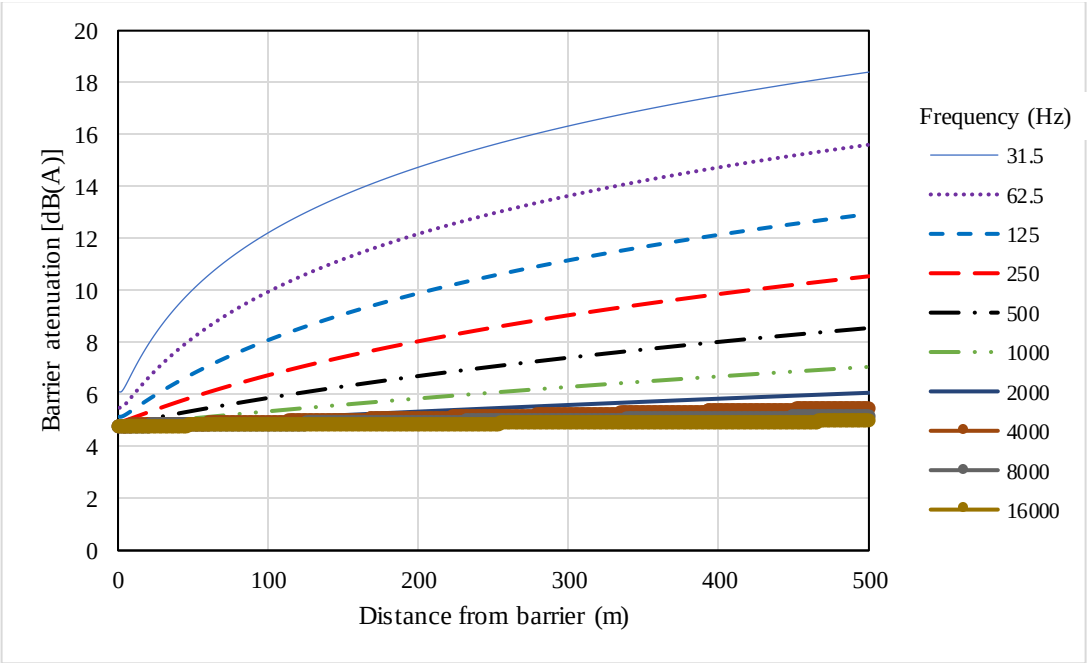

Figure 2.11: Variation of acoustic barrier attenuation with frequency

For the single barrier with a height of 3m and a width of 6m described as in the methodology section, the barrier attenuation in the hearing frequency range is sensitive to the z value (the difference between diffracted and direct sound length). As z increases, barrier attenuation increases for the lower frequency of 31.5Hz from slightly above 6dB(A) at 1.5m from the source, to 18dB(A) at 500m. For subsequent frequencies between 31.5 and 2000Hz, the attenuation levels decrease due to shortening of the wavelengths. Above 2,000 Hz, there is no significant difference in barrier attenuation as it is fairly constant at 4.9 dB(A) throughout the range from 1.5m to 500m, mainly due to the shorter wave lengths (below 17mm) at these frequencies. In order to achieve higher attenuation values, thicker materials and in some cases double barrier configurations are employed. This method is effective in the control of specific components of noise contributions to the overall noise level at given centre frequencies in order to minimize NIHL risks.

Similar analysis of the use of acoustic barrier has been studied by Jiaxin et al., (2020), who achieved higher noise reduction with the use of two parallel surfaces positioned perpendicularly between the source. However, this arrangement may be considered

to be similar to the use of a canopy (an acoustic enclosure), which are capable of substantially reducing the radiated noise.

The use of plants and other vegetative features have also been studied (Akay & Onder, 2021). Vegetation and moving water bodies as a noise-suppression features have been studied and found to be effective when used in areas including airports, where it may be difficult to implement and maintain a physical acoustic barrier due to the scope of area affected by landing and take-off noise (Martijn et. al., 2018).

2.14.3 Hearing Protection

The use of hearing protection equipment should be adopted as the last resort when deriving solutions for a noise control problem. This is because its use only provides a shield from the offending noise. Should there be any leakages caused by improper fit, or manufacturing defects, then the protection provided will not be effective as intended. It is therefore important to ensure that the hearing protection solution provided is most suitable for the type of noise pollution present and that the user is properly trained on the use of the equipment and well informed on the consequences of exposure to excessive noise. In addition, support must be provided during the use of hearing protection in form of implementation of an effective noise control and hearing conservation programme.

Rating systems have been developed for identification of hearing protection equipment (HPE's). These systems are used to provide a basis for comparison of different HPE's for a particular noise problem. The advantage of this is that the user is able to select a suitable product that will provide personal preferences in addition to the designed noise protection. In order to prescribe a hearing protection solution to the noise problem, the magnitude and characteristics of the noise should first be determined, and then coded into the three systems that define the HPE identifier.

There are three rating systems currently in use. The first one is the Single Number Rating method that provides a single number identifier (Ljunggren et al., 2014); the higher the number the more protection the product gives in a noisy environment. The second system is the High, Medium, Low (HML) method that estimates noise reduction of hearing protection at High, Medium, and Low frequencies. The third

system is the Octave Band Analysis method is considered more accurate as it allows for the detailed analysis of the noise at each of the centre frequencies within the hearing range (Rossi et al., 2019). in order to provide specific solution to the offending noise at particular frequency.

Research into the use of hearing protection as a control strategy for excessive noise exposure yielded a number of solutions. These include several types of hearing protection such as ear muffs and ear plugs as illustrated in **Plate 2.2**.

Earmuff Earplugs

Plate 2.2: Hearing protection devices

(Source: Pelton TM Optime)

Earmuffs are available in different configurations and designs depending on the manufacturer. They are designed to cover the ear canal, protecting the ear against sound energy, and can be used alone or as attachments to other protective gear such as helmets or hard hats. Earmuffs are available for hearing protection against high frequency noise up to 95 decibels. Some designs of the earmuff provide a mechanism for noise cancellation or reduction through a feedback control system that ensures that the offending noise is reduced.

On the other hand, ear plugs are made from soft plastic, polyvinyl chloride, silicon, and polyurethane, and are inserted either partially or fully into the ear canal. Ear plugs are useful for protection from low-frequency noise.

Effectiveness of the use of ear muffs depends on the design and construction, fit (Murphy et al., 2016), and activities being carried out by the worker (Feder et al., 2017). The use of hearing protection should also consider the environmental conditions such as humidity, which may lead to undesirable effects as infection of the ear. This would in turn greatly affect the efficiency of protection. Hearing protective devices should be personalized in order to derive the maximum benefit from their use. Certain types may be effective for a given group of people while others may result in discomfort, which may lead to ineffective usage.

2.15 Legislations relating to Noise Prevention and Control

Kenya has enacted a number of legislations for the prevention and control of noise both at the workplace and in the general environment. These are discussed in detail in the following subsections.

2.15.1 Occupational Safety and Health Act of 2007

The main objective of the Occupational Safety and Health Act of 2007 in Kenya is prevention of occupational accidents and ill health, and to provide for welfare of workers. The Act applies to all places where persons are lawfully engaged on employment. The general guidelines in the Act aims at elimination or minimization of workplace risks and hazards, with specific duties and responsibilities apportioned to both the occupier and the employee. Actions to address noncompliance are also clearly stipulated, in order to ensure safe and healthy workplaces.

The responsibilities of implementation of the Act are bestowed upon the Directorate of Occupational Safety and Health Services (DOSHS) under the Ministry of Health. The Directorate has offices in Nairobi and in all the 47 counties. Occupational Safety officers monitor activities of the workplace through inspection and review of annual reports. When major nonconformities are identified, the Safety officers issue improvement notices or stops any dangerous activities, and institutes legal proceedings in courts of law. Approved persons are engaged to advice occupiers on occupational safety and health issues, carry out training and inspections, audits, medical examinations on workers, and to prepare and submit reports to the Directorate.

Specific details of major aspects of the Act are contained in subsidiary legislations. These include Medical Examination Rules of 2005, Nose Prevention and Control Rules of 2005, Fire Risk Reduction Rules of 2007, Examination of Plant Order, and Woodworking Machinery Rules. With regards to noise, the Noise prevention and control Rules specifies action limits that inform actions to be taken to protect the worker. Permissible exposure to noise is capped as exposure to a continuous equivalent of 90 dB(A) in eight hours within any 24 hours duration. The premise here is that the human ear is capable of recovering from impacts of this exposure when noise level is not continuously at the peak value (Jin et al., 2018).

Where noise exceeds 85 dB(A), the Act requires that hearing protection be provided, and the occupier to develop and implement an effective noise control and hearing conservation programme. This programme should include training and provision of information to employees, periodic medical examination, monitoring of noise levels, and annual review of the hearing protection programme. In addition, the permissible peak sound level has been set at 140 dB(A) at any given time.

Intermittent noise exposure defined in the Act should not exceed a resultant sum equivalent to 90 dB(A) in an 8-hour duration within any 24 hours. In this category, intermittent noise includes noise resulting from the passing of a train, the flying past of an aircraft, or an equipment operating in circles. The occupier should therefore identify sources of intermittent noises within the workplace and take them into consideration when evaluating the overall impact of the noise on workers.

Shortcomings of the OSHA, 2007 in protecting workers against noise-induced hearing loss include brief guidelines on continuous and intermittent noise, and lack of legislation on other types of noises that are potentially injurious to hearing. Omitted noise types include impulsive noise (as experienced when firing an ammunition is fired from a firearm), low frequency noise (such as the humming of an electrical transformer), and high frequency noise (such as results in the release of air from a boiler venting exhaust outlet). There are also no proper guidelines on how to evaluate the noise types covered by the Act. While limits for noise from workplaces to the neighbourhoods during the day and night have been set at 55 dB(A) and 45 dB(A)

respectively, no provisions are given for other working environments such as construction sites, airports, and sensitive areas such as hospitals, schools, and other learning environments where noise control is critical.

Excessive vibrations have also been found to lead to occupational ill health (de Alwis & Garme, 2021). Vibrations mostly result from rotation or oscillation of machine parts. Noise may also induce vibrations as the acoustic waves propagate (Vavakou et al., 2021). The Occupational Safety and Health Act 2007 only requires that vibrations that are likely to result in health effects be controlled. However, the Act does not specify any threshold limit values or exposure action values to guide in decision making, neither does the Noise Prevention and Control Rules identify and address vibration as a risk. This is a gap that requires to be addressed when reviewing the Act. Consequences of not specifying safe vibration levels may include challenges in enforcing compliance with provisions of section 89 on control of excessive vibrations, and section 90 on redeployment due to adverse health effects. The occupier may fail to identify vibration as an occupational health risk and therefore not take the necessary action, since the Act does not give definitive guidelines.

2.15.2. Noise and vibration legislation

The International Labour Organization (ILO) developed Conventions and Recommendations to regulate the levels of noise exposures in workplaces. Member states ascribing to these Conventions and Regulations are bound by the requirements, and are obligated to domesticate the guidelines in form of statutory legislations. This is to ensure structured implementation measures are put in place for monitoring and control in order to minimize hazardous exposures at workplaces.

Convention C148 (No. 148 of 1977) on Working Environment (Air Pollution, Noise and Vibration requires that national laws shall prescribe measures to be taken for the control of, and protection against occupational hazards in the working environment due to air pollution, noise and vibration. It provides for the general criteria for implementation of measures, which include engineering and administrative controls, and the use of individual and collective protective devices of equipment.

Protocol P155 of 2002 to the Occupational Safety and Health Convention, 1981 requires member states to designate a competent authority to ensure establishment and application of means of collecting, collating and publishing statistics of occupational accidents and diseases at organizational and national levels, and publication of information on measures taken to minimize occupational accidents, injuries, and other injuries to health arising from the workplace.

In terms of global environment, public health issues capture well pollution associated issues arising from workplaces. Of significance in this category and relevant to this study is air pollution that include noise, vibration and pollutants from combustion processes. There are deliberate efforts by the World Health Organization (WHO), ILO and other international organizations to consolidate their efforts in minimizing adverse effects of environmental pollution.

In Kenya, while the Factories and Other Places of Work (Noise Prevention and Control) Regulations 2005 – a subsidiary legislation to the Occupational Safety and Health Act of 2007 – caters for the workplace, the Environmental Management and Coordination Act (Revised) 2015, caters of the general environment. In both cases, management and control of environmental pollutants are covered. The two legal instruments are detailed below in terms of occupational noise provisions.

2.15.3 The Factories and Other Places of Work (Noise Prevention and Control) Rules 2005

In these Rules, a "worker" is defined as a person who has entered into or works under a contract of service or apprenticeship; written or oral, express or implied, whether by way of manual labour or otherwise. In addition, a "workplace" is defined as to include any land, premises, location, vessel or thing at, in, upon or near which a worker performs his duty in accordance with his contract of employment. The overall objective of these Rules is prevention of injury to hearing by setting exposure limit values (ELV's) and outlines key measures that need to be taken by the occupier and employee with respect to noise exposure.

The lower exposure limit (LEL) is defined as 85 dB(A). Above this level, the occupier is required to put in place a noise prevention and hearing conservation programme.

The programme should include noise monitoring and measurement at least once a year, employee education and training, engineering control at source and hearing protection, administrative controls such as posting of hazardous noise notices and mandatory requirement to wear hearing protection. Other administrative measures to include adoption of less noisy methods and procedures. The programme should be renewed annually to ensure efficiency and effectiveness.

The upper exposure limit (UEL) is capped at 90 dB(A). No worker is to be exposed to noise level in excess of the continuous equivalent of 90 dB(A) in eight hours within any one day. Where noise is in excess of 90 dB(A), hearing protection must be provided, or segregation of the noise source be done using suitable sound absorbing enclosure. In addition, where noise level is such that interference with verbal or sound communication is likely to occur, alternative means of communication must be provided such as visual signs or the use of special lights. No worker is to be exposed to peak sound level of 140 dB(A) at any given time. Where intermittent noise is produced, no worker is to be exposed to noise in excess of the sum of the partial noise exposure equivalent to continuous sound level of 90 dB(A) in eight hours duration in any given day. Duties of both the worker and occupier are clearly spelt out in the Rules. While the worker is required to observe all the rules and regulations in place for prevention and control of noise pollution within the working environment, the occupier is required to put in place all possible measures to ensure that excessive noise is adequately controlled.

In the Rules, consideration is also provided for noise emission to neighbourhood of workplaces. During daytime, this level should not exceed 55 dB(A), while at night 45 dB(A) should not be exceed.

2.15.4 The Environmental Management and Coordination (Noise and Excessive Vibration Pollution) (Control) Regulations 2009

While there is a thin line between occupational and environmental settings, they share common features in terms of impact to the worker. The Environmental Management and Coordination Act 2015 is an Act of Parliament for the management of the environment. The Act gives entitlement to clean and healthy environment, and caters

for the broader scope that include occupational, aquatic, atmosphere, stratosphere, troposphere, and land. Compared to the Occupational Safety and Health Act, the Environmental Act provides for more information for the management of noise and vibrations, among other environmental health risk factors. Further details on exposure limits are provided in subsidiary legislation – The Environmental Management and Coordination (Noise and Excessive Vibration Pollution) (Control) Regulations 2009. The scope of coverage in the management of noise and vibrations in section 14 of the subsidiary legislation include construction sites, demolition sites, mining and quarrying sites. These are however not mentioned in the Occupational Safety and Health Act despite them being workplaces.

Part V of the environmental Act defines maximum permissible noise levels for different locations, which are detailed in the First Schedule to the Act; which specifies permissible equivalent 14-hour noise levels for silent zones (40 dB(A) during day and 35dB(A) during night); mixed residential with commercial zones (55 dB(A) during day and 35dB(A) during night); purely commercial zones (60 dB(A) during day and 35 during night). Maximum permissible noise levels for construction sites for different zones have also been specified as follows; measured from within health facilities and educational institutions (60 dB(A) during day and 35 dB(A) during night); measured from within residential zones (60 dB(A) during day and 35 dB(A) during night); measured from within areas other than those specified earlier (75 dB(A) during day and 65 dB(A) during night).

Maximum permissible noise levels for mines and quarries have also been specified. These are 109 dB(C) within health facilities and educational institutions, and 114 dB (C) within industrial and commercial facilities. The challenge with this definition of maximum permissible noise level is that it does not specify whether the noise is of the continuous or the impulsive type. These two noise types are generated in quarries and mines, and therefore clear distinction ought to have been made. The Noise Prevention and Control Rules 2005 sets the maximum limit as 140 dB(A) peak for continuous noise at any given time and no indication for impulsive noise, while the environmental legislation defines 114dB(C) as the maximum limit without specifying whether this is

for continuous or impulsive noise. Another contrast in the definition of noise limits between the two legislations is that the environmental values are based on 14-hour exposure duration, while the occupational is limited to the standard work shift of 8 hours. The environmental legislation is silent on other types of noises including impulsive, intermittent, low-frequency and high frequency. However, limit for noise from accelerating motor vehicle has been set at 84 dB(A).

Excess vibration in the environmental legislation has been set based on the presumed "safe" location that is the property boundary or 30m from any moving source. The maximum permissible vibration level is given as $0.5m/s^2$. The same limit is prescribed at the same location, and is defined for construction, demolition, mining and quarrying sites. These are active worksites, with residual effects affecting the surrounding environments and activities, which is why limits have been set in the environmental legislation.

The Environmental legislation allows for one to apply for a license to emit noise. This contradicts the spirit of the Act that aims at environmental protection from hazards. Though provisions in Schedule 7 of EMCA Noise and excessive vibration pollution control Regulations 2009 permit emission of noise in excess of specified limits, the applicant is required to state methods to be employed to minimize noise pollution. This leeway is difficult to monitor and control for environmental activities such as public rallies and outdoor advertising that use amplifiers and powerful loudspeakers mounted on vehicles or on site.

It remains a challenge, especially on exposure to noise, to determine the extent of contribution to adverse health effects on workers by environmental noise sources outside the workplace. While occupational environment may be controlled, there are many predisposing environmental factors that are difficult to account for. This makes it difficult to determine the exact cause of the onset of noise-induced hearing loss. It would therefore be important to expunge from the Act the requirement to seek permission to make noise. Activities including outdoor advertising, open-air public rallies, and playing of loud music in public service vehicles, contribute to environmental pollution whose impact is wide, and cannot be easily mitigated by the

permit applicant due to lack of professional knowledge. In addition, the permit applicant may not have the means to establish the effectiveness of any noise control measure proposed or put in place.

2.16. Noise measurements

The intensity of noise or sound is measured in decibels. The decibel is a logarithmic scale that approximates the ears dynamic range. A sound level meter is usually used to measure sound levels. The three main components of the meter include a microphone, a signal processing circuitry that detects and converts any air pressure variations associated with the sound being measured to electrical signal variations, which are calibrated and displayed in decibels, and a user interface.

Sound level meters available in the market for general applications or professional use are usually compact hand-held devices, which may be attached onto tripods for prolonged measurements. While the general application types give basic noise readings (Class 2), the professional types are constructed with additional features that are capable of providing detailed analysis and higher accuracy of the noise or sound being measured (Class 1). The class describes the accuracy as defined by the international standard IEC 61672.

In-built parameters and features of sound level meters include frequency weighting filters (A, C, and Z) that attempt to replicate the sensitivity of the human ear, octave bands (1:1 or 1/3), time-weightings in fast or slow modes, internal storage memory and data logging functions, capabilities for data transfer to analysis softwares, auto/manual range adjustment, audio recording, and output values such as peak sound pressure values and time-weighted average values. These options and features allow for measurement and analysis of noises including continuous, impulsive or intermittent types.

When sampling noise, the microphone is usually covered with a spherical sponge structure that minimizes the influence of reflected sound. The instrument should be positioned at a location above and away from reflecting surfaces. For personal noise sampling, special configurations of noise meters including noise dosimeters and

badges that are specially designed, are used to capture noise levels at the workers hearing zone.

2.17. Research gaps

The effects and epidemiological impacts of occupational noise exposure on hearing have been well researched and documented, though there are challenges in identification of the onset of occupational noise-induced hearing loss (Themann & Masterson, 2019). This is because the worker also encounters noise on a daily basis from activities outside of the work environment. Though the workplace noise may be well regulated and controlled, sources of noise outside of the workplace are hard to account for. These latter sources may include transportation (road and rail), entertainment in public or private, public rallies and activities, and tools and equipment used at home. In addition, development of engineering control interventions for residual noise control remains one of the underexplored research areas in the occupational safety and health field. Specific solutions for noise controls are developed and patent-protected by companies, and therefore further research on them becomes difficult.

While there is information on clinical implications research (Lubner, et al., 2022) and (Moyano et al., 2022), engineering solutions to address impacts of infrasound and ultrasound on workers have not been well documented.

CHAPTER THREE

MATERIALS AND METHODS

3.1 Study design

The research adopted a quantitative approach to occupational noise control, in which a proposed intervention was studied. Experiments were done to test causal relationships between input engine noise and the output resultant noise levels. In addition, investigation of the overall performance in terms of transmission loss by variation of the geometry of the continuous inclined barrier was done.

3.2 Profiling of a 1500cc VVT-i internal combustion engine noise

A test rig was assembled for profiling the engine noise and testing of the prototypes. A four-stroke, variable valve timing with intelligence (VVT-i) 1,500 cubic centimeters (cm^3) gasoline internal combustion engine was used for this study (**Plate 3.1**). This engine is classified under category M in the British Standards Institute (2019) Section 3.2 i.e., power-driven vehicle having at least four wheels and used for the carriage of passengers. It was mounted on a frame structure and installed with all the necessary controls to enable monitoring of test parameters including the engine speed in revolutions per minute. The engine was subjected to a range of no-load speeds between 1,000 and 4,500 rpm in order to study the behaviour or response of the various muffler prototypes used. Rotational speed of the engine was determined directly from the revolution counter attached to the engine.

Plate 3.1: A 1,500cc VVT-i gasoline engine noise source and test rig

Plate 3.2: Pulsar Nova sound level meter Model 45 Class 1

Plate 3.2. presents the integrating sound level meter used in data collection. This is a Class 1 industrial, occupational and environmental measurement product – a high performance sound level meter that is IEC 61672-1:2002 compliant. It has a dynamic measurement range of between 20 to 140 dB(A) with an accuracy of 0.1dB and supported by AnalyzerPlus data logging software, serial number PN1123 supplied with an acoustic calibrator (Model N0105).

The equipment was used to collect real-time noise frequency data for analysis of noise characteristics emanating from the engine without muffling, and the fabricated models attached to the engine test rig. The equipment time history data rate was set to 2

seconds, meaning that measurements were automatically repeated after every 2 seconds over the sampling time of 2 minutes, and the final results obtained as average data. An average of three readings was used to plot noise measurements for the different engine speeds.

3.2.1 Test site

A suitable test site was identified in a level open area away from large reflecting surfaces within a three-meter radius from the microphone location and any point of the test engine. The ground was partly covered with grass, though this did not have significant effects on sound reflection since the height of the lowest reference point was about 0.5m.

3.2.2 Meteorological conditions

Tests were carried out under metrological conditions without rain and 85% cloud cover. Wind speeds were less than 5 metres per second (m^{-s}). Humidity of 74%, atmospheric pressure of 1,013.2mBar, and ambient temperature of 22^0C were also registered.

3.2.3 Background noise level

Readings on the measuring instrument produced by ambient noise and wind was established to ensure that it was at least 10 decibels (dB) below the A-weighted sound pressure level to be measured. The background noise level measured was 39.2 dB(A). A suitable windshield was fitted over the microphone to take care of any possible reflections.

3.2.4 Test procedure

i. Positioning and preparation of the engine

The gear lever controlling the power transmission was set in the "Parking" position, with the engine assembly and supporting auxiliaries including the cooling fan that have automatic actuating mechanisms operating as designed. Before each series of measurements, the engine was brought to its normal operating temperature, as specified by the manufacturer.

ii. Microphone position

The microphone was located at a distance of 0.5m ± 0.01m from the reference point of the exhaust pipe defined in **Figure 3.1** and at an angle of 45 degrees ± 5 degrees to the vertical plane (**Figure 3.2**) containing the flow axis of the pipe termination. This location ensures that the impacts of reflections at the edge are minimized. The microphone was maintained at the height of the reference point, but not less than 0.2m from the ground surface. The reference axis of the microphone was maintained in a plane parallel to the ground surface and directed towards the reference point on the exhaust outlet.

iii. Noise measurement points were conveniently selected to ensure ease of setting, and taken for different engine speeds in steps of 500 revolutions per minute (rpm) from 1,000 to 4,500 rpm first with the exhaust system attached, and later with the exhaust removed. The two sets of measurements (with and without the exhaust system) allowed for establishment of insertion loss characteristics of the exhaust system, and determination of the magnitude of noise without any engineering intervention. These measurements also formed basis of comparison with the proposed design solution.

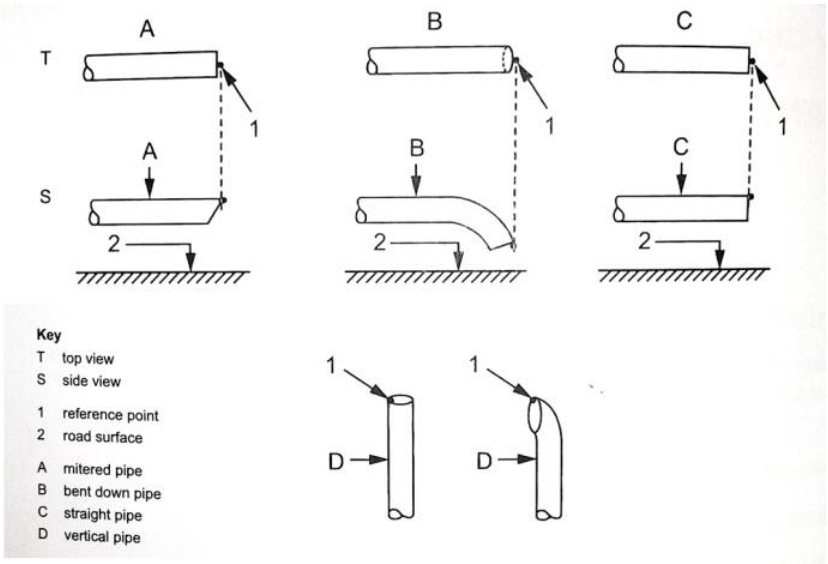

Figure 3.1: **Location of exhaust pipe reference points**

Source: ISO 7235:2003E

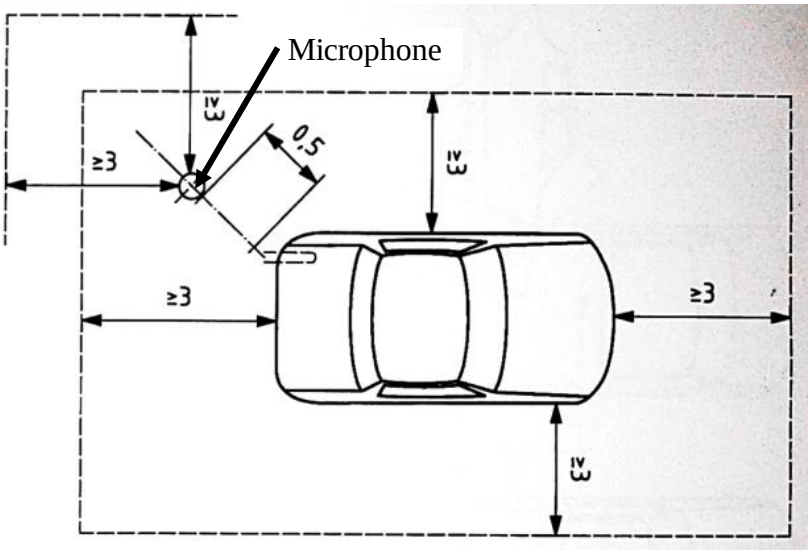

Figure 3.2: Location of microphone relative to reference point

Source: ISO 7235:2003E

Figure 3.2 illustrates the plan location of the sampling microphone, which is also applicable to all ventilating systems handling exhaust gases. It is important to note that a different engine specification may give totally different results, and hence the need to use a particular model.

Sampled data were downloaded from the integrating sound level meter for analysis using the AnalyzerPlus software.

3.3 Development and performance testing of muffler

The design methodology used in this research was based on that developed by Suganeswaran, et al. (2014). Performance parameters were established for the identified Engine model. Acoustic performance requirements for the proposed silencer were also established to form the critical input data for the development of the base model. From this stage, a number of design alternatives were derived based on structural and flow analysis, which were fed into a final alternative solution. Validation of the best solution was done prior to prototyping and eventual testing.

Due to lack of acoustic laboratory and equipment at JKUAT, some of the research studies including simulation and testing were carried out at the Aeroacoustics laboratory of Tottori University in Japan.

3.3.1 Parameters for the base model

The base model was defined initially by parameters of the test engine to be used, which included the engine type (spark ignition), number of cylinders (4 in-line), firing cycle (1-3-4-2), unmuffled noise (108dB(A), maximum power output developed (81 kilowatts at 6,000 revolutions per minute (rpm)), maximum torque developed (142 Newton-metres at 4,200 rpm) type of fuel (gasoline), exhaust temperature (650^0C), engine displacement (1497 cubic centimetres), compression ratio (10.5:1) and backpressure target for optimal performance. For the proposed model, parameters to be fixed included transmission loss target, insertion loss target, and noise and corresponding frequency targets. Sizing of the silencer chamber was done according to the guidelines specified in a technical paper by Ahmedov et. al., (2018) This gave a length to diameter ratio of of the expansion chamber of 3 and muffler volume to engine displacement ratio of 4. AutoDesk Inventor design software was used to model the shape.

3.3.2 Flow parameters

In order to refine the base model, flow analysis was evaluated to predict transmission loss, insertion loss, back-pressure and noise level. These were carried out using design (Autodesk Inventor) and analysis (ANSYS Fluent) softwares. Validation of the parameters defined was undertaken before prototyping and testing.

3.3.3 Prototyping

In order to first study the characteristics of the muffler, three prototype models were constructed from acrylic material. These were the Simple Expansion Chamber – Model 1; the Simple Expansion Chamber with helicoid (Continuous Inclined Barrier) – Model 2; and the SEC with Helicoid and central tube section – Model 3. These models are as shown in **Plate 3.3**, **Plate 3.4**, and **Plate 3.5**.

Plate 3.3: Model 1 - A Simple Expansion Chamber

Plate 3.4: Model 2 - A Simple Expansion Chamber with Helicoid

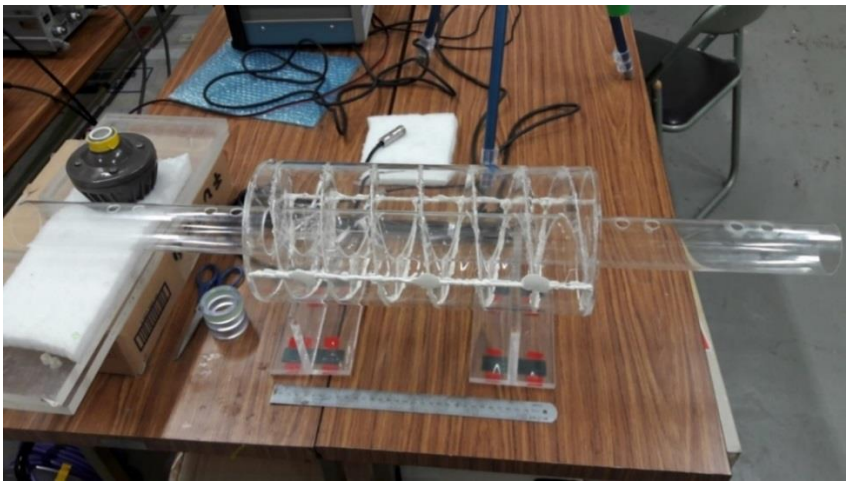

Plate 3.5: Model 3 - SEC with Helicoid and Central Tube

The general proportions of the models were as indicated in the drawing in **Figure 3.3**.

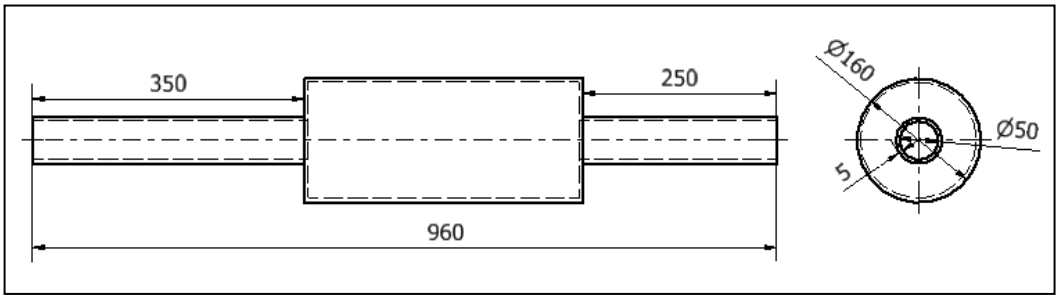

Figure 3.3: General proportions of muffler prototype

Other models used were variations of the prototypes shown in **Plate 3.4** and **Plate 3.5**, in which the pitch of the helicoid was varied and tests done with and without the central tube. Generally, the pitch variation was chosen to vary from 350mm (length of the expansion chamber) to the diameter of the inlet and outlet pipes (50mm).

Fabrication of the models was also done in Stainless Steel sheets grade 304 and in Mild Steel sheets produced to BS EN 10142. Major production methods included shearing to size, roll forming, lap jointing, drilling and welding. Sections of the helicoid were successfully welded to form the desired profiles before enclosing the ends of the expansion chamber and addition of the inlet and outlet pipes.

The SEC was improved by insertion of a central tube. This was welded in place from the middle outwards on either ends of the chamber. Once the helicoid was welded in place the sudden expansion and sudden contraction covers were secured to the chambers and connected to the inlet and outlet pipes.

3.3.4 Simulation of 3D models of muffler

The prototypes were also modelled using Autodesk Inventor 3D modelling software and then imported into ANSYS simulation software. Here, the complex internal fluid volume geometry of each model was extracted using ANSYS Space Claim Direct Modeller and resulting output meshed. The effects of fluid-structural interactions were ignored in this analysis since this was considered a purely acoustic problem. Transient computational fluid dynamics (CFD) was done to solve unsteady flow equations when ANSYS reads and maps CFD results to acoustic mesh and calculates aero-acoustic sources based on transient dynamic analysis.

Simulation of the models was carried out at the Aeroacoustics laboratory of Tottori University in Japan.

Prior to computation, the following boundary conditions were defined;

a. No-flow conditions
b. Medium – Air. Basic parameters for the acoustic medium;
   - density 1.2041 $kg.m^{-3}$
   - sound speed of 343$m.s^{-2}$
c. Analysis frequency range **0 – 2,000Hz** with 50Hz solution intervals
d. Port definition to locate specific acoustic regions in order to define transfer admittance matrix between the two ports
e. Absorbing fluid element, that is, the extracted fluid volume of the respective models used
e. Solution method set to "Full"
f. Anechoic termination at the outlet
g. Non-reflecting boundary conditions at the inlet and outlet respectively
h. Acoustic pressure of 1 Pascal at the inlet

Topology optimization was done following the steps below;

i. Identification and specification of input parameters that may alter the response. These included the muffler geometry, pressure loading, mesh element size, density, speed of sound, acoustic body sound speed, acoustic body mass density, acoustic body bulk viscosity, acoustic body dynamic viscosity, and acoustic normal surface velocity amplitude of normal velocity.
ii. Identification and specification of output parameters. These are the responses of the system of interest, and included frequency of maximum transmission loss, geometry internal volume, mesh elements, mesh nodes, acoustic sound pressure level, maximum pressure amplitude, maximum input sound power level, average transmission loss, average input sound power level, average return loss, and average absorption coefficient.

iii. Evaluation of parameter sensitivity; individual strengths and correlation with other parameters, curve fitting and adjustment to get optimum parameter combination,

iv. Design of experiments (DOE) by taking the weighted inputs from parameter correlation and distributing sample points optimally within the design space.

v. Curve fitting the DOE results. Response surfaces (indicating relationships between input and output verification points) were used to predict results at any point within the design envelop

vi. Determination of optimum design configuration. These are presented in optimization charts including candidate points, trade-offs, samples, sensitivities, and history.

ANSYS provided two methods of analysis of parameter correlation. These were the Pearson and Spearman correlation analysis. The former was used to measure the degree of relationship between linearly related variables. Assumptions when using the Pearson ***r*** correlation are that both variables should be normally distributed, and that there is a straight-line relationship between each of the two variables besides data being equally distributed about the regression line. The Pearson correlation is referred to as parametric statistical procedure as it relies on the shape of the distribution in the underlying data.

The following formula was used to calculate the Pearson ***r*** correlation:

$$\gamma = \frac{N\sum xy - \sum(x)\,(y)}{\sqrt{N\sum x^2 - \sum(x^2)\ [N\sum y^2 - \sum y^2]}} \qquad (13)$$

where,

r = Pearson ***r*** correlation coefficient

N = number of observations

$\sum xy$ = sum of the products of paired scores

$\sum x$ = sum of x scores

$\sum y$ = sum of y scores

$\sum x^2$= sum of squared x scores

$\sum y^2$= sum of squared y scores

On the other hand, Spearman rank correlation, a non-parametric test, was used to measure the degree of association between two variables. The Spearman rank correlation test does not carry any assumptions about the distribution of the data and is the appropriate correlation analysis when the variables are measured on a scale that is at least ordinal.

The following formula was used to calculate the Spearman rank correlation:

$$\rho = 1 - \frac{6 \sum d_i^2}{n(n^2 - 1)} \qquad (14)$$

ρ = Spearman rank correlation

d_i = the difference between the ranks of corresponding variables

n = number of observations

The assumptions of the Spearman correlation are that data must be at least ordinal and the scores on one variable must be monotonically related to the other variable.

Both the Pearson and Spearman correlation analysis methods were used in evaluating the parameters.

3.3.5 Instrumentation

The following instruments, available at the Aeroacoustics Laboratory in Tottori University in Japan, were used to carry out tests on the prototypes;

1. FFT Hardware

This scientific instrument shown in **Plate 3.6** was used to make acoustic signal measurements within the prototypes. It consists of a number of other complementing units such as the signal generator, amplifier, speaker, multi-channel analyser, and microphones.

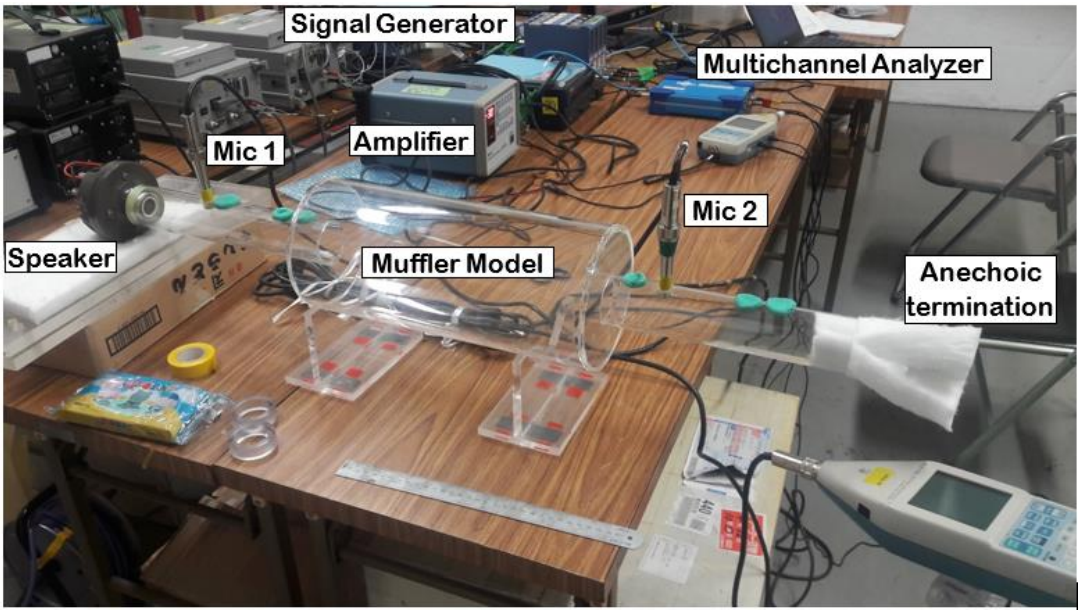

Plate 3.6: FFT Hardware and experimental setup

Appropriate cabling is provided for the interconnection of the various components and to the input and output units, including sound level meters and computer screen.

Four provisions made in the inlet and outlet sections of the muffler prototypes to accommodate insertion of reference and sampling microphones were used as sampling points. After calibration, sampling using two integrating sound level meters was done in two locations at a time, with the rest being plugged using modelling clay. At the inlet there was attached a sound source while at the other end anechoic termination in the form of sound absorbing material was used to plug it off.

Sampling was then taken with the positions of inlet, outlet, and reference microphone locations reversed and real-time data collected. Results were captured through the FFT hardware and software. The necessary transfer function elements were obtained by moving one microphone & using the other as reference. Data collected was then used to determine the overall transmission losses. A detailed procedure of data collection for the determination of transmission loss is provided below.

Transmission loss is a muffler property that is independent of the noise source, and requires an anechoic termination at the downstream end. Anechoic termination is an arrangement that transforms a duct of finite length into an acoustically infinite duct to

provide a non-reflecting condition at the end of the pipe. It involves plugging the end with an acoustic material such as polyester fiber. Transmission loss is the difference between the power level incident on the muffler and that transmitted downstream into an anechoic termination. Basic assumptions made in calculating the transmission loss include the following;

1. The medium is an ideal fluid without viscous properties, and sound waves propagate in the medium without energy loss
2. Sound propagation is an adiabatic process, and there is no heat exchange with the external environment
3. The sound wave propagates in the medium with a small amplitude, and the acoustic field parameters in the medium are first order small quantities, which is described by a linear wave equation.

Method for calculating the transmission loss involved calculation of sound pressure and vibration velocity of the muffler inlet and outlet. Four methods are commonly used to measure the transmission loss of a muffler. These are the transfer function method, acoustic wave decomposition method, the two-sound source method, and the two-load method. The first two measurement methods require that complete noise elimination is achieved at the end of the system. The last two methods do not require sound absorbing materials, but require two measurements. The difference between the two methods is that the former obtains the system parameters based on the characteristics of the sound source generated by the two measurements, whereas the latter obtained the system parameters based on changes in the acoustic impedance conditions at the end of the muffler.

The two-load technique is easy to implement and widely used, and was therefore used in this study. The quadrupole transfer matrix method was used to realize the two independent test states needed to determine the two-port data by changing the loads at the termination instead of moving the sound source to the other end thus generating four equations with four unknowns. The basic setup for laboratory test was as shown in **Figure 3.4** (Damray, et al., 2022).

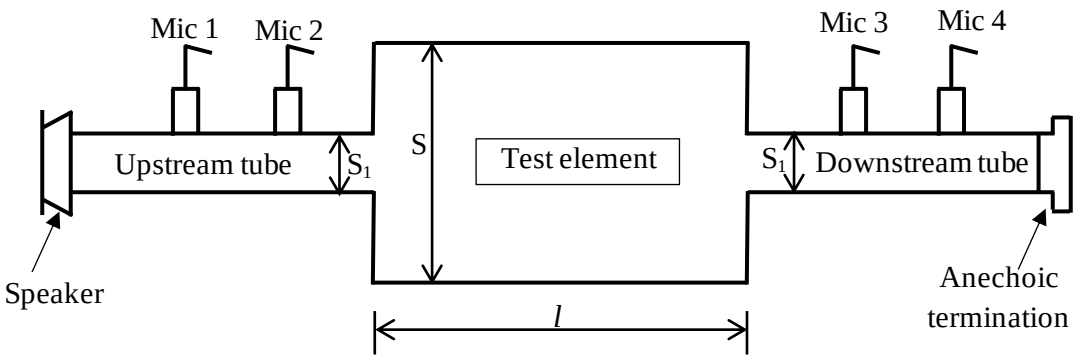

Figure 3.4: Experimental setup for the two-load transmission loss determination

The speaker was connected to a signal generator and a power amplifier in order to provide a monotone sound to the test element. Microphone readings were recorded for positions 1, 2, 3 and 4 through a conditioning amplifier and a multichannel signal amplifier. For non-flow condition, transfer matrix of the test object was determined as follows;

$$\begin{bmatrix} p_1 \\ v_1 \end{bmatrix} = \begin{bmatrix} A & B \\ C & D \end{bmatrix} \begin{bmatrix} P_2 \\ v_2 \end{bmatrix}, \tag{15}$$

where p1 and p2 are the sound pressure of the muffler inlet and outlet respectively, and v_1 and v_2 are the vibration velocity of the muffler inlet and outlet respectively. Transfer matrix parameters in equation (15) are defined as follows;

$$\begin{cases} A = (p_1/p_2)\,]_{v_2=0,\ v_1=l} \\ B = (p_2/v_2)\,]_{p_2=0,\ v_1=l} \\ C = (v_1/p_2)\,]_{v_2=0,\ v_1=l} \\ D = (v_1/v_2)\,]_{p_2=0,\ v_1=l} \end{cases} \tag{16}$$

For the same temperatures at the inlet and outlet of the muffler (in this case the test object) and the same cross-sectional areas of inlet and outlet, the transmission loss obtained by the quadrupole transfer matrix method is as follows

$$TL = 20log\left\{\frac{1}{2}\left|A + B\left(\frac{S_1}{c}\right) + C\left(\frac{c}{S_2}\right) + D\right|\right\} \tag{17}$$

where S_1 denotes the cross-sectional area of the inlet and outlet, and c denotes the sound velocity in the air. The quadrupole transfer matrix may be expressed as;

$$[T] = \begin{bmatrix} cos(kl) & j\frac{c}{S}sin(kl) \\ j\frac{S}{c}sin(kl) & cos(kl) \end{bmatrix} \quad (18)$$

Substituting equation (18) into equation (17), the transmission loss is obtained as defined in equation (7)

4. Integrating Sound Level Meter capable of measuring sound in A-weighting scale and in frequency bands

This instrument was used to determine sound energy over the period under investigation. Appropriate connectors were used to transfer the output in real-time for analysis and eventual storage.

Three different models were used to collect data depending on the location of data sampling. **Plate 3.7** shows the third model used in this research. It is a ½ inch pre-polarized condenser microphone with a preamplifier that is equipped with 1/3 octave band analyser and can be connected to an external data logger. It has a pistonphone calibrator and can measure instantaneous and equivalent continuous sound pressure level. Measurement range is between 10 and 140 dB(A) in 7 ranges, and with frequency range of 20 to 12,500 Hz.

Plate 3.7: RION Integrating Sound Level Meter Model NA-27A

3.3.6 Evaluation of performance of the design

A second major test on the prototype was carried out on the engine test rig and performance characteristics of each model compared with simulation results. Procedures used when testing were as set out in the following sampled standards;

1. **BS ISO 15619:2013** – Reciprocating Internal Combustion Engines: Measurement Method for Exhaust Silencers. Sound Power Level of Exhaust Noise and Insertion Loss Using Sound Pressure and Power Loss Ratio.
2. **ISO 6798-1:2020** Reciprocating internal combustion engines — measurement of sound power level using sound pressure — Part 1: Engineering method.
3. **ISO 6798-2:2020** Reciprocating internal combustion engines — measurement of sound power level using sound pressure — Part 2: survey method.
4. **ISO 11820:1996(E)** Acoustics – Measurements on Silencers in-situ.
5. **ISO 7235:2003(E)** Acoustics – Laboratory Measurement Procedures for Ducted Silencers and Air Treminal Units – Insertion Loss Flow Noise and Tonal Pressure Loss.

3.3.7 Engine test results

Outputs were obtained in form of fabricated acrylic, stainless steel and mild steel models. While the acrylic models were used for bench measurement in no-flow conditions, these were used to output real-time acoustic pressure phase and magnitude values at intervals of centre frequency. These were used to compute transfer matrices and subsequently transmission loss values, results of which are presented in TL verses frequency plots.

For the output from simulation software, data obtained were presented in TL vs frequency plots, and acoustic maps within the fluid volume elements of the models under investigation. Comparison of the two was made to identify trends and differences.

For the models fabricated out of steel, real-time data was collected via integrating sound level meter and plots of sound levels against frequency bands plotted. These were used for comparison with other models to evaluate insertion loss (IL) and Transmission Loss (TL) characteristics of the muffler. While IL was determined by getting the difference between acoustic power levels with and without the muffler installed at the outlet of the exhaust pipe, TL was determined graphically by plotting computed transmission loss values for each of the eight centre frequencies within the 0-2,000 Hz hearing range.

Key design parameters were also determined through simulation in order to achieve a good performance characteristic for the designed engineering solution. Optimization results were also obtained as a function of input and output parameters to satisfy desired performance characteristics.

These parameters were subjected to parameter-correlation analysis (using ANSYS simulation software) to establish the strength of relationship among the variables. These relationships are important in order to identify significant parameters that affect muffler performance and to reduce subsequent computation time by excluding non-significant parameters. One hundred (100) samples were used for the design space with mean value accuracy of 0.01, standard deviation accuracy of 0.02 and convergence frequency set at 10 for both analysis methods.

3.4 Determination of residual noise hazards

Sampling information from the integrating noise level meter were downloaded through the AnalyzerPlus software for analysis of octave bands. Analysis of Variance (ANOVA) was used to establish relationships between and within profile data for the different engine speeds. For the human hearing range of 33.5 to 2,000 hertz, resulting graphs were compared with the threshold of hearing limit and perception limit. The noise characteristics were used to establish whether the resulting exposure would interfere with conversation, and also to give specific indication of the noise component values at different frequencies to define the noise profile.

Comparisons were then made with established permissible exposure limits as defined in the Occupational Safety and Health Act (2007) and the Environmental Management and Coordination Act 2015 to determine whether such limits were exceeded.

3.5 Residual noise hazard mitigation

3.5.1 Use of distance solution

The first step was to define the Noise Reduction design goal by considering the residual noise and specifying the safe noise levels required at the receiver location. Safe noise levels used were based on provisions from the Occupational Safety and Health Act and the Environmental Management and Coordination Act. The two

categories considered were for silent zones (where concentration levels are expected to be high and recognition of acoustic cues critical), and industrial settings (where workers are to be protected against exposure to high noise levels and to ensure that audible warnings can be easily identifiable).

Determination of the location of the receiver using the Noise Reduction value obtained in step 1 by using expression 13.

$$r_2 = r_1 \times 10^{\frac{NR}{20}} \quad (19)$$

where NR = noise intensity level (dB reduced by moving from location 1 to location 2);

r_1 = the distance from location 1 to the sound source;

r_2 = the distance from location 2 to the sound source ($r_2 > r_1$)

Since the intensity of sound decreases with increase in distance, the use of equation 15 provided for computation and determination of the minimum safe distance in order to comply with zoning requirements as provided in the environmental and occupational Acts.

3.5.2 Acoustic barrier in free-field solution

This solution was provided by obstructing the path of travel of the sound waves from the source, thereby resulting in reduction of the noise level at the receiver location. This was achieved by assuming the use of a single barrier 3m high (typical height of an industrial wall) and 6m wide. The barrier insertion loss characteristic (IL) of the acoustic barrier was determined using a procedure developed by Wang, Luo, and Cai (2018) and defined in 3.5.1.1.. The equivalent frequency for the entire noise spectrum within the hearing range was used to determine the barrier attenuation (equation 11).

3.5.3 Hearing protection solution

Octave band analysis data and the residual noise hazards identified in section **3.4** were used to determine hearing protection solution to ensure that those exposed are effectively protected. The Octave Band rating was determined by application of (equation 16) to components of each centre frequency. Selection of the correct hearing protection was done with consideration that over-protection may result in reduced

communication with the working environment or surrounding while at the same time ensuring comfort.

$$Attenuation(dB) = 10log_{10}\sum_{i}^{n} 10^{\left(L_{Ai}/_{10}\right)} + 10^{\left(L_{A(i+1)}/_{10}\right)}..+ 10^{\left(L_{An}/_{10}\right)} \text{ ... (20)}$$

CHAPTER FOUR

RESULTS AND DISCUSSIONS

4.1 Introduction

In this chapter, results obtained from each of the tests conducted are presented and discussed. Comparison with results from other data collection methods was made and observations highlighted. Salient features of the results that relate to occupational safety and health are identified and discussed, with the main aim of minimizing the risks associated with NIHL and industrial accidents.

4.2 Noise profile of a 1500cc VVT-i internal combustion engine

A 1500cc VVT-i IC engine mounted on a stationary rubber-damped stand and subjected to varied engine speed tests gave a distinctive noise profile as presented in **Figure 4.1**.

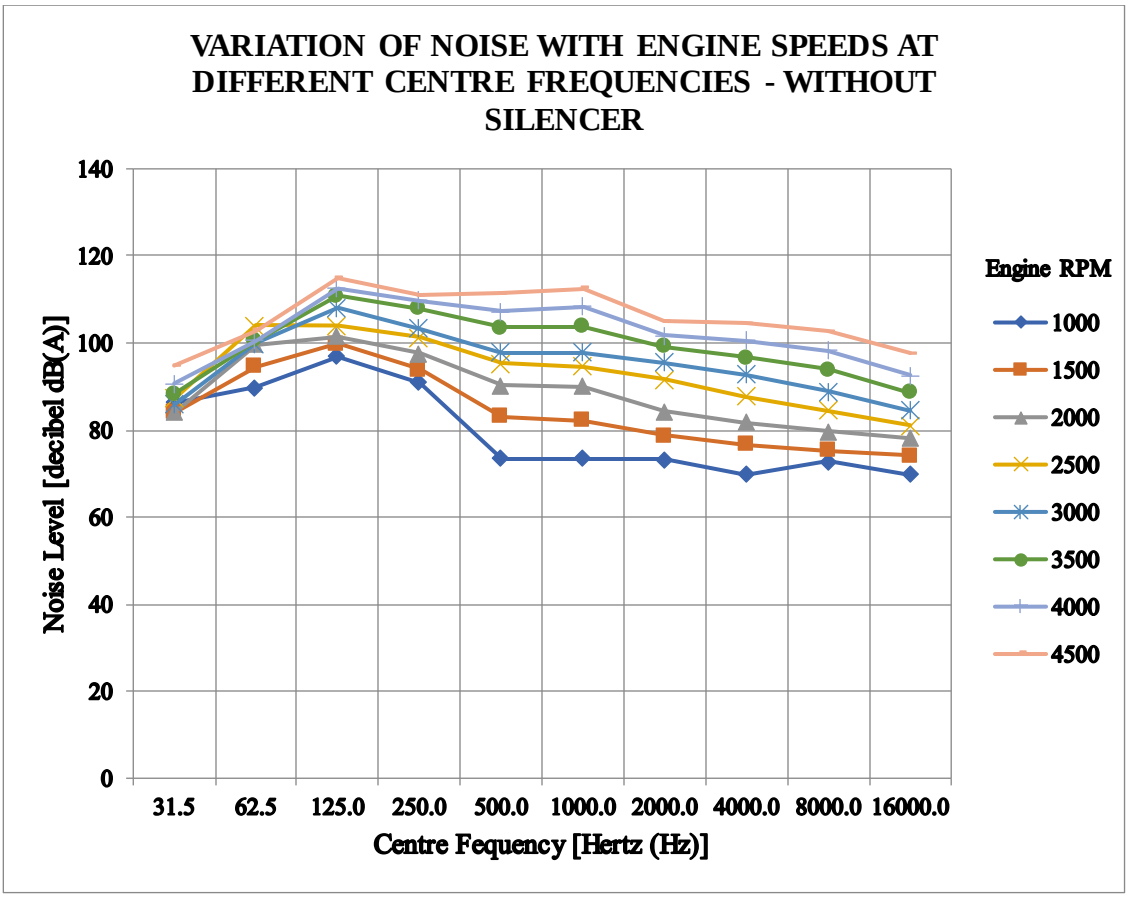

Figure 4.1: Frequency profile of engine noise without silencer

For each of the engine speeds investigated, the general noise spectrum tended to sharply increase from 31.5 to 125 Hz and then gradually decrease at higher frequencies. For all the engine speeds investigated, a maximum noise level was recorded at the center frequency of 125 hertz. This maximum point (125 Hz) indicates a characteristic property of the muffler in which resonance occurs. The occurrence of maximum noise levels at a particular frequency is a good indication that a noise control strategy may be designed around 125 hertz. This makes it a one-size fits-it-all solution that may be employed to flatten the general profile of the noise curves. The most significant change in noise levels throughout the hearing spectrum was observed at 1,000 rpm engine speed, with the lowest noise level [68 dB(A)] occurring at 4,000 Hz and highest [94 dB(A)] at 125 Hz. The 1,000-rpm engine speed is unique in noise profile as it marks the transition between idling (no-load) and loaded (acceleration) condition.

Higher engine speeds tended to give a uniform decrease in noise level, possibly because the wavelength of sound at higher frequencies becomes shorter. It was also observed that the higher the engine speed, the higher the noise levels throughout the hearing frequency range of 20 Hz to 20,000 Hz. This observation is similar to findings by Chaynov et. al., (2018), who carried out experimental and computational analysis of noise levels for different engine speeds of a power plant with an 8-cylinder V-shaped 8CN 12/13 type automobile diesel engine.

Unsilenced internal combustion gasoline engine exhaust noise was found to be broadband with the highest levels occurring at lower frequencies. Similar analysis of engine noise carried out under static condition by Arana et. al., (2022) confirms that engine noise is broadband in nature throughout the hearing frequency range. However, in their case, the engine size was not specified, but the fuel used was hydrogen. The results further indicated that due to high reactivity of the hydrogen fuel, noise levels were high while air pollutants discharged to the environment were reduced compared with those arising from the use of gasoline fuel. For the case of this study, no analysis of combustion products was done as this was outside the scope of research.

Research on levels of noise emanating from biofuels powered engine by Patel et al., (2019) showed that it was possible to obtain lower combustion noise and vibrations. However, biodiesels showed higher carbon monoxide, hydrocarbons and nitrous oxide emissions. In this case, the size of the engine was not fully specified, but indication of the use of a single cylinder engine was presented. From the foregoing discussion, it can be observed that it is possible to reduce noise levels by changing the type of fuel used. However, a decision would have to be made on what to compromise between resulting noise levels and the levels of gaseous pollutants, and particulate matter released to the environment.

For the experimental setup in this research, the values of the average noise levels for the frequency components increases by between 6% and 50% with increase in engine speed. The peak noise level average was 106.1 dB(A) at 125 Hz. At the same frequency of 125 Hz, the unmuffled noise levels at 4,500 rpm was found to be 118 dB(A). Between 500 to 2,000 Hz, the levels of noise were below the action limit of 80 dB(A) while at engine speeds above 1,000 rpm, noise levels were found to be beyond the recommended action limit of 85 dB(A), both determined at a background noise level of 39.2 dB(A). It would therefore be necessary to apply additional controls to protect the worker against exposure to noise at engine speeds beyond 1,000 rpm.

Guidelines provided in the Factories and Other Places of Work (Noise Prevention and Control) Rules 2005 stipulates a peak noise value of 140 dB(A) at any given time. The peak noise obtained at 125 hertz of 106.1 dB(A) was less than the statutory requirement. However, exposure to this noise without any form of protection violates section 4 of the Noise Prevention and Control Rules, 2005. In this section, a threshold limit value of 90 dB(A) exposure for 8-hours in any 24 hours period is permitted. The Rules further specifies in sections 9, 10 and 11 interventions to be taken by the occupier to reduce noise levels and limit its spread. These interventions should include enclosing such a noisy source (in a canopy or using a sound-proof casing configuration), segregation (isolating the machine from workers by enclosing it in a room), and suppression (of the noise at source as done using a muffler or silencer) as engineering controls.

Administrative control interventions stipulated for noise beyond 90 dB(A) include provision of training to workers, comprehensive information to workers on the impacts of exposure to such high noise values, monitoring of noise levels to inform decisions, job rotation to minimize adverse effects hearing protection, and periodic medical examination. In addition, the use of personal and collective hearing protective devices should be implemented. To protect a worker exposed to noise above 90 dB(A), the Act requires the occupier to develop and implement an effective noise control and hearing conservation program, that must be periodically reviewed.

4.3. Development of an innovative inclined barrier

Simulation and experimental data were collected for the basic muffler geometry for comparison with modelling data. Four configurations each of the CIB in a SEC were also modelled and simulated before fabrication and results compared. The following sections present the outcomes.

4.3.1. Simple Expansion Chamber

Simulation results of the simple expansion chamber using ANSYS for frequency range between 0 and 2,000 Hz is as shown in **Figure 4.2**.

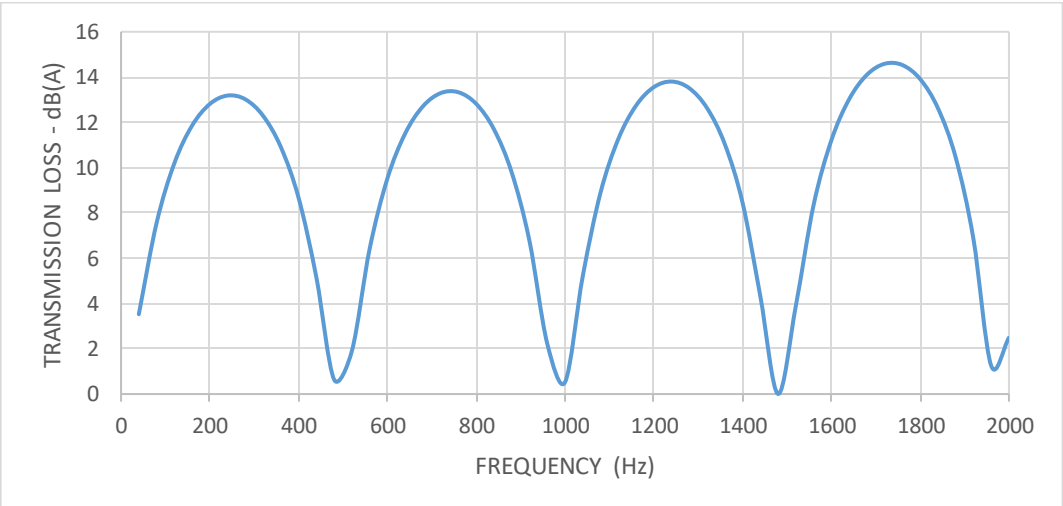

Figure 4.2: Theoretical transmission loss curve for simple expansion chamber

The average transmission loss as determined by equation 7 was found to be approximately 14 dB(A) with peaks and troughs spaced in approximately uniform intervals. The expansion chamber had a predictable TL curve having maxima at $f_c \leq$

(1.84c/πD); where f_c represents frequency, c represents speed of sound, and D represents diameter of the expansion chamber. This is a theoretical indication of plane wave propagation for the frequency range considered that may not be observed in practical applications. When a larger frequency range was analysed – say up to 20,000Hz, a different form of results of transmission loss was observed. Beginning from approximately 2,500Hz, the profile ceases to exhibit a uniform shape and there is a sudden rise or jump in the level of TL, which approaches 50 dB(A). This is an indication that complex pressure fields are at play indicating that wave propagation is not planar anymore and they will not favour acoustic propagation. The wave propagation ceases to be plane wave and becomes three-dimensional. **Figure 4.3** indicates also that beyond this frequency, the profile of the TL-frequency curve was no longer uniform and TL values become fairly high.

These results were in agreement with findings reported by Kalita and Singh (2018). In their study on a simple expansion chamber (length to diameter ratio of 1.3), plane wave propagation was observed for frequency range between 50 and around 2,480 hertz and transmission loss value of 22dB. The onset of complex waves in this case was reported to occur at frequencies above 2,500 hertz.

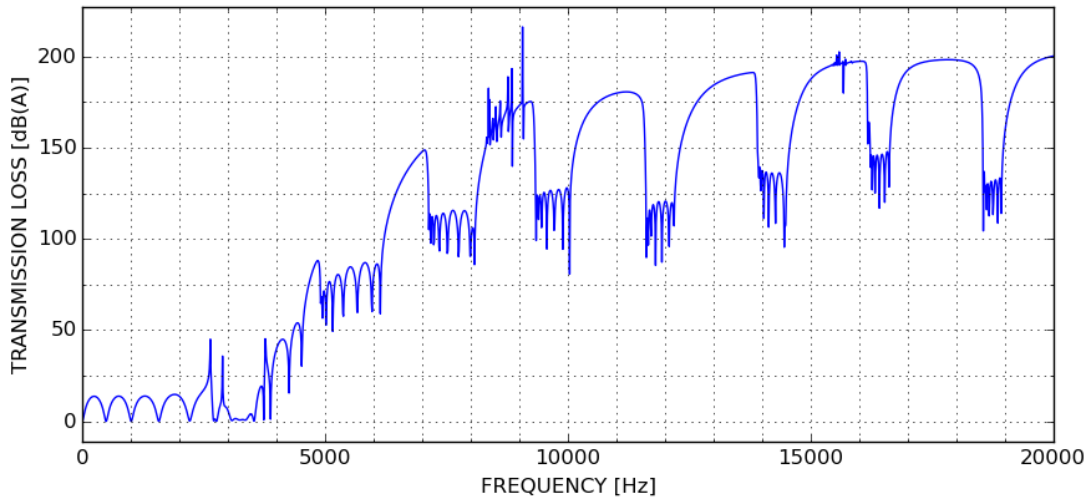

Figure 4.3: Transmission loss characteristics of a Simple Expansion Chamber

Comparison of simulation results of transmission loss characteristics of the simple expansion chamber and elliptic expansion chamber was done by Badya et al., (2011).

These results indicated good performance of the elliptic expansion chamber compared to the simple expansion chamber. The difference in performance was attributed to the position of the exit port on the elliptic expansion chamber (side outlet), and the expansion ratio.

Plate 4.1: Simple Expansion Chamber data collection setup

Plate 4.1 shows experimental setup of data collection for the simple expansion chamber. Results obtained from this setup are as indicated in **Figure 4.4**. Here, it is observed that there is some undesired behaviour at the beginning indicating instability of the plane wave propagation, which stabilizes thereafter. The troughs occur at around 500 and 100Hz similar to that obtained in the simulation result (**Figure 4.2**).

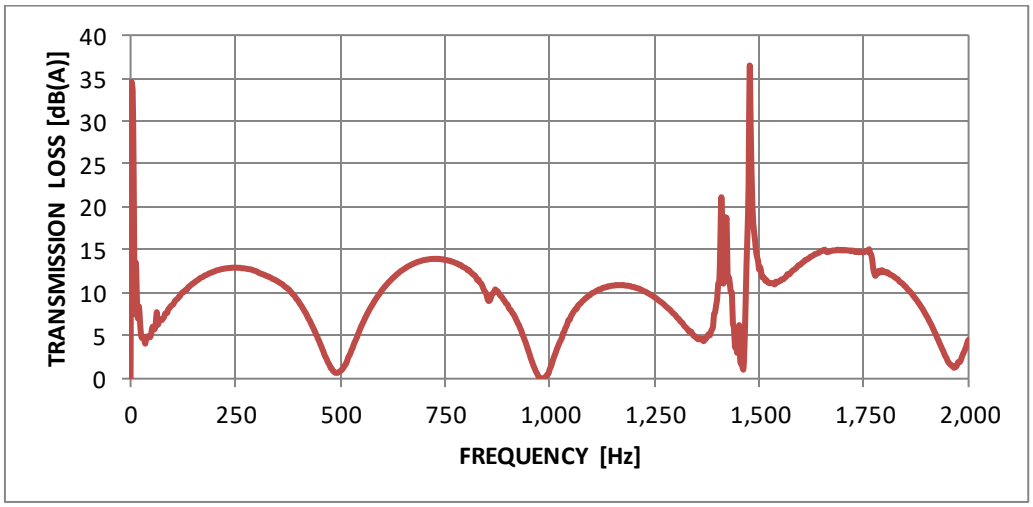

Figure 4.4: Experimental results of Simple Expansion Chamber

Beyond 1,000 Hz, the shape of the TL curve becomes unstable and a TL value of about 36 dB(A) is recorded at about 1,490 Hz. This indicates a cut-on frequency in which

resonance occurs. This is a deviation from the theoretical result obtained from simulation and indicates a point of resonance. **Figure 4.5** shows this comparison.

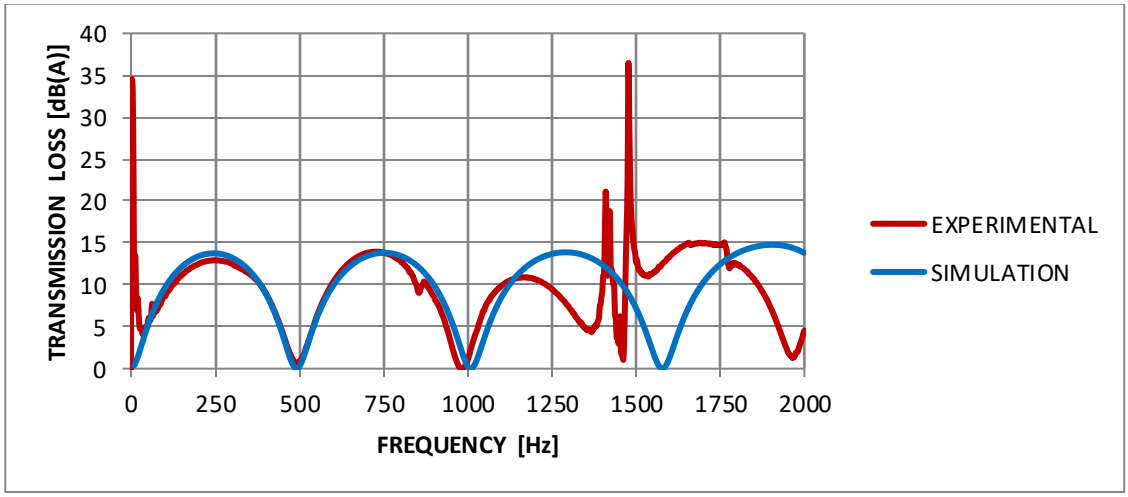

Figure 4.5: Comparison of TL curves for Experimental and Simulation results

Generally, from the results obtained, the critical frequencies are those in the lower range (0 to 2,000 Hz) which are not attenuated with this arrangement. This explains why the SEC is not used for noise attenuation in internal combustion engines. The SEC has been used as a basic structure in the study and development of mufflers and silencers as it provides the fundamentals upon which complex shapes are derived. Further, the low transmission loss values (15dB) obtained from the SEC configuration does not provide sufficient noise reduction for the VVT-i engine noise.

4.3.2. Simple Expansion Chamber with Helicoid

The impact of the modified SEC on sound attenuation was visualized through 3-D acoustic maps of sound pressure fields. These are shown in **Plate 4.2** to **Plate 4.8**. Post processed results of the SEC modified using pitch variations of the helicoid, beginning with a single pitch of 350mm and halving it every other consecutive time (to obtain 175mm, 116mm and 87.5mm respectively), are presented.

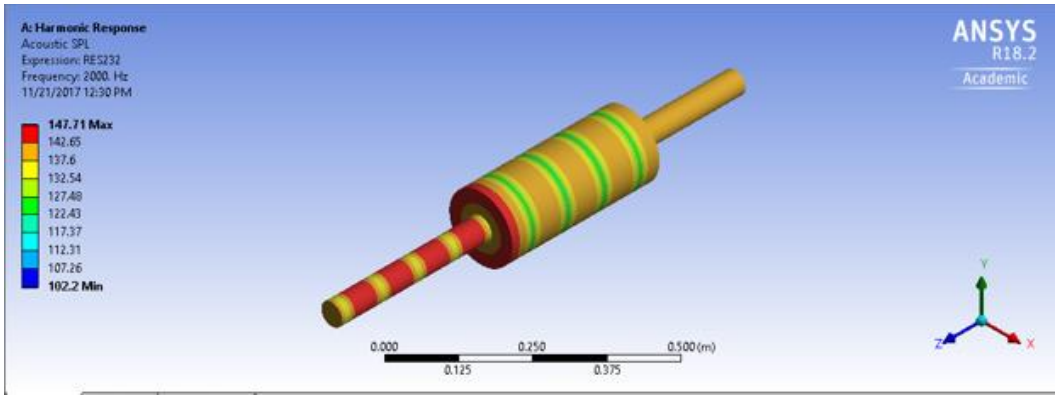

Plate 4.2: Acoustic sound pressure map for SEC

Harmonic response results of the SEC (**Plate 4.2**) give basic harmonic profiles that indicate clearly distinctive regions of high acoustic pressure levels followed by regions of low acoustic pressure levels upstream (on the right) of the expansion chamber. Immediately after the expansion chamber there is a region of high acoustic pressure followed by alternate regions of relatively low and high acoustic pressure levels compared with the upstream results. After the reduction in cross-sectional area a uniform acoustic pressure is observed that corresponds to the high value within the SEC. This arrangement is not suitable for noise attenuation since the sudden changes in cross-sections may result in high back pressure and poor noise attenuation characteristics. Typically, a uniform periodic transmission loss graph is obtained from computational results of the SEC (**Figure 4.2**).

With the introduction of the helicoid within the SEC (**Plate 4.3** to **Plate 4.8**), regions of fairly low acoustic pressure were observed. As the wave propagates downstream, there was a general reduction in acoustic pressure levels with patterns indicating noise cancellation. As the number of turns of the inclined barrier increases from one (350mm pitch) to four (87.5mm pitch), the pattern also modifies to give an overall low acoustic pressure downstream. This phenomenon translates to an improved transmission loss characteristic of the geometry.

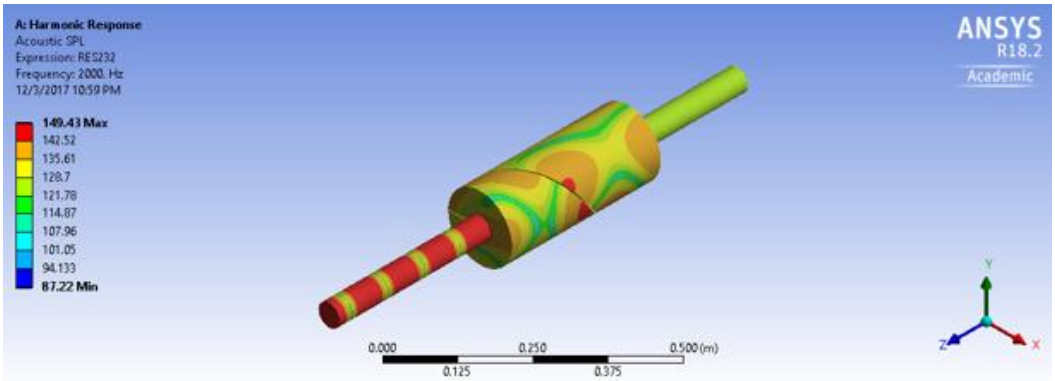

Plate 4.3: Acoustic sound pressure map for 350mm pitch helicoid

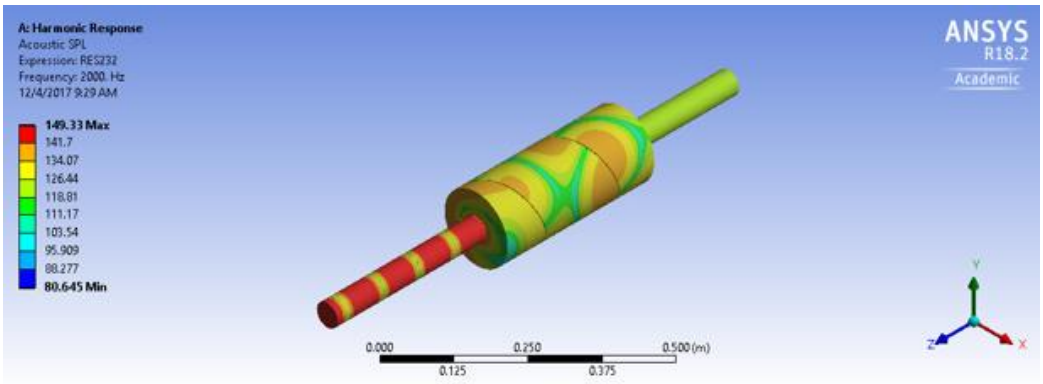

Plate 4.4: Acoustic pressure map for 175mm pitch helicoid

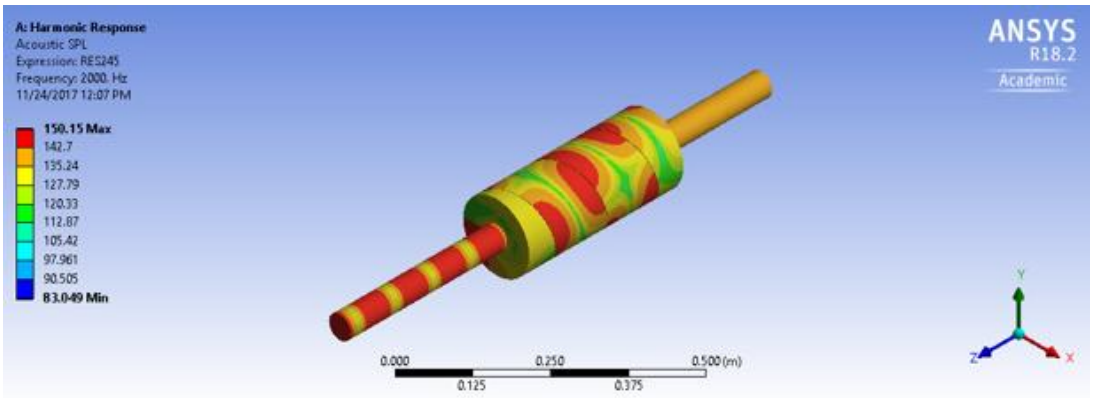

Plate 4.5: Acoustic sound pressure map for 116mm pitch helicoid

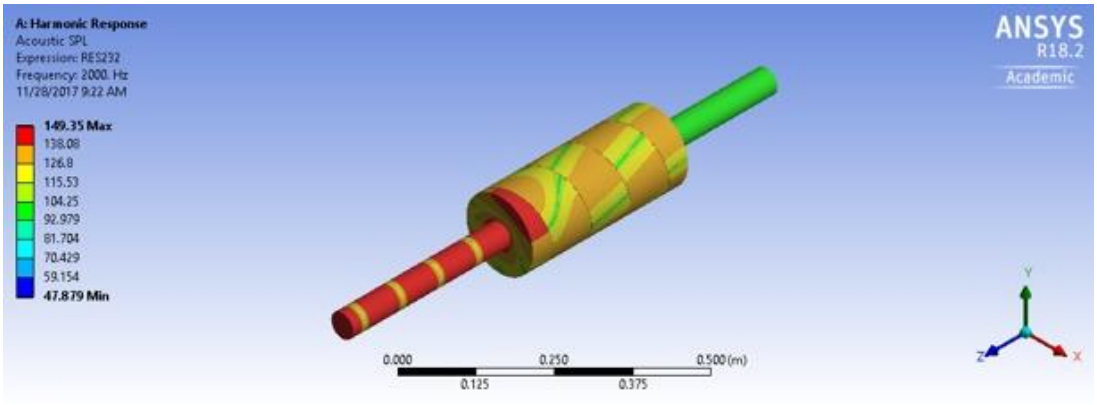

Plate 4.6: **Acoustic pressure map for 87.5mm pitch helicoid**

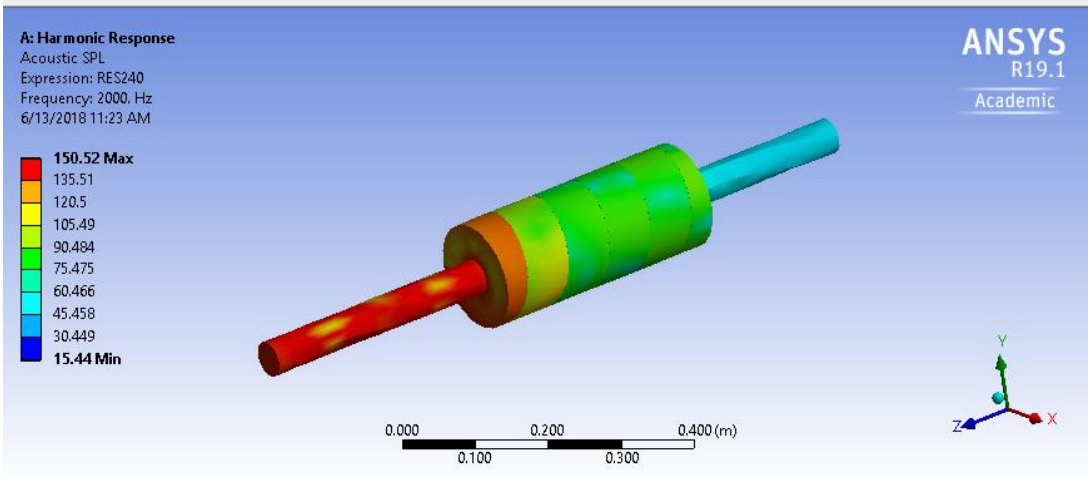

Plate 4.7: Acoustic pressure map for 70mm pitch helicoid

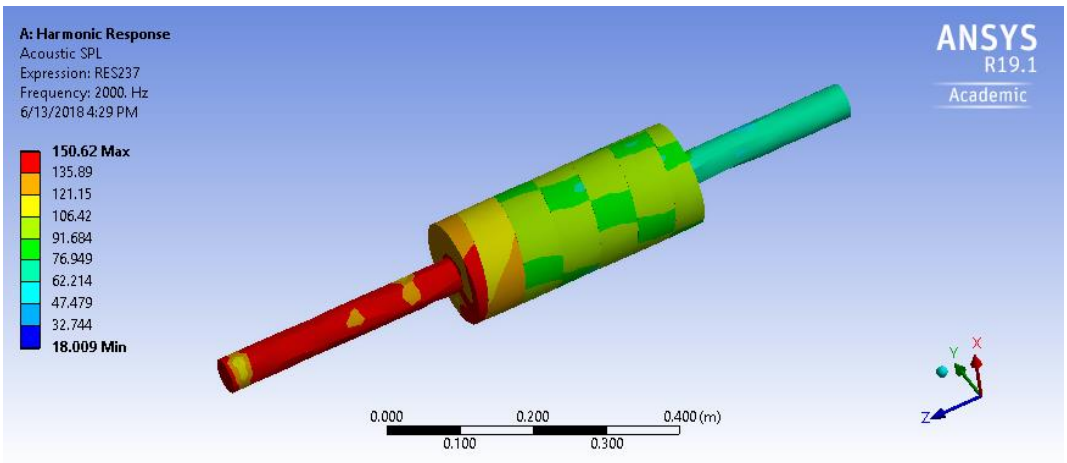

Plate 4.8: Acoustic pressure map for 58.3mm pitch helicoid

From the results, it was observed that the effective parameters along the direction of propagation within the helicoid were dependent on helicity as the pitch varied when other geometric parameters remain constant. This result compares well with findings on helicoidal resonators studied by Lapka (2018). Results of the changes of acoustic propagation properties are demonstrated in **Figure 4.6**.

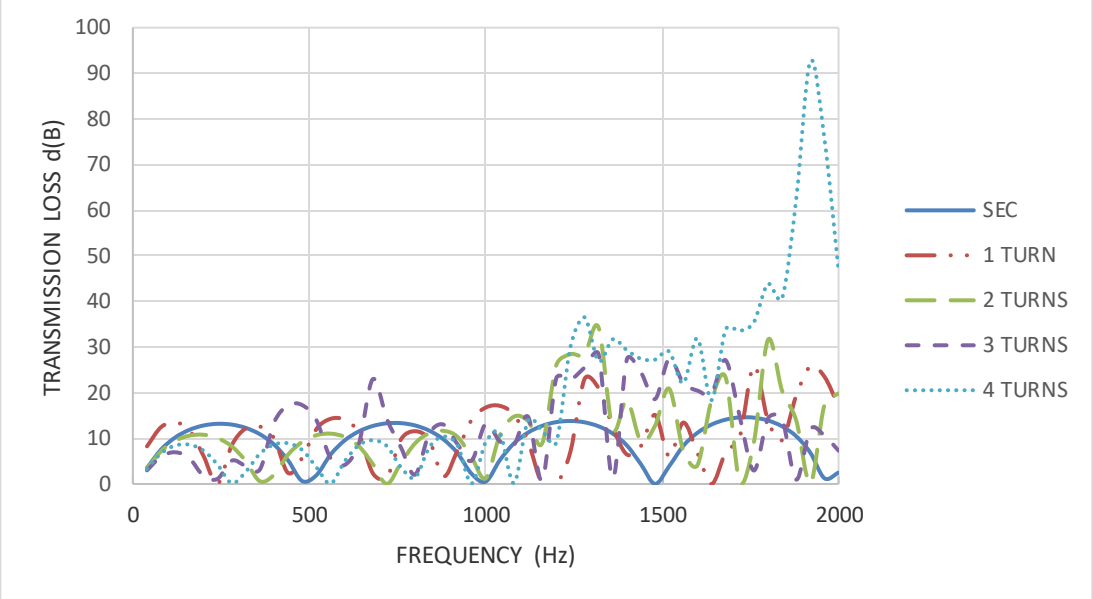

Figure 4.6: Comparison of TL of the four helicoidal pitch configurations

Comparisons of transmission loss versus frequency for the four geometric configurations of the helicoid in a SEC under study are presented in **Figure 4.6**. The plots are indicative of the transmission loss as a function of natural frequency for models with 350mm (1 turn), 175mm (2 turns) and 87.5 mm pitch (4 turns) and the loss is a minimum when the natural frequency matches with the frequency of the source. This is in comparison with TL results of the simple expansion chamber (Onyango et al., 2017). For model with 116mm pitch (3 turns), a different behaviour is observed where the TL is almost a minimum at frequencies of about 240; 1,360; and 1,860 Hz. In between these values the minimum TL values are not a function of the natural frequency. Also, up to about 1,200Hz, most of the noise from the source is limited to the firing frequency and its first few harmonics. At around 1,920Hz, the TL value for the 4 turns model reached 93dB(A) representing a cut-on duct mode for circular duct of order 2. This shows good performance at the given frequency.

TL values from the simulation results indicates an average of 15 dB for model with 350mm pitch, 12 dB for model with 175mm pitch, and 10 dB for model with 87.5mm pitch. Compared with the simple expansion chamber that exhibits 13 dB transmission loss, there is a general decline in the TL values as more turns are used. This is a unique finding of this configuration. It can also be observed that the number of natural frequencies decrease for models with 175mm and 116mm pitches while those of models with 350mm and 87.5mm pitch remain five. However, these could be improved by further redesign or modification of the geometry. It is also possible to get higher values of transmission loss at higher frequencies.

At lower frequencies, results of the models show plane wave propagation characterized by uniform and periodic shape of the transmission loss graph. This can also be seen in the pressure field map of respective models downstream and upstream of the expansion chamber (**Plate 4.3** to **Plate 4.8**). At higher frequencies however, complex pressure fields are formed indicating that wave propagation is not planer anymore and thus will not favour acoustic propagation. This is indicated in the pressure field map in the simple expansion volume by the different pressure levels with the different colour shades. An interpretation of this on the transmission loss graph is the high transmission loss values that follow the plane wave propagation profile on the graphs.

Local pressure and density of air will impact local speed of sound and consequently modify acoustic propagation through the duct as presented by equation 4.

$$c(x) = \sqrt{\gamma RT(x)} \tag{21}$$

$$c(x) = \sqrt{\frac{\gamma p(x)}{\rho(x)}} \tag{22}$$

Also, a mean flow velocity modifies the acoustic wave propagation when the second term in the numerator the expression in equation 23 varies due to energy scattering into neighbouring modes occasioned by an incident propagating mode.

$$\lambda(x) = \frac{c(x) \pm v_o(x)}{f} \tag{23}$$

Results confirm that the models are effective in low frequency bandwidth. This result compares well with findings on the study of reactive mufflers by Xue and Sun (2018). The cutoff frequency of the design is approximately 1,240 Hz based on equation 23. A further analysis was done for the SEC with the helicoidal pitch equal to the ratio of the expansion chamber to the diameter of the inlet/outlet pipe (350/50). Here, all other parameters remained as in the reference model as illustrated in **Figure 4.7**.

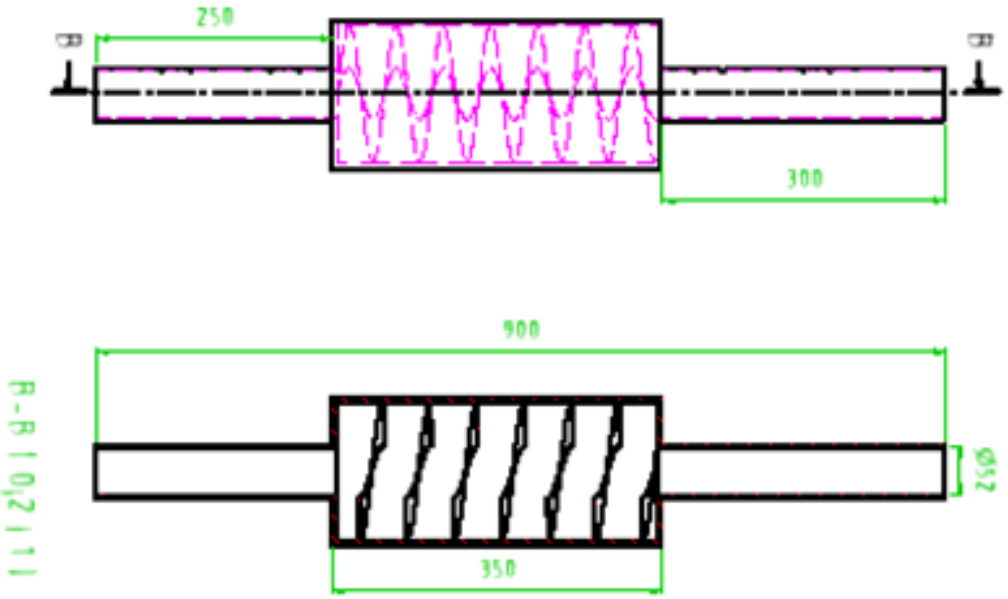

Figure 4.7: Layout of the SEC with helicoid pitch of 50mm

Acoustic pressure map for this arrangement (**Plate 4.9**) yielded the following unique pattern of alternating low acoustic pressures after every two successively high pressure, and a ring of relatively low pressure (approximately 113dB(A)) radially disposed between the hollow section and the wall of the expansion chamber. A section of the muffler confirms this. This very interesting phenomena resulted in a final exit acoustic pressure of about 142dB(A). The exit acoustic pressure value of 142dB(A) is higher than the engine maximum of 118dB(A), and therefore does not represent a reduction as anticipated of a muffler.

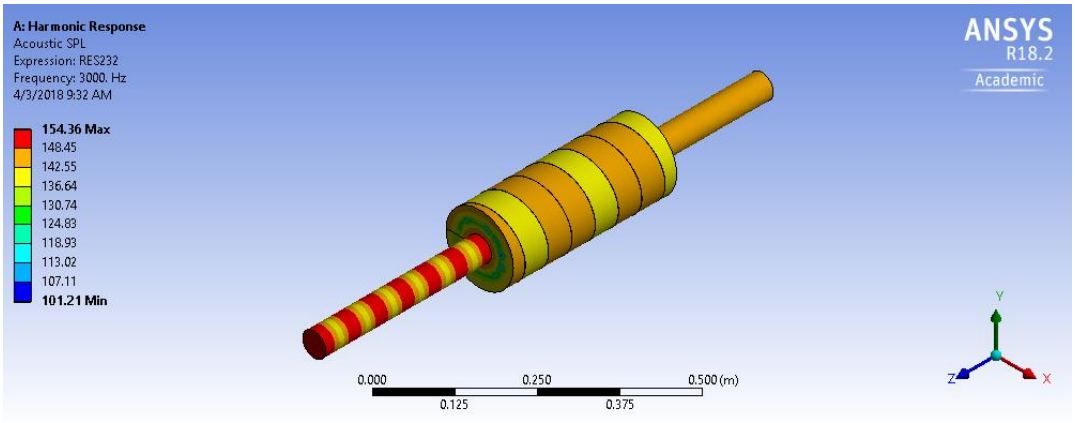

Plate 4.9: Acoustic pressure map for SEC with 50mm pitch helicoid

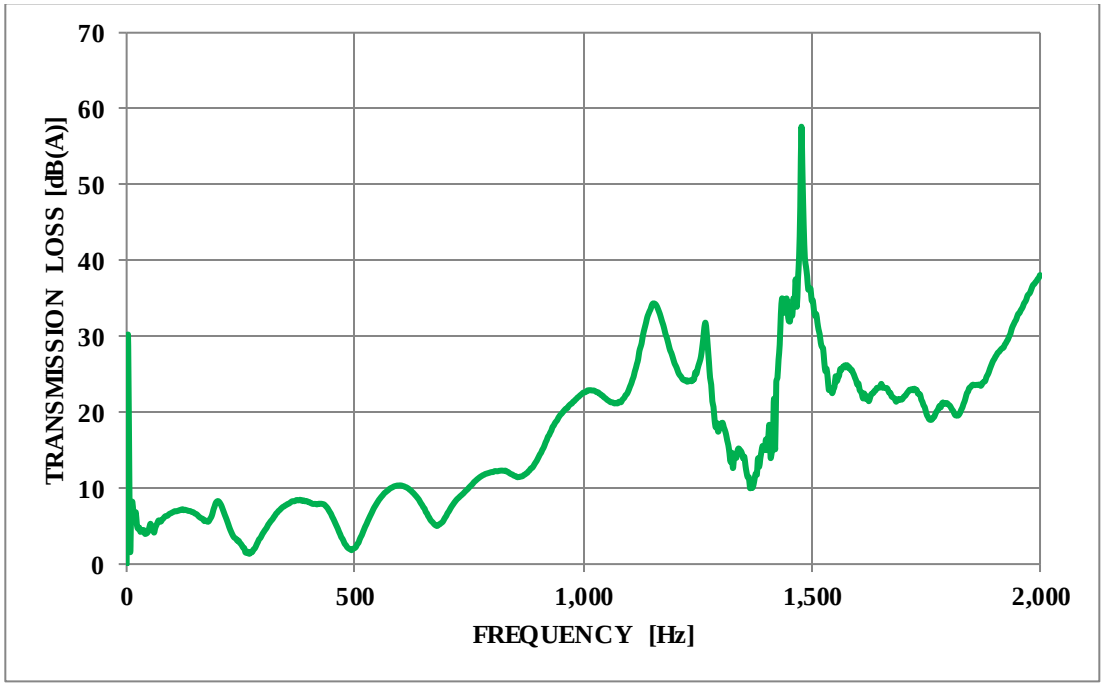

Figure 4.8: Transmission Loss curve for SEC with 50mm pitch helicoid

Plane wave propagation was experienced in the frequency range between 200 and 700 Hz above which 3-D wave propagation set in. Resonance occurred at about 1,450 Hz with a maximum of about 60 dB(A) being recorded. This is presented in **Figure 4.8**. The occurrence of resonance indicates that, if well harnessed, the phenomena lead to high transmission loss that is desirable in achieving an overall reduction of noise.

4.3.3. Simple Expansion Chamber with Helicoid and Central Tube

Comparison of Acoustic plots of Models without and with the central tube arrangements are as shown in **Figure 4.9.**

S.NO.	MODEL A – WITHOUT TUBE	MODEL B – WITH TUBE
1.	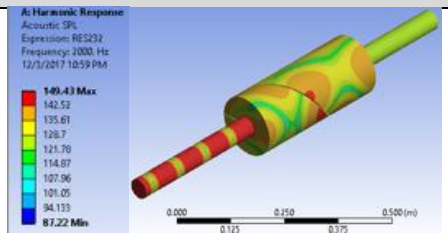 Model 1a	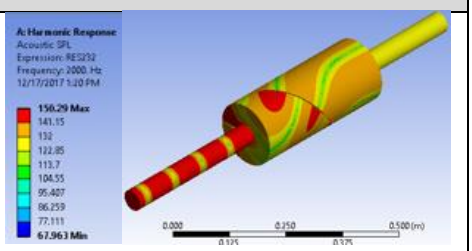 Model 1b
2.	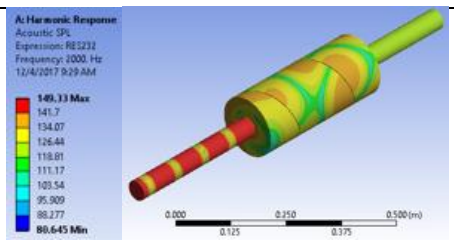 Model 2a	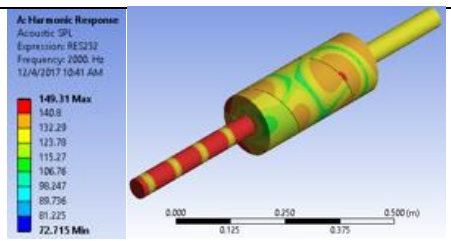 Model 2b
3.	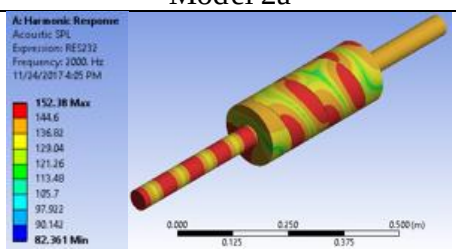 Model 3a	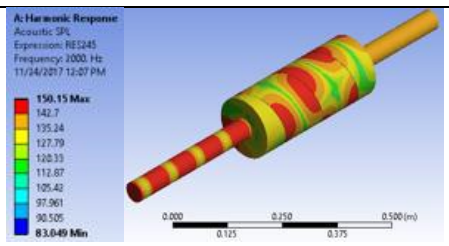 Model 3b
4.	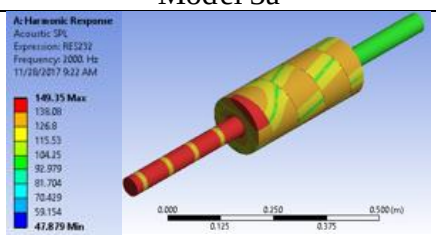 Model 4a	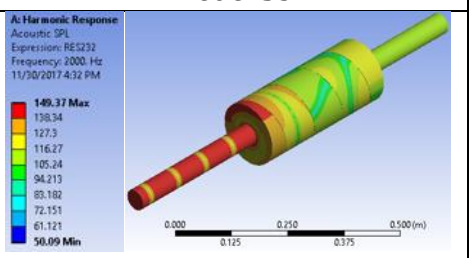 Model 4b

Figure 4.9: Acoustic pressure maps for models with and without central tube

The results of the acoustic pressure maps in **Figure 4.9** show plots of the real part of the acoustic pressure in order to visualize resonance observed in the TL plot for each of the models evaluated (Model A column 1 and Model B column 2). These are

distinctly different in configuration from those observed for the SEC. The helicoid introduces a torsional effect in the regions of low and high acoustic pressures, thereby accounting for the different profiles of the TL's. In these models, the influence of the helicoid is caused by centrifugal effects of the vortex that results in pressure drops and acoustic power dissipation giving rise to a dipole sound field. Model 1A exhibits characteristics of plane wave propagation up to about 1,200 Hz where 3D acoustic wave propagation starts. TL is a maximum at about 1,300 Hz. In comparison with Model 1B, 3D acoustic wave propagation is experienced after 400 Hz with maximum TL occurring at around 900Hz. These TL variations are illustrated in **Figure 4.10**.

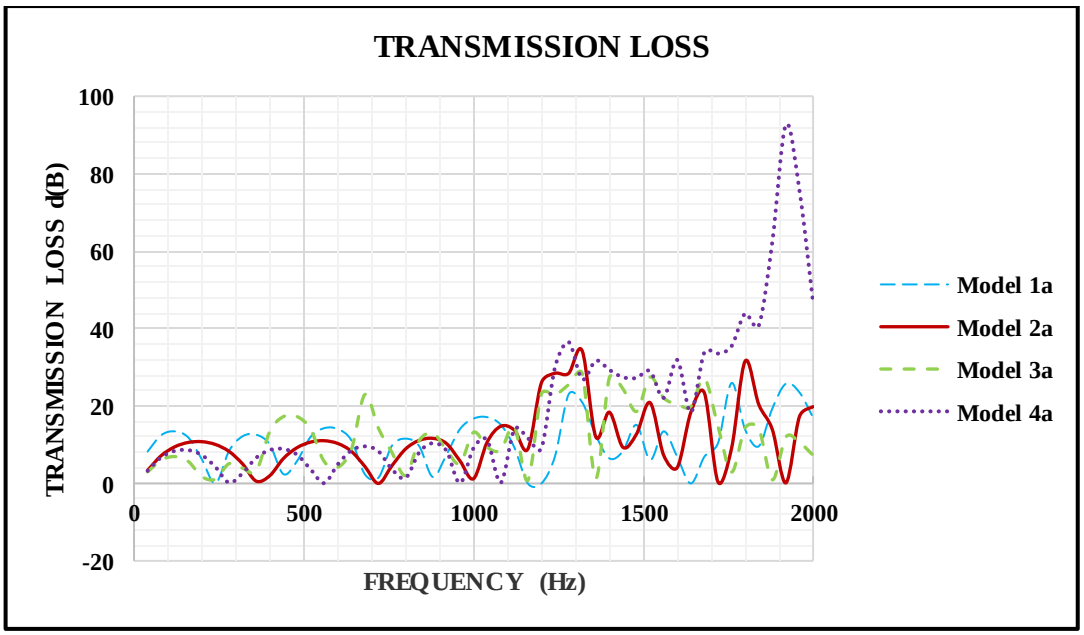

Figure 4.10: Transmission loss of helicoid without central tube

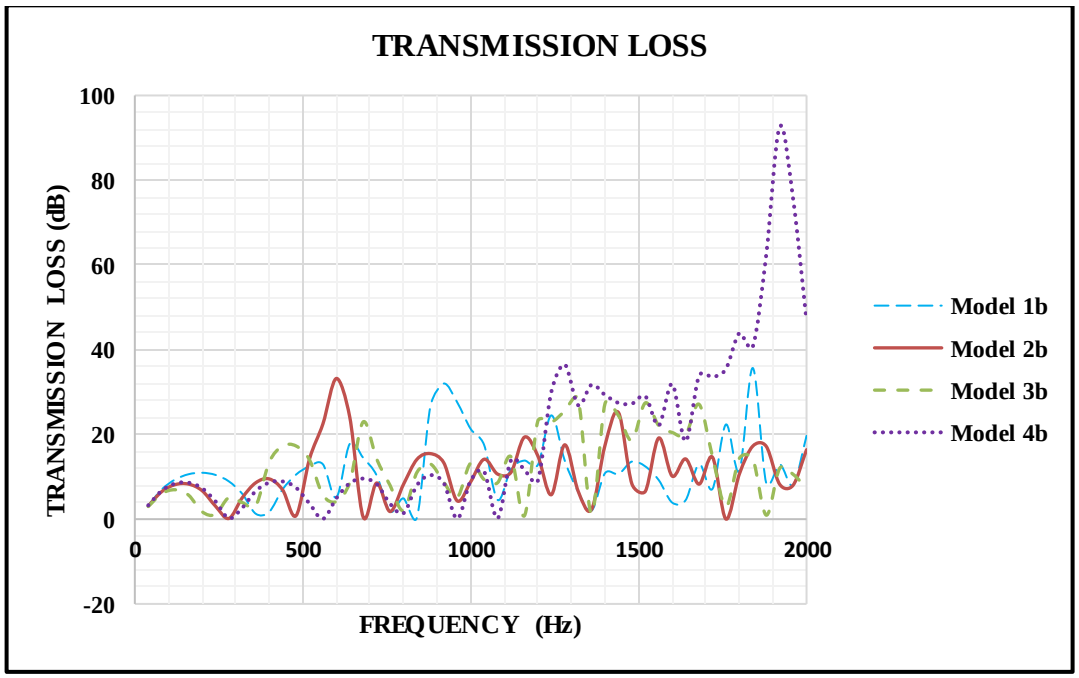

Figure 4.11: Transmission loss of helicoid with central tube

For Model 2A, a sudden spike in the value of TL sets in at about 1,150 Hz while for Model 2B (**Figure 4.11**), this occurs much early at 600 Hz. For Model 3A, the sudden spike in the value of TL is observed at 700 Hz while for Model 3B this occurs at about 450 Hz. For these three sets of models, effects of 3D wave propagation are experienced much earlier with the central tube in place as compared with when the tube is not included. Both models 4A and 4B exhibit the same characteristics where effects of 3-D wave propagation set in at about 1,400 Hz with a maximum TL of 92 decibels occurring at 1,900 Hz. A broadband attenuation is observed for Model 4 for frequency range between 1,400 Hz to 1,900 Hz. However, the similarities in TL characteristics do not reflect in the acoustic pressure maps, but the geometries with and without the central tube appear to produce the same TL characteristics.

With the introduction of the helicoid within the SEC, regions of fairly low acoustic pressure are observed throughout this section. As the wave propagates downstream, there is a general reduction in acoustic pressure levels with patterns indicating noise attenuation. As the number of turns increases from one to four, the pattern also modifies to give an overall low acoustic pressure downstream. This phenomenon

translates to an improved transmission loss characteristic of the geometry. The effective parameters along the propagation direction within the helicoid are dependent on helicity as the pitch varies when other geometric parameters remain constant.

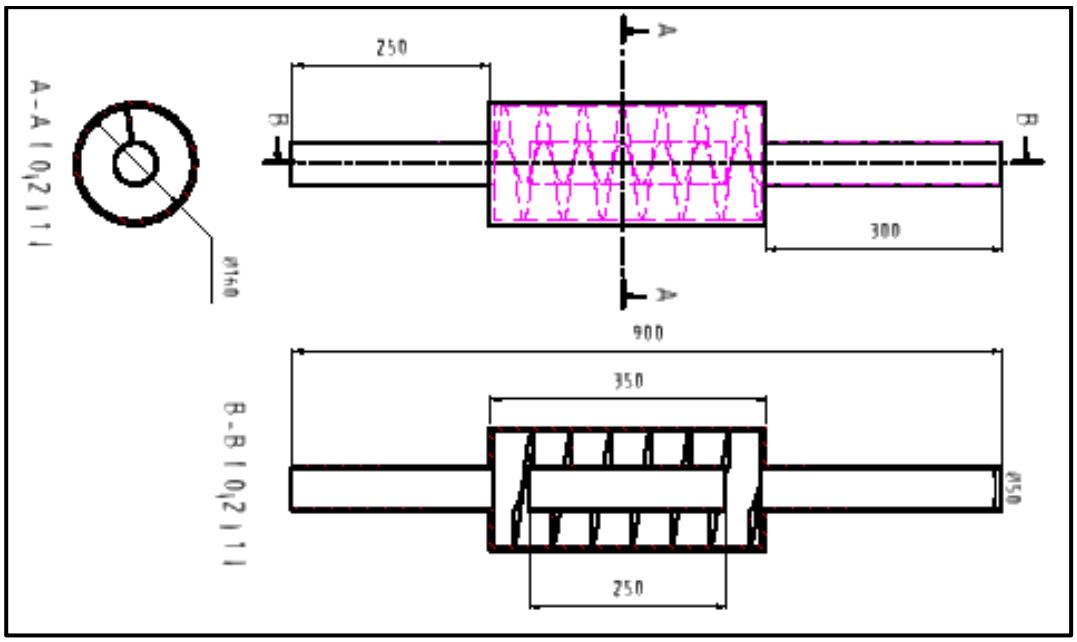

Figure 4.12: Geometry of the SEC with 50mm pitch helicoid and central tube

Data was collected for frequencies between 0 and 2,000 Hz since it is at this range where the impact of engine noise is significant. Data obtained from the experimental setup were used to compute transmission loss using the transfer matrix method as proposed by Mohamad, Jalics, and Kermani (2019).

The data obtained from the experiments conducted were tabulated and used for the analysis of the performance of the SEC with helicoid, and SEC with helicoid and Central tube (**Figure 4.12**).

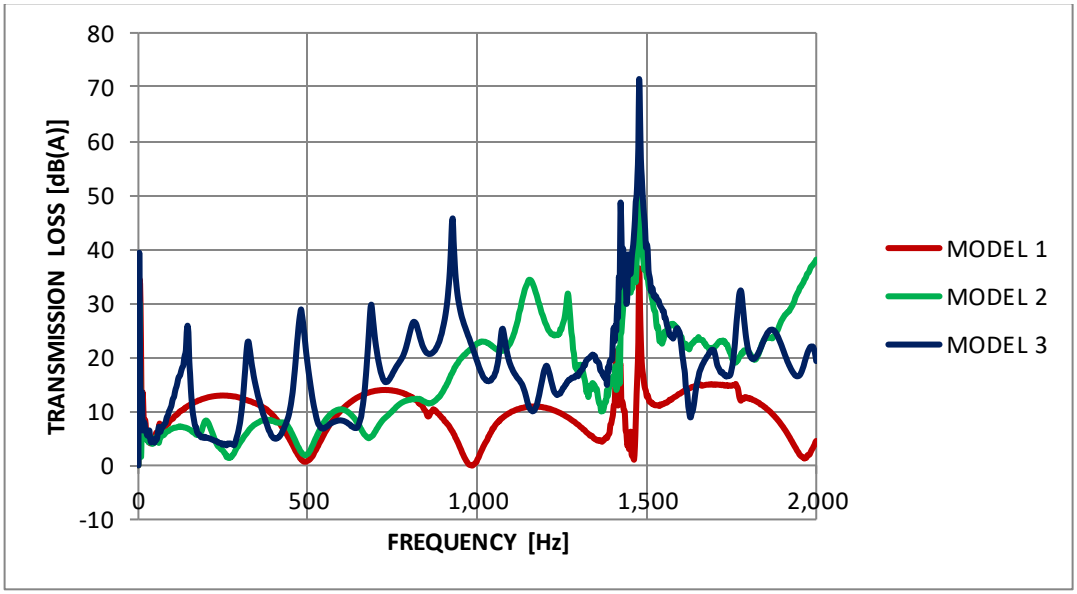

Figure 4.13: Comparison of Transmission Loss of the SEC 50mm pitch with and without central tube

Comparing the results in **Figure 4.13**, it is evident that a common resonance frequency occurs at approximately 1,490 Hz. The helicoid within the expansion chamber gave lower values of transmission loss compared with the other two configurations. With improvement of the internal geometry by insertion of a cylindrical pipe through the helicoid, the value of TL improved from an average of about 8 to 28 decibels for the range of frequencies of interest. Peak frequencies f_a of Model 3 are defined by the expression

$$f_a = \frac{nc}{2(L_h - L_s)} \qquad (24)$$

where L_h = length of the helicoid path, and

L_s = length of the inner straight pipe

n = 1,2,3, *(representing successive peaks)*

These peaks occur by superposition of the sound waves propagated through both paths.

Transmission loss value results of the simple expansion chamber measurements were compared with theoretical values (computed from equation 7) and this showed good correlation especially at lower frequencies (**Figure 4.13**). Typically, such results are valid for plane wave propagation, in this case up to about 1,000 Hz. Results compare

well with findings of other researchers such as Gupta and Mathur (2015), and Jena and Panigrahi (2017) who have used the SEC as the basic unit for comparison with result outputs of modeling and design. The TL for the SEC is slightly below 15 decibels, but a good muffler would be one in which this value is as high as possible.

It can also be observed from **Figure 4.13** for both experimental and simulation results that, up to 1,000 Hz, transmission loss is a maximum for frequency (f_b) corresponding to the following condition;

$$f_b = \frac{(2n-1)c}{4L} \tag{25}$$

where c = speed of sound,

L = length of expansion chamber, and

n = 1, 2, 3, ….

It is also observed that TL is a minimum for frequencies corresponding to half multiples of the maximum frequency

$$f_c = \frac{nc}{2L} \tag{26}$$

The spikes around 1,400 Hz correspond to the cut on frequency of the first circumferential mode of the expanded duct given by

$$f_d = \frac{0.586c}{D}, \tag{27}$$

where D = diameter of the expansion chamber

The spike indicates higher transmission loss value that is desirable for noise attenuation. The higher this value the better the performance of the muffler.

4.4 Performance of the innovative inclined barrier silencer design

Insertion loss performance of the fabricated model of muffler 4b configuration subjected to tests on a stationery engine is presented. Outputs of this exercise for engine speeds from 1,000 rpm to 4,500 rpm in steps of 500 rpm are represented in **Figure 4.14**. There was a clear distinction in the frequency distribution pattern for noise emitted with and without the silencer. Engine exhaust noise varied significantly with increase in engine speed for both cases, with noise levels generally reduced when the designed silencer was connected.

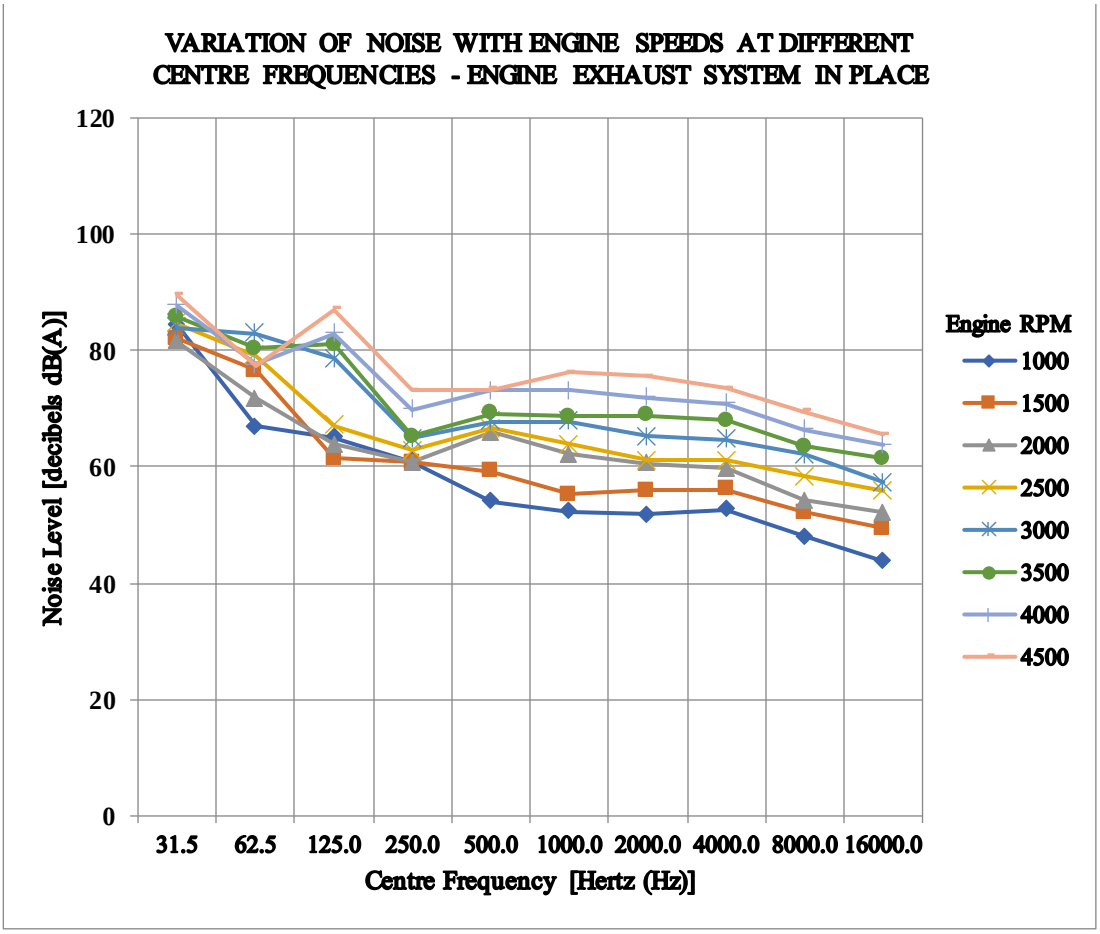

Figure 4.14: Frequency profile of engine noise with muffler 4b

At lower engine speeds (≤ 2,500 rpm), the average noise profile acquired decreasing trend between 31.5 and 125 Hz while for higher engine speeds (≥ 2,500 rpm) results indicated a spike in average noise levels at 125 Hz center frequency before decaying thereafter – observations being made with the silencer in place. This spike illustrated in **Figure 4.14** showed that acoustic resonance of the exhaust noise at higher engine speeds occurred at a low frequency of 125 Hz, which was within the low frequency range of 20 – 2,000 Hz.

The noise level for the arrangement with the exhaust system in place was also observed. The peak average noise level was found to be 84.9 dB(A) at a frequency of 31.5 Hz while that without the exhaust system the peak average noise level was 106.1 dB(A) at 125 Hz. At the same frequency of 125 Hz, the unmuffled noise level at 4,500 rpm was found to be 118 dB(A) which was way beyond the recommendation for the

conservation of hearing as set out in the Occupational Safety and Health Act of 2007. The former (noise level with model 4b model) was just about the upper action limit while the latter was beyond the recommended action level of 85 dB(A), both determined at a background noise level of 39.2 dB(A). Flow rate varied with engine speeds and ranged between 8.45ms^{-1} at 1,000 rpm to 10.9ms^{-1} at 2,500 rpm with a peak of 11.2ms^{-1} recorded at 1,500 rpm.

The results indicate that exposure to unmuffed engine noise exceeded set threshold limit value of 90 dB(A), and this could result in noise-induced hearing loss. It would therefore not be healthy to operate the engine without muffling. In addition to muffling, noise above threshold limit value was realized, which required additional layers of control. Though the fabricated model 4b was able to reduce the noise levels to below 90 decibels, significant levels were observed with engine speeds above 2,500rpm at 125 hertz. Ideally, operation of the VVT-i engine beyond the 3,000rpm mark leads to excessive vibration, which contributes to higher noise levels at 125 hertz as observed in **Figure 4.14**. The vibration of the engine as a result of operation at speeds above 2,500rpm and the increase in noise levels also indicate that 125 hertz indicate a point of resonance frequency of the engine. In order to develop engineering interventions to minimize noise, actions around this frequency should be avoided.

Comparison of results obtained in **Figure 4.1** with results of **Figure 4.14** for engine operating at 4,500rpm and at 125 Hz Centre frequency indicates an insertion loss value of 31.0 dB(A). This implies that by simply introducing the new design to the unmuffed engine, noise is reduced by 31 decibels. This property (insertion loss) is one of the basic parameters used to evaluate performance of a muffler in addition to the transmission loss that is dependent on the internal design of the muffler.

4.4.1. Design parameters optimization

Optimization results for the SEC were obtained through an iterative process presented in the following illustrations from ANSYS software. This is a step further after harmonic response analysis of the various configurations of the muffler as presented in section **4.2** and **4.3** above.

Illustration in **Figure 4.15** shows a typical project schematic in ANSYS in which the harmonic Response Parameters for the model have been fully defined, updated, and results obtained.

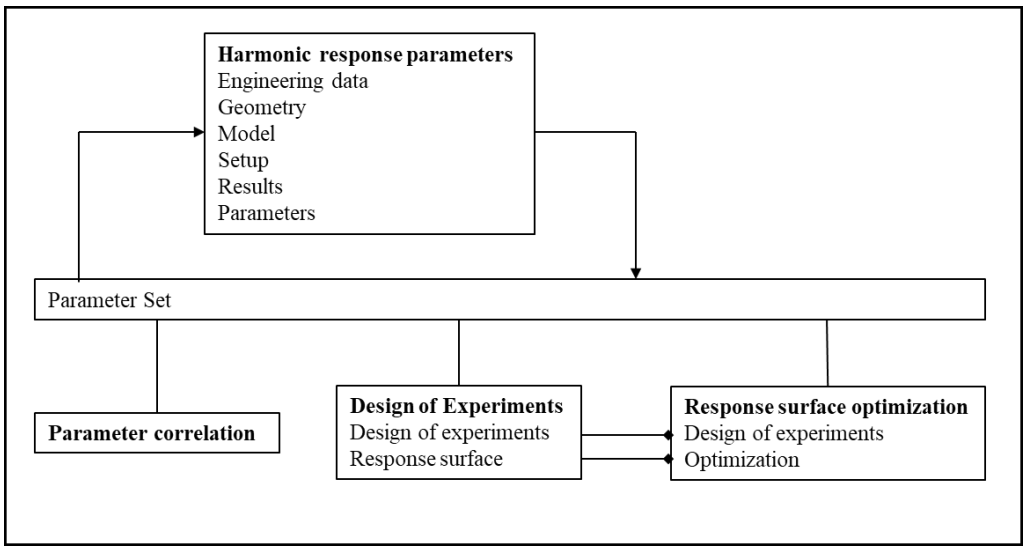

Figure 4.15: Project schematic for the SEC parameter optimization

The schematic also indicates the relationship between the input and output parameters and the link between these parameters and properties including Parameter Correlation, Response Surface and Six Sigma Analysis. Each of these are covered in details in the following sections.

The first step in Parametric Correlation started with eight (8) input parameters and twelve (12) output parameters as indicated in **Table 4.1**. The output of this relationship is a quadratic determination matrix that identifies the strength of linkage of input and output parameters.

Table 4.1: Harmonic response input and output parameters of the SEC

Input Parameters		Output Parameters	
Identifier	Description	Identifier	Description
P1	Density	P4	Acoustic Power Result Plot Frequency of Maximum TL
P2	Speed of Sound	P5	Acoustic Power Result Plot Maximum TL

P6	Acoustic Body Sound Speed	P8	Geometry Volume
P7	Acoustic Body Mass Density	P10	Mesh Elements
P9	Mesh Element Size	P11	Mesh Nodes
P12	Acoustic Body Bulk Viscosity	P15	Acoustic Sound Power Level (SPL) Maximum
P13	Acoustic Body Dynamic Viscosity	P16	Acoustic Time-Frequency Plot Maximum Pressure Amplitude
P14	Acoustic Normal Surface Velocity Amplitude of Normal Velocity	P17	Acoustic Power Result Plot Frequency of Maximum Input Sound Power Level
		P18	Acoustic Power Result Plot Average TL
		P19	Acoustic Power Result Plot Average Input SPL
		P20	Acoustic Power Result Plot Average Return Loss
		P21	Acoustic Power Result Plot Average Absorption Coefficient

From **Table 4.1**, the following observations are made;

i. Increase in any of the input parameters has a corresponding positive increase in the geometry volume (P8) and the frequency of maximum input sound power level (P17)

ii. All the other output parameters (P4, P5, P10, P11, P15, P16, P18, P19, P20 and P21) are insignificantly affected by variations in the input parameters.

A detailed comparison of relationships between input and output parameters is presented in a quadratic determination matrix in **Figure 4.16**.

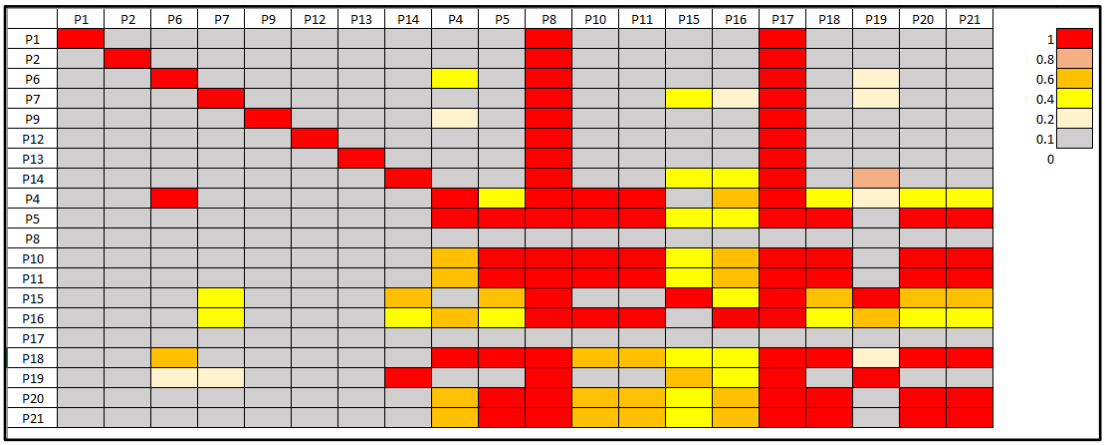

Figure 4.16: Quadratic determination matrix for the SEC

Other than determination matrix obtained from the parameter correlation tool, additional relevant aspects to help identify input parameters deemed to be unimportant including correlation matrices, correlation scatter plots, and sensitivity charts were obtained. These are identifiable as computational results in **Table 4.2**. The correlation matrix shown in **Table 4.2** indicates there is strong positive relationship (+1) between P6, P9 and P14 input parameters showing best relationship against output parameters P4, P5 and P8 respectively. Though equally significant, the impact of P7 and P1 on P16 and P5 respectively are not as strong.

Table 4.2: Additional computational results of parameter correlation tool

1.	Filtering Method	
2.	Relevance Threshold	0.5
3.	Configuration	Filtering on Correlation Value and R2 Contribution, with a maximum of 5 major input parameters
4.	Filtering Output Parameters	P4 – Acoustic Power Result Plot Frequency Of Maximum TL, P5 – Acoustic Power Result Plot Maximum TL, P8 – Geometry Volume, P10 – Mesh Elements, P11 – Mesh Nodes, P15 – Acoustic Sound

		Power Level (SPL) Maximum, P16 – Acoustic Time-Frequency Plot Maximum Pressure Amplitude, P17 – Acoustic Power Result Plot Frequency of Maximum Input Sound Power Level, P18 – Acoustic Power Result Plot Average TL, P19 – Acoustic Power Result Plot Average Input SPL, P20 – Acoustic Power Result Plot Average Return Loss, P21 – Acoustic Power Result Plot Average Absorption Coefficient		
5.	Major Input Parameters				
6.		Best Relationship with Filtering Output Parameter			
7.	Input Parameters	Relevance	Output Parameter	R2 contribution	Correlation Value
8.	P6 – acoustic Body Sound Speed	1	P4 – Acoustic Power Result Plot Frequency of Maximum TL	0.36944	0.7357
9.	P9 – Mesh Element Size	1	P5 – Acoustic Power Result Plot Maximum TL	0.087867	0.29642
10.	P14 – Acoustic Normal Surface Velocity	1	P8 – Geometry Volume	1	1

	Amplitude of Normal Velocity				
11.	P7 – Acoustic Body Mass Velocity	0.96842	P16 – Acoustic Time-Frequency Plot Maximum Pressure Amplitude	0.20352	0.57457
12.	P1 – Density	0.92101	P5 – Acoustic Power Result Plot Maximum TL	0.068647	-0.25262

Major and minor parameters with impacts on relationships with filtering output parameters are presented in **Table 4.3**.

Table 4.3: Major and Minor input parameters for the SEC model

1.	Filtering Method	
2.	Relevance Threshold	0.5
3.	Configuration	Filtering on Correlation Value and R2 Contribution, with a maximum of 5 major input parameters
4.	Filtering Output Parameters	P4 – Acoustic Power Result Plot Frequency of Maximum TL, P5 – Acoustic Power Result Plot Maximum TL, P8 – Geometry Volume, P10 – Mesh Elements, P11 – Mesh Nodes, P15 – Acoustic Sound

		Power Level (SPL) Maximum, P16 – Acoustic Time-Frequency Plot Maximum Pressure Amplitude, P17 – Acoustic Power Result Plot Frequency of Maximum Input Sound Power Level, P18 – Acoustic Power Result Plot Average TL, P19 – Acoustic Power Result Plot Average Input SPL, P20 – Acoustic Power Result Plot Average Return Loss, P21 – Acoustic Power Result Plot Average Absorption Coefficient		
5.	Major Input Parameters				
6.		Best Relationship with Filtering Output Parameter			
7.	Input Parameters	Relevance	Output Parameter	R2 Contribution	Correlation Value
8.	P6 – Acoustic Body Sound Speed	1	P4 – Acoustic Power Result Plot Frequency of Maximum TL	0.36944	0.7357
9.	P9 – Mesh Element Size	1	P5 – Acoustic Power Result Plot Maximum TL	0.087867	0.29642
10.	P14 – Acoustic Normal Surface Velocity	1	P8 – Geometry Volume	1	1

	Amplitude of Normal Velocity				
11.	P7 – Acoustic Body Mass Velocity	0.96842	P16 – Acoustic Time-Frequency Plot Maximum Pressure Amplitude	0.20352	0.57457
12.	P1 – Density	0.92101	P5 – Acoustic Power Result Plot Maximum TL	0.068647	-0.25262
13.	Minor Input Parameters				
14.		Best Relationship with Filtering Output Parameter			
15.	Input Parameters	Relevance	Output Parameter	R2 Contribution	Correlation Value
16.	P2 – Speed of Sound	0.82089	P11 – Mesh Nodes	0.16207	0.19922
17.	P13 – Acoustic Body Dynamic Viscosity	0.77673	P5 – Acoustic Power Result Plot Maximum TL	0.041176	-0.040239

18.	P12 – Acoustic Body Bulk Viscosity	0.69174	P20 – Acoustic Power Result Plot Average Return Loss	0.039751	-0.079025

From the Pearson correlation analysis results, a medium association (+0.41227) was observed between P6 and P19 that was not evident with the spearman correlation. In addition, a higher association (+0.53774) was observed between P6 and P4 confirming observations made with the Spearman analysis method. A weak negative correlation (-0.15343 and -0.15409) of output parameters P20 and P21 resulting from the influence of input parameter P6 was observed. This implies that increasing P6 decreases P20 and P21. This is a sharp contrast to the observation made from the Spearman analysis. Essentially, this difference may have resulted in the accuracy associated with the number of samples used for each of the methods and the assumptions made of the distribution of data.

P14 was found to have a negative and large association with P19 (-0.80277) and P15 (-0.61523), implying that increase of P14 leads to a corresponding decrease of P19 and P15. This observation was not the case with the Spearman analysis results.

Table 4.4: Pearson parameter correlation matrix

		Output parameters											
		P4	**P5**	**P8**	**P10**	**P11**	**P15**	**P16**	**P17**	**P18**	**P19**	**P20**	**P21**
Input parameters	**P1**	-0.08534	-0.25262	0	-0.01793	-0.01672	-0.09205	0.131652	0	-0.24954	0.047944	-0.2557	-0.25538
	P2	0.045959	-0.04908	0	0.147002	0.147057	-0.01531	-0.06308	0	-0.04742	-0.02461	-0.00584	-0.0057
	P6	**0.53774**	-0.10585	0	-0.1554	-0.15494	-0.09907	0.095708	0	-0.04215	**0.412273**	-0.15343	-0.15409
	P7	0.018331	-0.01101	0	0.058745	0.058897	**0.572205**	0.439229	0	-0.00896	0.380362	-0.0178	-0.01759
	P9	-0.26341	-0.24226	0	-0.18712	-0.18652	-0.16496	0.170882	0	-0.25249	-0.08639	-0.23286	-0.23405
	P12	-0.07937	-0.05593	0	-0.06501	-0.06459	-0.03903	0.047857	0	-0.06004	-0.03397	-0.07902	-0.07882
	P13	0.040816	-0.04024	0	0.107773	0.107899	-0.01987	-0.04261	0	-0.0354	0.009496	-0.01375	-0.01352
	P14	-0.03023	-0.03331	0	0.009299	0.009124	**-0.61523**	-0.46179	0	-0.03624	**-0.80277**	-0.00524	-0.00578

Table 4.5: Spearman correlation parameter analysis matrix

		Output parameters											
		P4	**P5**	**P8**	**P10**	**P11**	**P15**	**P16**	**P17**	**P18**	**P19**	**P20**	**P21**
Input parameters	**P1**	-0.11638	-0.11758	0.01316	-0.08554	-0.08554	-0.07865	0.160087	0.01316	-0.12766	0.039728	-0.15372	-0.15289
	P2	0.006122	0.010043	0.025022	0.010946	0.010946	-0.03905	-0.01765	0.025022	-0.00351	-0.05383	-0.04306	-0.04309
	P6	**0.735696**	**0.665294**	0.023278	-0.04177	-0.04177	-0.10176	0.031008	0.023278	**0.744292**	0.396512	**-0.76095**	**-0.7602**
	P7	-0.01177	0.35786	-0.04889	-0.05289	-0.05289	**0.571243**	**0.57457**	-0.04889	0.119542	0.36684	-0.39394	-0.39477
	P9	-0.18573	-0.21346	-0.00628	-0.19416	-0.19416	-0.1615	0.105529	-0.00628	-0.20973	-0.07881	-0.11577	-0.11797
	P12	-0.06935	-0.08834	-0.03129	-0.04404	-0.04404	-0.03196	0.035708	-0.03129	-0.09155	-0.03546	0.010711	0.011379
	P13	-0.00825	0.000965	0.010699	-0.02643	-0.02643	-0.00022	0.00914	0.010699	0.009388	0.034595	-0.0066	-0.00408
	P14	-0.05549	-0.02758	0.066852	-0.01048	-0.01048	**-0.61896**	**-0.57432**	0.066852	-0.05487	**-0.80169**	-0.02892	-0.02992

Input parameters P2, P12 and P13 had insignificant impact on the output parameters. This is true for the Spearman correlation analysis method as well.

From the Spearman correlation analysis results, strong and positive correlation was established between input parameter P6 and the following output parameters;

i. P18 (+0.744292)
ii. P4 (+0.735696)
iii. P5 (+0.665294)

This implies that increasing input parameter P6 increases parameters P18, P4 and P5. This is a very important relationship that ensures that maximum transmission loss is achieved thereby contributing to the desired noise reduction.

In contrast, a strong and negative correlation (-0.76095 and -0.7602) exist between P6 and P20 and P21 respectively, implying that increasing P6 decreases P20 and P21.

From the foregoing discussion and observations, the major input parameters were identified as P6 and P14 while the significant output parameters that affect muffler performance were P5, P14, P15, P18, P19, P20 and P21. Their relationships in summarized form are presented in **Table 4.6** and **Table 4.7**.

Table 4.6: Pearson correlation matrix - major parameters

	P4	**P5**	**P15**	**P18**	**P19**	**P20**	**P21**
P6	**0.53774**	-0.10585	-0.09907	-0.04215	0.412273	-0.15343	-0.15409
P14	-0.03023	-0.03331	**-0.61523**	-0.03624	**-0.80277**	-0.00524	-0.00578

Table 4.7: Spearman correlation matrix - major parameters

	P4	**P5**	**P15**	**P18**	**P19**	**P20**	**P21**
P6	**0.735696**	**0.665294**	-0.10176	**0.744292**	0.396512	**-0.76095**	**-0.7602**
P14	-0.05549	-0.02758	**-0.61896**	-0.05487	**-0.80169**	-0.02892	-0.02992

Input parameter P14 is represented as having the same impacts to output parameters P15 and P19 for both analysis methods, such that as the magnitude of parameter P14 increases, parameters P15 and P19 decreases.

In order to improve results of Spearman correlation analysis, the sample size was increased to 200 in order to achieve convergence. However, the optimization results did not vary much from those obtained with 100 samples. The new Spearman correlation matrix with 200 samples is shown in **Table 4.8**.

Table 4.8: Spearman correlation matrix with 200 sample points

		Output parameters											
		P4	**P5**	**P8**	**P10**	**P11**	**P15**	**P16**	**P17**	**P18**	**P19**	**P20**	**P21**
Input parameters	**P1**	-0.030880	-0.056808	-0.008762	-0.026954	-0.052552	-0.028004	0.076333	-0.008762	-0.055642	0.035613	-0.062994	-0.062628
	P2	0.008343	-0.000364	0.031142	0.031096	0.030690	0.007005	0.015509	0.031142	-0.012954	0.002712	-0.030506	-0.031194
	P6	**0.774446**	**0.683729**	-0.001454	-0.062884	-0.044596	-0.077830	0.018186	-0.001454	**0.778435**	0.393141	**-0.741957**	**-0.741692**
	P7	-0.001537	0.385187	-0.005471	-0.024402	-0.023650	**0.620534**	**0.614239**	-0.005471	0.139051	0.420442	-0.419904	-0.419968
	P9	-0.076595	-0.097501	0.013275	-0.057910	-0.023166	-0.062657	0.076824	0.013275	-0.094037	-0.015476	-0.137011	-0.138196
	P12	0.012312	0.009214	-0.049550	0.000555	-0.015605	0.021856	0.015147	-0.049549	0.004341	0.006752	0.032631	0.032598
	P13	0.045383	0.032835	0.006330	0.062400	0.092444	0.021527	-0.068016	0.006330	0.051122	-0.000440	0.055968	0.056827
	P14	-0.033696	-0.055750	0.013318	-0.005988	0.014895	**-0.632694**	**-0.608797**	0.013318	-0.051069	**-0.802578**	-0.019586	-0.019843

Global sensitivity

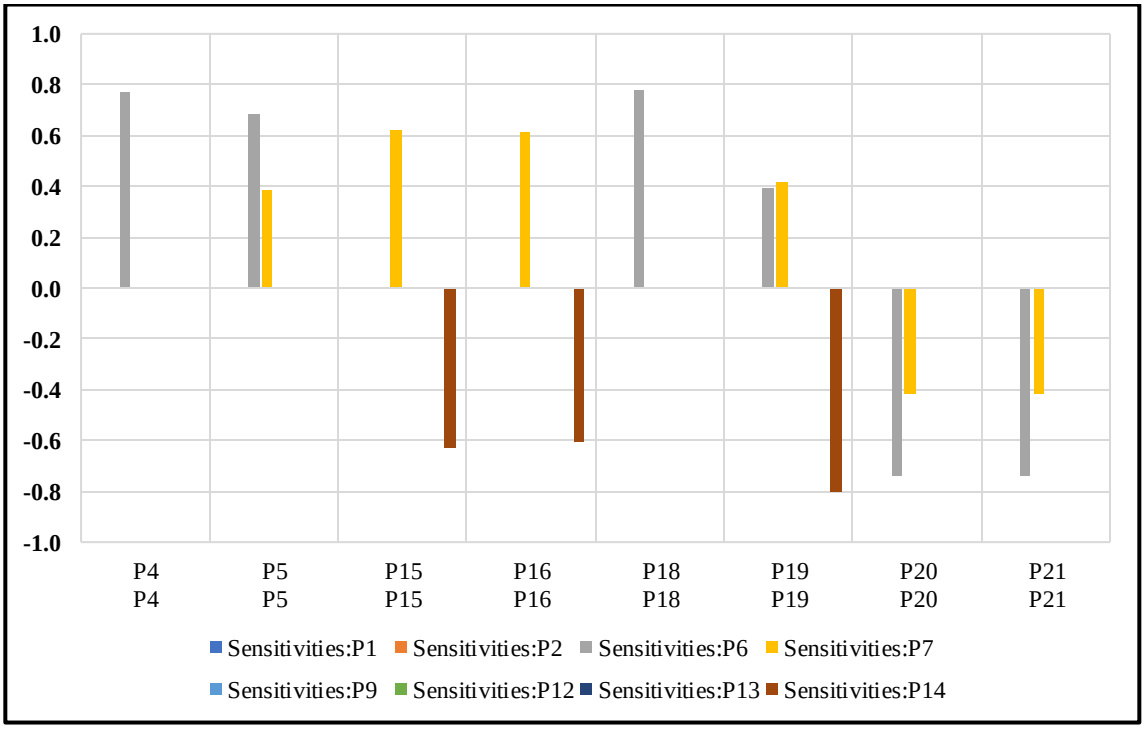

Figure 4.17: Global sensitivity chart for the SEC model

From **Figure 4.17** and **Figure 4.19**, it may be noted that a positive sensitivity of about +0.75 indicates that increasing P6 increases P4 and P18, while a negative sensitivity of about -0.75 indicates that increasing P6 decreases P20 and P21 (**Figure 4.20** and **Figure 4.21**). In addition, increasing P14 (sensitivity of -0.8) decreases P19 as observed in **Figure 4.22**. These statistical sensitivities are based on the Spearman Rank Order Correlation coefficients that take both those aspects into account at the same time.

Correlation Scatter Charts

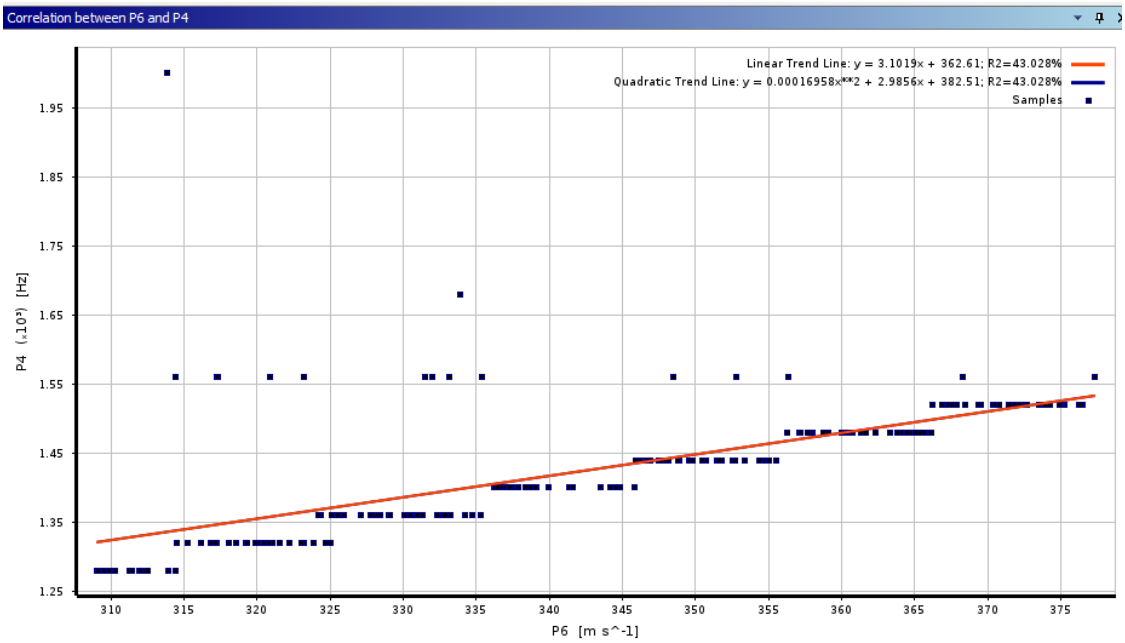

Figure 4.18: Correlation between parameter P6 and P4

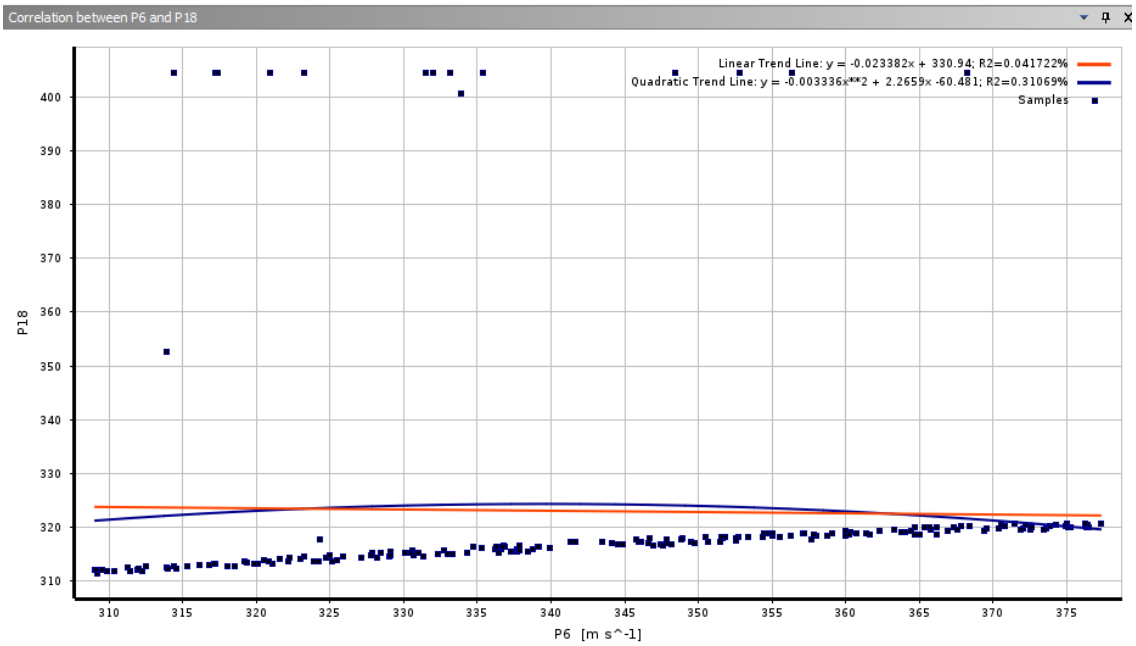

Figure 4.19: Correlation between parameters P6 and P18

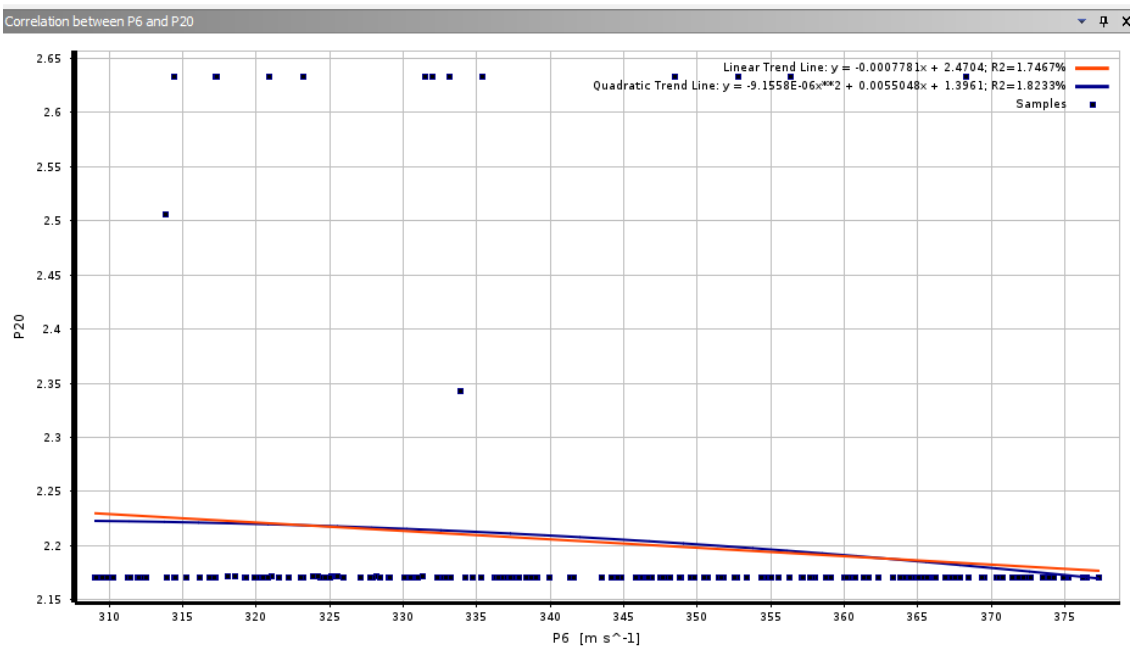

Figure 4.20: Correlation between parameters P6 and P20

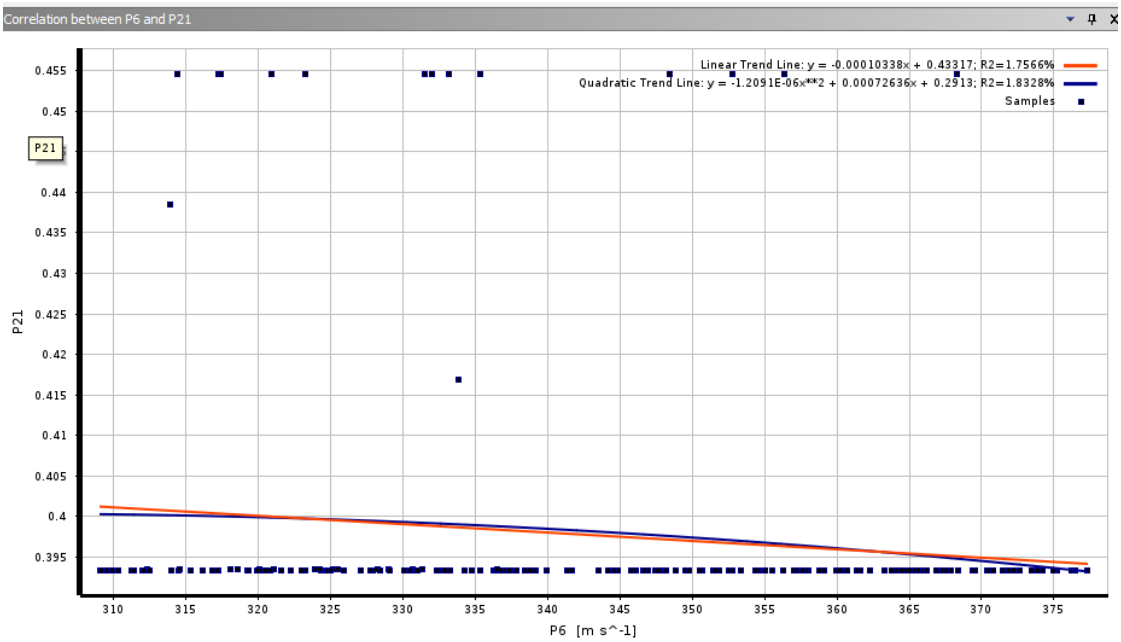

Figure 4.21: Correlation between parameters P6 and P21

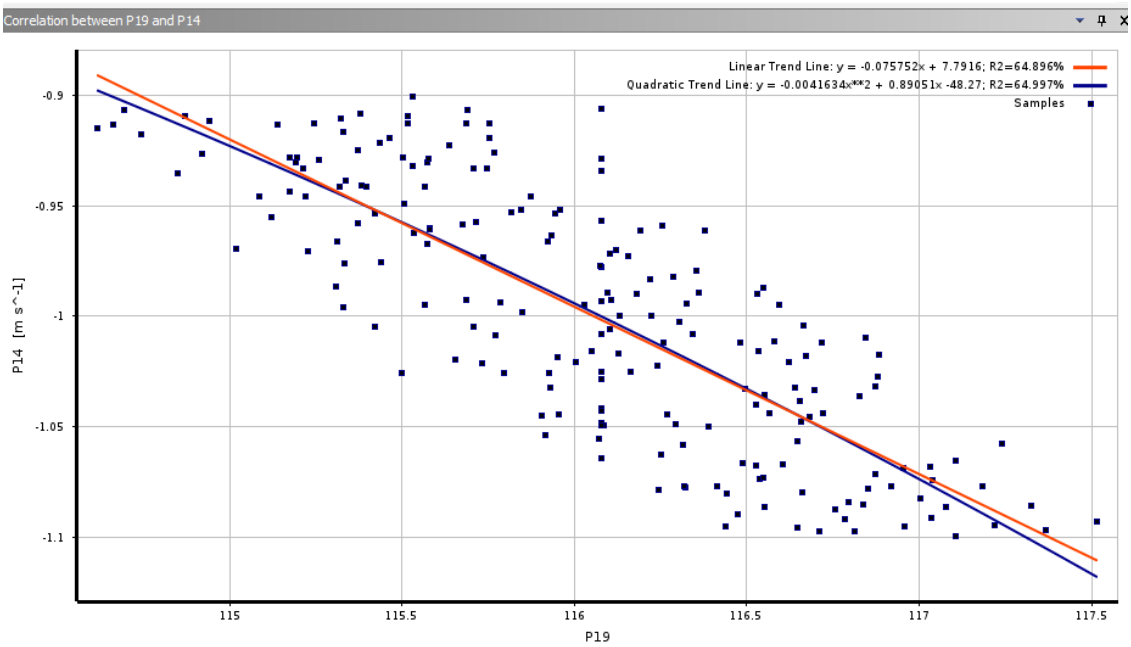

Figure 4.22: Correlation between parameters P19 and P14

These plots provide visual presentation of relationships of the parameter pair that indicate the strength and direction properties at the same time. The charts convey graphical presentation of the degree of correlation between the parameter pair in linear and quadratic trends.

4.4.2. Coefficient of determination

Nonlinear associations between parameter pairs as indicated in **Figure 4.18** to **Figure 4.22** were also evaluated. Results of coefficient of determination from relationships in **Figure 4.18** to **Figure 4.21** were not feasible since they exhibited determination coefficients lower that the given threshold. The lower values imply that other factors such as mesh error or an insufficient number of points may be the cause of the output variations.

For relationship between P14 and P19, a Determination Histogram is presented in **Figure 4.23**. Here, variability of the output parameter that can be explained by linear or quadratic correlation between the input (P14) and the output (P19) is 64.896 and the value for the linear and quadratic determination ranges between 95.09 and 95.217%. Since this value is closer to 100%, it indicates that variations of P19 are as a result of P14. Impacts of P6 and P7 on P19 are much lower than that of P14.

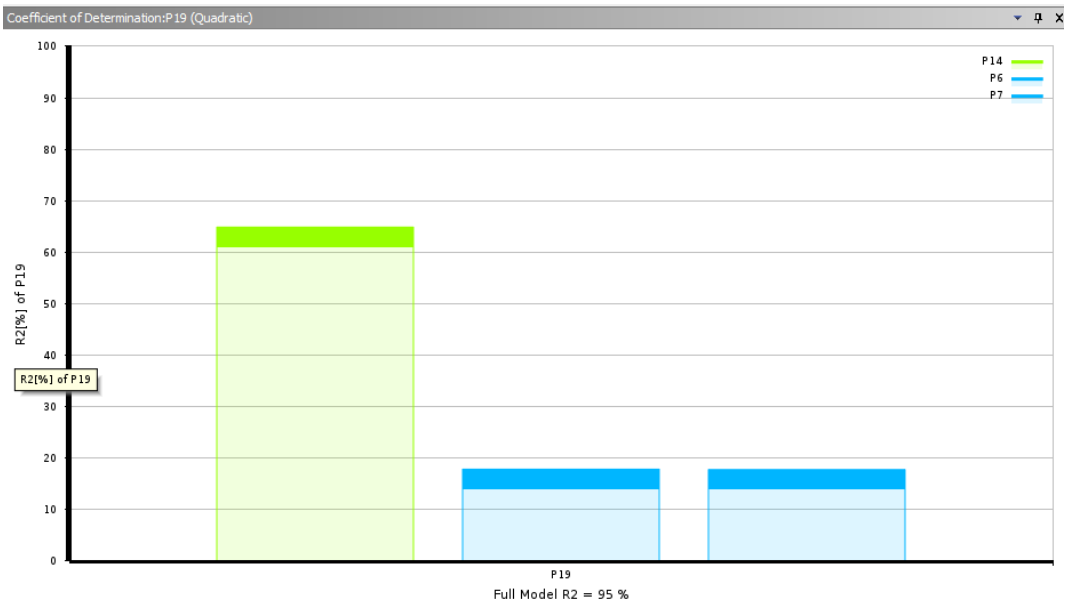

Figure 4.23: Determination histogram for relationship between P14 and P19

Response surface

Design Exploration function in ANSYS software was used to study the analysis response of the model. Using a Goal Driven Optimization method, the solution was parametrized and an interpolated response surface for the parameter ranges generated. A number of relationships were explored between an output parameter and two predictor variables, and their response surfaces presented and discussed in the following section.

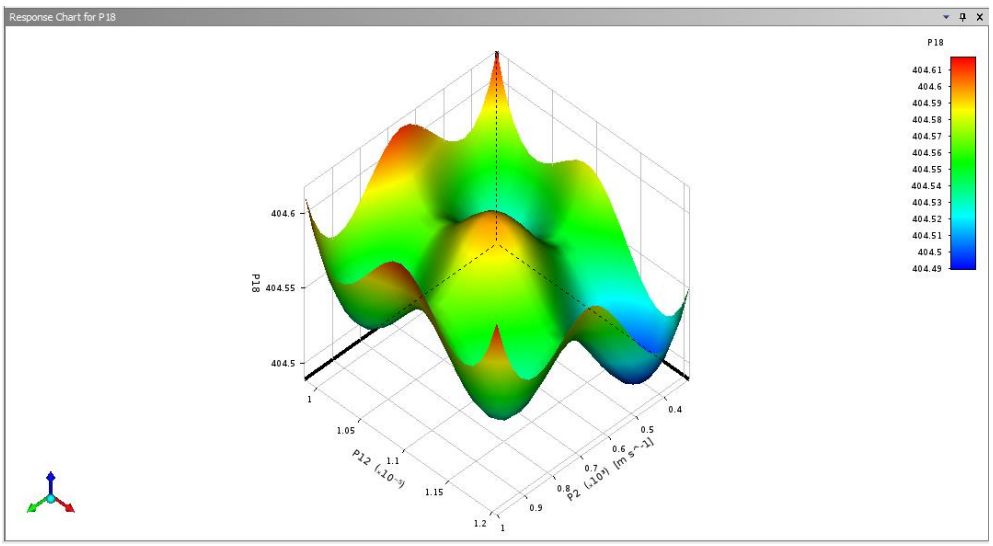

Figure 4.24: Response surface relationship between P18, P12 and P2

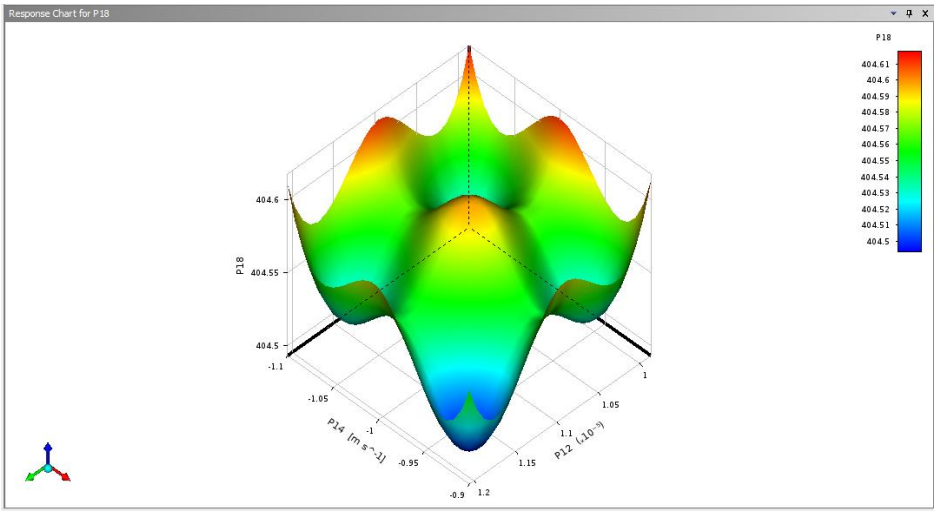

Figure 4.25: Response surface relationship between P18, P14 and P12

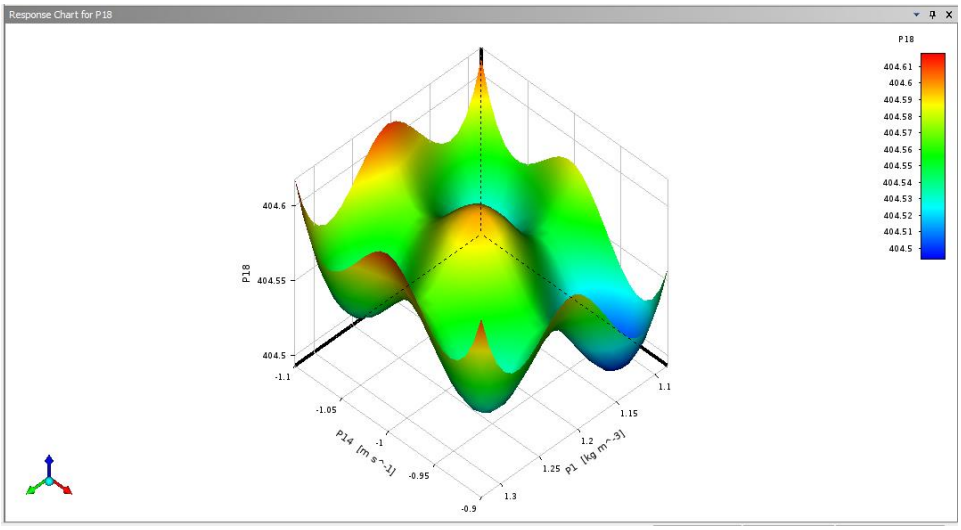

Figure 4.26: Response surface relationship between P18, P14 and P2

Within the parameter bounds defined at the onset for each individual parameter, complex 3D surface relationships were observed for output parameter P18 as influenced by input parameters P1, P2, P12, and P14. A common peak is observed at the center of each of the three relationships in **Figure 4.24**, **Figure 4.25**, and **Figure 4.26**. This peak indicates a combination of the three parameters that gives the highest value of average transmission loss for each of the three cases above.

Another common occurrence in the three relationships discussed is the four valleys (minima's) around the peak phenomenon. These valleys correspond to combinations of parameters on the x and y axis that produce minimal values of transmission loss.

These are undesirable since the objective of improving the design is to maximize on the TL values.

In order to improve the performance of the sample model, a number of objectives and constraints were defined based on results of the previous analysis. These settings were as follows;

i. Minimize geometry internal volume to a lower bound of $0.0245m^{-3}$
ii. Maximize the value of the maximum transmission loss to be above 45 decibels
iii. Hold the amplitude of the input normal sound velocity at $0.9ms^{-1}$
iv. Maximize the value of the average transmission loss, with minimum value being 12 decibels

It was found that in order to increase the value of the average transmission loss of a muffler, considerations have to be made to alter the characteristics of the amplitude of the normal surface velocity and the bulk body viscosity. These aspects may be achieved by the use of the continuous inclined barrier to modify the behaviour of the normal surface velocity, together with a network of perforations and resonance chambers within the helicoidal geometry to create appropriate thermal gradients that would alter the bulk viscosity of the exhaust gases.

4.5. Residual noise hazard quantification

The objective of hazard quantification was to establish the levels of compliance with applicable statutory occupational and environmental requirements with regards to industrial settings as well as silent zones. Silent zones include areas where high concentration is required, or in a hospital environment, where noise could affect the patients' recovery. Definitions of the noise zones are as provided in the Occupational Safety and Health Act of 2007, and the Environmental Management and Coordination Act of 2015.

Residual hazardous noise levels for the muffed and unmuffed engine were identified for different speeds. The results are as summarized in **Table 4.9**.

Table 4.9: Residual noise hazards arising from engine noise source

S.NO.	Engine condition	Noise level dB(A)	Residual hazard – dB(A)	
			Industrial setting	Silent zones
1.	Unmuffed (idling)	**106.1**	26.1	66.1
2.	Muffed (idling)	**84.9**	4.9	44.9
3.	Unmuffed (4,500rpm)	**118.0**	38.0	78.0
4.	Muffler design 1 (engine idling)	**94.1**	14.1	58.1
5.	Muffler design 1 (4,500rpm)	**106.0**	26.0	66.0
6.	Muffler design 3 (engine idling)	**78.1**	-	38.0
7.	Muffler design 3 (4,500rpm)	**90.0**	10.0	50.0

Residual hazardous noises were considered for industrial setups where the statutory limit for safe level is set at 80 dB(A) and that for silent zones within the workplace set at 40 dB(A). Higher risk was noted from unmuffed engine operating at 4,500rpm, potentiating noise-induced hearing loss within the vicinity of the noise source (38 dB(A) residual noise) and disruption at silent zones (78 dB(A) residual noise). While noise from the unmuffed engine may require several layers of control due to the high residual hazard level, residual hazard from the muffed engine (noise source) may only require a simple control solution in order to protect the worker.

Exposure to unmuffed engine was found to be well beyond the threshold limit value as set out in the Occupational Safety and Health Act 2007 and its subsidiary legislation (Noise Prevention and Control Rules 2005). The Act specifies that when noise levels exceed 85 decibels, the worker is exposed to excessive noise. The occupier should therefore mitigate against this by monitoring the noise levels in order to determine

suitable control measures, providing training and education to those workers exposed, conducting periodic medical examination to workers, and communicating results with implications to those affected. The Act also requires the occupier to develop, implement, and maintain an effective noise control and hearing conservation programme, which should include posting of notices in noisy areas, provision of periodic hearing tests, and annually reviewing the programme.

The Act also requires that noise emitted from a workplace to the neighbourhood should not exceed 55 dB(A) during the day and 45 dB(A) during the night. This implies that unmuffed noise from the engine at idling and at 4,500rpm must be reduced to minimize the risk of noise pollution at neighbouring locations. Sensitive areas where worker concentration is critical and which is located in the neighbourhood of the engine noise location will be seriously affected by noise levels that are above 90 dB(A). Appropriate action will have to be taken to prevent adverse effects of excess noise on the worker such as annoyance, poor concentration and low productivity.

4.6 Management of residual hazard arising from excessive noise exposure

Impacts of residual noise hazards range from interference with speech and hearing, discomfort, pain and eventually to hearing loss increases in that order as the magnitude of residual noise increases above the threshold limit value. Hazard control strategies are usually based on a hierarchy of controls and take into consideration the magnitude of the hazard. This hierarchy ranges from the most effective to the least effective. Several interventions or layers may be applied together to increase the effectiveness of control. The most effective is one that will require as minimal human intervention as possible while at the same time reducing the risk to as low as reasonably possible. Using engineering interventions to design out the hazard method is considered the most effective. The least effective control is the use of personal or collective protective devices since it only serves as a barrier between the user and the hazard. When the barrier is damaged, then the user is exposed to the hazardous agent and therefore may suffer some damage. Other layers of control include administrative controls, which do not form part of strategies discussed here.

Based on the results of residual noise (hazard) obtained, three risk management strategies have been proposed and are detailed in the following sections. The strategies are aimed at achieving at least an in-ear noise exposure level between 70 and 80 dB(A), with 75 to 80 dB(A) being considered good attenuation.

4.6.1 Use of distance solution

In order to address residual risks identified in **Table 4.9**, the relationship provided in **Figure 2.8** was used to determine the minimum distances in free field required for each of the engine configuration listed. Results are as detailed in **Figure 4.27.**

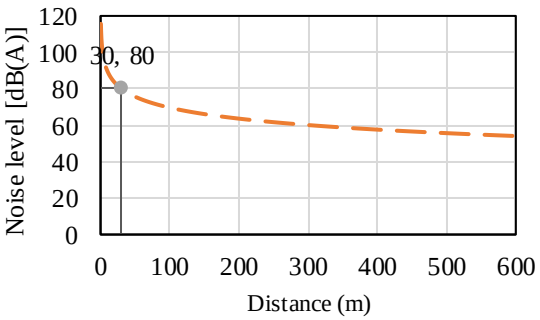

a. Muffed [idling – 106.1 dB(A)]

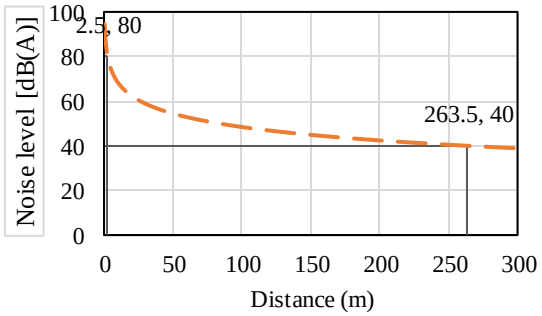

b. Muffed [idling – 84.9 dB(A)]

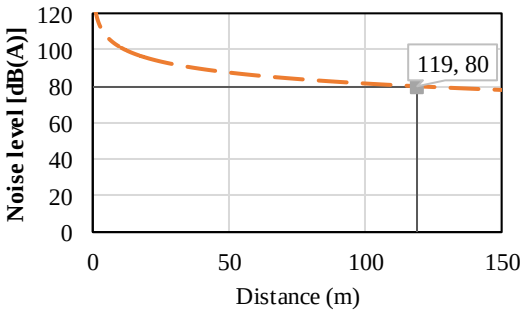

c. Unmuffed [4500rpm, 118dB(A)]

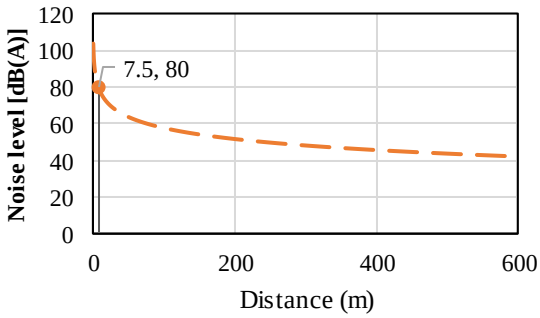

d. Muffed design 1 idling 94.1 dB(A)

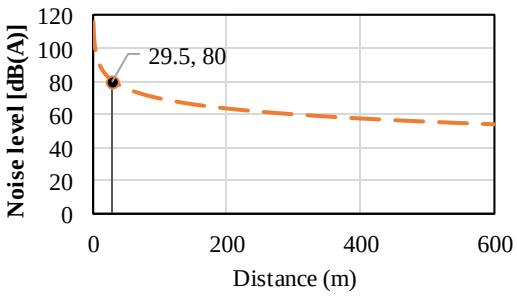

e. Muffed design 1 [4500rpm, 106 dB(A)]

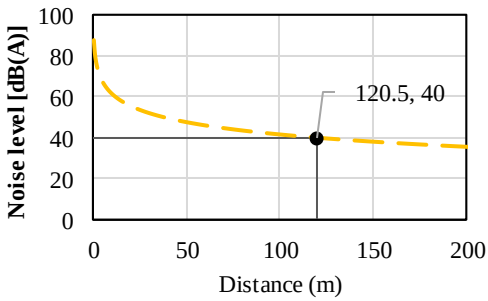

f. Muffed design 3 [idling 78.1 dB(A)

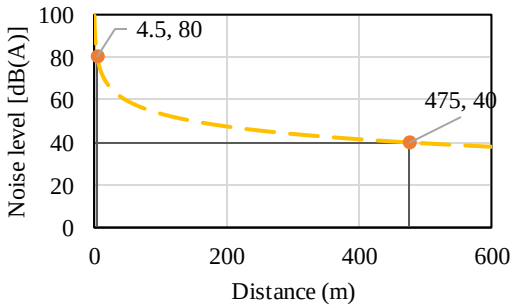

g. Muffed design 3 [4500rpm, 90 dB(A)]

Figure 4.27: Minimum safe distances in free field required for noise reduction

From **Figure 4.27**(a), a distance of 30m is required to attain noise level of 80 dB(A). however, to locate a silent zone, more than 600m will be required for the muffed noise source generating 106.1 dB(A). In figure (b), in order to reduce the 4.9 residual noise, a distance of at least 2.5m is required, while 263.5m is sufficient to locate a silent zone. When the noise source is unmuffed and emitting 118 decibels – **Figure 4.27** (c), 119m is required to achieve 80 dB(A). A much longer distance would be required for the location of a silent zone. A distance of 7.5m is sufficient to locate a workstation from a noise source emitting 94.1 dB(A) as indicated in **Figure 4.27** (d).

The basic muffler design (a simple expansion chamber) installed in an engine and outputting 106 dB(A) requires 29.2m to reduce this value to 80dB(A) as indicated in **Figure 4.27** (e). When muffler design 3 is used to reduce engine noise, the resulting noise level is below the lower safe limit of 80 dB(A), and therefore does not require additional layer of protection in a typical industrial setup. However, in order to cater for a safe zone that requires 40 dB(A), a distance of 120.5m will be required. Finally, for a residual noise level arising from a reference measured value of 90 dB(A), a distance of 4.5 would be the minimum safe location for a worker, while a silent zone may be located at a distance of 475m.

Overall, additional layers of protection would be required to locate silent zones within 600m from the noise sources depicted in **Figure 4.27 a, b, c,** and **e**. Where space is not an issue and quieter work environment is required, the above results imply that location of such quiet workstations would be beyond 600m from the offending noise

source. This solution may be limiting and may not be suitable for practical applications due to space constraint.

Another method involving Fuzzy Logic has been used to predict noise decay with distance (Peng et al., 2020). In this method, time and frequency domain analysis was used to evaluate the influence of distance ratio on overall noise cancellation. Output of this study indicated that the best distance ratio between 7 Hz and 14 kHz had a significane influence on the broadband noise cancellation. This comparison with the current study indicate that, where distance is not an issue, suitable noise reduction can be achieved.

4.6.2 Acoustic barrier in free field solution

From **Figure 4.27** (a), it can be observed that for the muffed engine operating at 106.1 dB(A) operating at 30m from an industrial setup (80 dB(A), the use of an acoustic barrier would provide a maximum protection of 11 dB(A) for noise component at 31.5 Hz centre frequency. This indicates that the barrier would be effective for low-frequency noise attenuation. In contrast, for the muffed idling engine operating at 84.9 dB(A) - **Figure *4.27*** (b) – and targeting silent zone (40 dB(A)), at around 260m, a maximum attenuation of 16 dB(A) would be achieved at 31.5 Hz centre frequency, with lower frequency noise being attenuated above 6 dB(A) up to 1,000 Hz. Attenuation of noise above 1,000 Hz centre frequency would only achieve a maximum of 5 dB(A). When the distance between the noise source (unmuffed engine) and the worker at an industrial setup is 120 dB(A), the maximum protection achievable at 31.5 dB(A) would be 13 dB(A) as established from **Figure 2.11**.

For noise emanating from the muffed engine fitted with design 1 muffler idling at 94 dB(A) and running at 4500rpm respectively, the maximum barrier attenuation achievable would be 7 dB(A) for noise within the lower frequency range (31.5 to 250 Hz), while at the rest of the centre frequencies, attenuation of 5 dB(A) would be achieved. Muffler design 3 fitted to the engine and addling at 78.1 dB(A) would provide a maximum of 11 dB(A) at 31.5 Hz centre frequency when located at 120m from a silent zone (40 dB(A)), while a maximum of 17 dB(A) would be achieved with the same muffler (design 3) and the engine running at 4,500rpm for the same zone. In

the latter case, noise components up to 2,000 Hz centre frequencies would be attenuated beyond 5 dB(A).

The general observation here is that barrier attenuation would provide good protection to the worker against low frequency noise components from the VVT-I gasoline IC engine.

4.6.3 Use of hearing protection devices

Hearing protection devices aim to reduce noise levels to between 70 and 80 dB(A). When noise perceived at the ear is above 80 dB(A), the hearing protection is ineffective, while below 70 dB(A) the protection is over rated, and therefore may lead to lack of perception of important acoustic cues at the work environment. For the values determined using the centre frequency method, the frequency of interest range from 62.5 to 8,000 Hz. For protection against noise from the unmuffed engine running at 4,500rpm, a hearing protection device with the following rating (**Table 4.10**) at each of the 8 centre frequencies of interest will be appropriate.

Table 4.10: Hearing protector data for 4,500rpm muffed engine noise source

f (Hz)	62.5	125	250	500	1000	2000	4000	8000
L_f	66	78	82	85.9	83.7	86.6	89.4	80.9
A_f	21.9	19.7	17.7	17.6	21.8	32.8	38.9	33.4
A_{pv}	4.9	3.7	2.8	2.8	1.8	3.8	3.0	4.9
L_{Ai}	40.2	54.6	61.5	65.5	60.1	50	47.5	42.6

Source: 3M™ Hearing Protection Solutions product catalogue

Where f = frequency;

L_f = centre frequency noise level;

A_f = A weighting factor;

A_{PV} = Assumed protection value;

L_{Ai} = A weighted value at the ear for each centre frequency.

Applying equation 20, the calculated level at the ear according to ISO 4869-2:2018 (α = 1) is 70 dB(A). Allowing for 4 dB for real world factors, gives 74 dB(A) at the ear. Protector gives adequate protection and does not "overprotect". The worker would

then use hearing protection (earmuff) designated by values indicated in A_{PV} row for each of the critical centre frequency in protection against noise levels in the magnitude of 106 dB(A.) For this solution to be effective in protection, the worker must use it in the correct fit and at all times within the target workplace location.

For protection against noise from the unmuffed engine, a hearing protection device with the following rating (**Table 4.11**) at each of the 8 centre frequencies of interest will be appropriate.

Table 4.11: Hearing protector data for unmuffed engine noise source

f (Hz)	62.5	125	250	500	1000	2000	4000	8000
L_f	77	88	73	73	78	76	73	69
A_f	-8.8	-17.0	-24.0	-28.0	-36.9	-37.3	-39.3	-36.4
A_{pv}	3.9	3.2	2.0	29.5	3.3	4.9	3.2	3.9
L_{Ai}	64.3	67.8	47.0	15.5	37.8	33.8	30.5	28.7

Source: 3M™ Hearing Protection Solutions product catalogue

Using equation 20, the calculated level at the ear according to British Standards Instute (2018) ($\alpha = 1$) is 72 dB(A). Allowing for 4 dB for real world factors, gives 76 dB(A) at the ear. Protector gives adequate protection and does not "overprotect". The worker would then use hearing protection designated by values indicated in A_{PV} row for each of the critical centre frequency in **Table 4.11** for environments experiencing 118 dB(A). For this solution to be effective in protection, the worker must use it in the correct fit and at all times (8-hour work shift) within the target workplace location.

Conventionally, the use of hearing protective devices is recommended as a last resort where engineering and administrative controls fail to sufficiently minimize the noise risks. However, there are situations including military operations where hearing protection is the first line of defence and possibly the only viable option (Charles, Kurt, & Martin, 2019). Not only does the military personnel encounter impulsive and steady-state noise from various sources including ammunition, but also from transport equipment such as ground vehicles, planes and ships. For such cases, it would be important to put in place hearing conservation programmes as specified in the Noise

Risk Reduction Rules, and to ensure that the programmes are evaluated in order to reduce on the impacts of residual noise (Rabinowitz, et al., 2018).

In addition, the effective use of hearing protective devices (HPD's) depends on the comfort levels. When the user is not comfortable, this may present additional risks including lack of perception of the neighbourhood acoustic environment and exposure to the offending noise. For this reason, comfort and fit should be critical in achieving hearing protection. The challenge is that comfort is subjective and therefore varies from one use to the other. Olivier, et al., (2019) proposed that for the use of HPD's to be effective, suitable comfort attributes would be a critical input in the design of these devices.

The Occupational Safety and Health Act 2007 and the Noise Risk Reduction Rules require that training be given to workers using HPD's. This is well supported by Nasim & Talha (2019) who established that education and awareness strongly influence attitude, and aids the effective use of hearing protective equipment / devices (HPE) / HPD's.

CHAPTER FIVE

CONCLUSIONS AND RECOMMENDATIONS

5.1 Conclusions

This study aimed at evaluating the performance of a continuous inclined barrier configuration in a simple expansion chamber muffler design. In order to establish baseline data, the characteristics of an internal combustion engine noise were studied. Models of the muffler design were developed, simulated, optimized and evaluated for performance, with residual noise hazards being identified and additional controls proposed. A summary of the study findings and conclusions are presented;

1. Noise profile of a 1500cc VVT-i internal combustion engine is broadband in nature, with noise levels exceeding 90 dB(A) throughout the critical hearing frequency range of 125 to 2,000 Hz. From this finding, it can be concluded that exposure to unmuffed noise from the engine is likely to affect the worker and lead to noise-induced hearing loss. In addition, perception of acoustic cues will be interfered with when one works in the neighbourhood of the engine.
2. From this study, a continuous inclined barrier in a simple expansion chamber with a central tube configuration gave a maximum transmission loss value of 92 dB(A) at 1450 Hz, and an insertion loss of 31 dB(A). The efficiency of this new configuration improved as the value of the key design parameter (pitch) of the model is decreased. The use of a CIB in a SEC muffler design has the potential of providing noise cancellation for internal combustion engines, thereby contributing positively as an engineering solution to workplace noise pollution.
3. Residual noise risks were significant with unmuffed engine running at 4,500rpm at a value of 38 dB(A) for industrial settings, and 78 dB(A) for silent zones, while the proposed design had residual noise risk values of 10 dB(A) and 50 dB(A) for industrial and silent zones respectively. In order to protect workers in an industrial setting and who is exposed to the residual noise, additional layers of protection will have to be provided.

4. For an unmuffed engine emitting 118dB(A), a distance of 120m is needed to protect a worker in an industrial setting, while only a distance of 4.5m would be sufficient for the same worker when the engine is fitted with the muffler design. On the other hand, the unmuffed engine would be unsuitable for use near silent zones, but with the design solution, an average distance of 475m would be sufficient to ensure that a worker in a silent zone is safe. Further, the use of acoustic barrier for noise attenuation was found to be effective for low frequency noise (31.5 to 1000 Hz), and depended on the size of the barrier and distance between the source and the receiver. It is therefore not safe to locate a workstation near an unmuffed IC engine as this would lead to occupational noise-induced hearing loss.
5. In addition, hearing protective devices that result in 76 dB(A) at the ear can be used to protect the worker against unmuffed engine noise and to ensure that the worker operates within safe exposure limits.

5.2 Recommendations

From the results obtained, the continuous inclined barrier in a simple expansion chamber muffler configuration can be adopted to provide a noise-induced hearing loss intervention where elimination of the hazard in not feasible. The following are recommendations for further investigation;

1. Since the performance of the continuous inclined barrier in a simple expansion chamber configuration gave improved performance with decrease in pitch, further investigations may be carried out to establish the optimum pitch that provides the maximum transmission loss. The pitch of the continuous inclined barrier in this study was limited by production method (forming and welding). However, other advanced and more accurate methods could be used to fabricate configurations with smaller pitch sizes.
2. The range for which the muffler design was tested was broadband noise (between 32.5 and 16,000Hz). However, the possibility of use of the design to attenuate noise within the infrasound (0 to 20Hz) and ultrasound (above 20 KHz) could be investigated. In addition, the impacts of noise on hearing

generated within these two ranges have not been adequately investigated. This provides an area for future research.

3. While reactive mufflers are used for control of higher frequency noise levels (within the hearing frequency range of 33.5 to 16,000Hz), absorptive mufflers work well at lower frequencies. For the same range of configurations of the reactive muffler design investigated, modifications could be made by adding absorptive materials within the continuous inclined barrier spaces, thus converting it to an absorptive type. Comparisons can then be made of performance (transmission loss characteristics) of the two arrangements.
4. Improvements to the design may be made by addition of perforations and localized cross-sectional discontinuities to enhance noise cancellation and hence improved transmission loss.

REFERENCES

Agbo, C. O. (2019). Adaptive design and performance evaluation of compact acoustic enclosure build with GFRP for portable mini-generators. *Journal of Engineering Research and Reports*, 1-11.

Ahmedov, A., Beavis, N., Pezouvanis, A., Rogers, D., & Ebrahimi, K. (2018). *Design, development and performance evaluation of ICE exhaust silencer*. UK: Loughborough.

Akay, A., & Onder, S. (2021). An acoustical landscapind study; the impact of distance between the sound source and the landscape plants on traffic noise reduction. *Environ Dev Sustain*. Retrieved from https://doi.org/10.1007/s10668-021-01930-y

Akay, A., & Onder, S. (2022). An acoustical landscape study: the impact of distance between the sound source and the landscape plants on traffic noise reduction. *Environment, Development and Sustainability, 24*(10), 12036-12058.

Amos, A. E., Olisa, Y. P., & Kotingo, K. (2018). Design and performance evaluation of a soundproof enclosure for a 2.5kVA generator. *Journal of Applied Sciences and Environmental Management*, 1975-1978.

Arana, M., San Martin, R., Urroz, J. C., Dieguez, P. M., & Gandia, L. M. (2022). Acoustic and psychoacoustic levels from an internal combustion engine fueled by hydrogen vs gasoline. *Fuel*, 123505.

Arumugam, V., Mishra, R., Militky, J., & Tomkova, B. (2019). Noise attenuation performance of wrap knitted spacer fabrics. *Textile Research Journal*, 281-293.

Badya, M. F., A Dhaiban, A., Hassanie, H. M., S Soliman, M., & ELSebaie, M. G. (2011). Finite element simulation of acoustic attenuation performance of elliptic muffler chambers. *Journal of Engineeirng Sciences, 39*(6), 1361-1373.

Balakumar, P., King, R. A., Chou, A., Owens, L. R., & Kegerise, M. A. (2018). Receptivity and forced response to acoustic disturbances in high-speed boundary layers. *AIAA Journal, 56*(2), 510-523.

Bashir, I., & Carley, M. (2020). Development of 3D boundary element method for the simulation of acoustic metamaterials / metasurfaces in mean flow for aerospace applications. *Journal of Aeroacoustics, 19*(6-8), 324-346.

Basner, M., Babisch, W., Davis, A., Brink, M., Clark, C., Jannsen, S., & Stansfield, S. (2014). Auditory and non-auditory effects of noise on health. *The Lancet, 383*(9925), 1325-1332.

Been, K., & Moon, W. (2019). Reconsideration on Helmholtz-Kirchoff Integral solution for boundary points in radiation problems. *Acta Acoustics united with Acustics, 105*(5), 827-837.

Bi, F., Li, L., Zang, J., & Ma, T. (2015). Source identification of gasoline engine noise based on continuous wavelet transformation and EEMD-RobustICA. *Applied Acoustics, 100*, 34-42.

Bies, D. A., Hansen, C. H., & Howard, C. Q. (2017). *Engineering Noise Control* (5th ed.). Florida: CRC Press.

Biswas, S., & Mandal, G. (2013). An approach to reduce the product variants through design of hybrid muffler for commercial vehicle application. *(No. 2013-26-0096). SAE Technical Paper*.

Borghi, T. F., Barros, J. E., & Valle, R. M. (2014). Aeroacoustics investigation of an automotive exhaust muffler. *Advanced Materials Research Journal, 1016*, 529 - 533.

Bravo, T., & Maury, C. (2018). Sound attenuation and absorption by anisotropic fibrous materials: Theoritical and experimental study. *Journal of Sound and Vibration*, 165-181.

British Standards Institute. (2019). BS ISO 5130:2019. *Acoustics: Measurement of sound pressure level emitted by stationary vehicles*. London: BSI.

British Standards Instute. (2018). ISO 4869-2:2018. *Acoustics - Hearing protectors - Part 2 Estimation of effective A-weighted sound pressure levels when hearing protectors are worn*. London: BSI.

BS. (1995). BS ISO 7698:1995 - Reciprocating Internal Combustion Engines: Measurement of Emitted Airborne Noise. Engineering Method and Survey Method. London: British Standards Institute.

BS. (2013). BS ISO 7698:1995 - Reciprocating Internal Combustion Engines: Measurement Method for Exhaust Silencers. Sound Power Level of Exhaust Noise and Insertion Loss Using Sound Pressure and Power Loss Ratio. London: British Standards Institute.

Caviedes-Nozal, D., Heuchel, F. M., Agerkvist, F. T., & Brunskog, J. (2019). The effect of atmospheric conditions on sound propagation and its impact on the outdoor sound field control. *In INTER-NOISE and NOISE-CON Congress and Conference Proceedings. 259 No. 2*, pp. 7211-7220. Institute of Noise Control Engineering.

Charles, J., Kurt, Y., & Martin, B. R. (2019). Noise of military weapons, ground vehicles, planes and ships. *Acoustical Society of America*, 3832-3838.

Chaudhari, J. H., Patel, B. S., & Shah, S. A. (2014). Muffler design for automotive noise attenuation - A review. *International Journal of Engineering Research and Applications, 4*(1), 220-223.

Chaynov, N. D., Markov, V. A., & Savastenko, A. A. (2018). Structural noise and Acoustic Characteristics improvement of Transport Power Plants. *InIOP Conference Series: Materials Science and Engineering, 327*(2), 022069.

Cromer, G. C., Cromer, O. C., Foster, C. G., & Purdy, K. W. (2018, March 16). *Automobile - History of the automobile.* Retrieved from Britannica.com: https://www.britannica.com>technology

Damray, N., Mansouri, F., Khavanin, A., Jafari, A. J., Asilian-Mahabadi, H., & Mirzaei, R. (2022). Acoustical performance of a double-expansion chamber muffler: Design and evaluation. *Health Scope, 11*(1). doi:10.5812/jhealthscope-103226

de Alwis, M. P., & Garme, K. (2021). Effects of occupational exposure to shock and vibration on health in high performance marine craft occupants. *Proceedings of the institute of Mechanical Engineers Part M: Journal of Engineers for the Maritime Environment, 235*(2), 394-409.

Doijode, A. G., & Gajjal, S. Y. (2015). Experimental analysis of reactive silencer. *Internal Engineering Research Journal*(2), 775 - 779.

dos Reis, A. R., Biondi, D., & de Oliveira, J. D. (2022). The role of urban green areas in noise pollution attenuation. *Dyna, 89*(220), 210-215.

EMCA. (2015). Environmental Management and Coordination Act (Ammended). Nairobi: Government Printer.

European Environment Agency. (2020). *Environmental noise in Europe - 2020.* Copenhagen: European Environment Agency.

Feder, K., Michaud, D., McNamee, J., Fitzpatrick, E., Davies, H., & Leroux, T. (2017). Prevalence of hazardous occupational noise exposure, hearing loss, and hearing protection usage among representative samples of working Canadians. *Journal of occupational and environmental medicine, 59*(1), 92.

Fu, J., Xu, M., Zhang, Z., Kang, W., & He, Y. (2019). Muffler structure improvement based on an acoustic finite element analysis. *Journal of Low Frequency Noise, Vibration and Active Control, 38*(2), 415-426.

Gada, M. F. (2017, February 23). Ear Anatomy. *Glob J Otolaryngology, 4*(1). doi:555630. DOI 10.19080/GGJO.2017.04.555630

Gaidar, S., Karelina, M., Laguzin, A., & Quand, H. D. (2020). Impact of operational factors on environmental safety of internal combustion engines. *Transport Research Procedia, 50*, 136-144.

Gaidar, S., Karelina, M., Laguzin, A., & Quang, H. D. (2020). Impact of operational factors on environmental safety of internal combustion engines. *Transport Research Procedia*, 136-144.

Gaikoumis, E. G., Dimaratos, A. M., & Rakopoulos, C. D. (2011). Experimental Study of Combustion noise radiation during Transcient Turbocharged Diesel Engine Operation. *Energy, 36*(8), 4983 - 4995.

Ganiyu, S. A., & Ogunsote, O. (2010). A Study of Sources and Control of Environmental Noise Pollution on a typical street in Akure, Nigeria. *1st SET International Conference at Akure.* Akure: Federal University of Technology - Akure.

Ghazaly, N. M., & Moaaz, A. O. (2014). Current Research Trends in Sound Transmission Loss of Silencers. *Journal of Mechanical and Civil Engineering, 11*, 22-26.

Gilles, P., & Rieusset, L. (2016). *The Navier-Stokes Problems in the 21st Century* (1st ed.). New York: Chapman & Hall.

Guo, W., Li, T., Zhu, X., Miao, Y., & Zhang, G. (2017). Vibration and acoustic radiation of a finite cylinder shell submerged at finite depth from the free surface. *Journal of sound and vibration, 393*, 338-352.

Hansen, C. H., & Hansen, K. L. (2021). *Noise Control: from concept to application* (2nd ed.). London: CRC Press.

Heywood, J. B. (2018). *Internal combustion engine fundamentals* (2nd ed.). New York: McGraw-Hill.

Holmberg, A., Kierkegaard, A., & Weng, C. (2015, June 23). A frequency domain linearized Navier-Stokes method including acoustic damping by eddy viscosity using RANS. *Journal of Sound and Vibration, 246*, 229-247.

Hosseini, S. A., Zandi, S., Fallah, A., & Nasiri, M. (2016). Effects of geometric design of forest road and roadside vegetation on traffic noise reduction. *Journal of forestry research, 27*(2), 463-468.

Ikechiamaka, F. N., Okpala, C., & Lawal, A. (2017). Design and implementation of a low cost hearing aid device. *FUDMA Journal of Sciences, 1*(1), 115-122.

ISO. (1996). ISO 11820:1996(E) Acoustics - Measurements on Silencers in situ. Switzerland: International Organization for Standardization.

ISO. (2003). ISO 7235:2003(E) Acoustics - Laboratory Measurement Procedures for Ducted Silencers and Air Tremina Units - Insertion Loss, Flow Noise and Total Pressure Loss. International Standardization Organization.

Jacobsen, F., Poulsen, T., Rindel, J. H., Gade, A. C., & Ohlrich, M. (2011). *Fundamentals of Acoustics and Noise Control.* Department of Electrical Engineering, Technical University of Denmark.

Jena, D. P., & Panigrahi, S. N. (2017). Numerically estimating transmission loss of a reactive muffler with and without mean flow. *Measurement, 109*, 168-186.

Ji, J., Lui, X., Tan, S., Wang, M., & Ni, W. (2019). Preparation and performance analysis of Foam-Concrete sound absorbing material prepared purely from solid wastes. *Annales De Chimie-scienceDes Materiaux*, 37-42.

Jiaxin, Z., Baicun, C., Jiancheng, T., & Xiaojun, Q. (2020). The performance of active noise control systems on ground with two parallel reflecting surfaces. *The Journal of the Acoustic Aociety of America*, 3397-3407.

Jin, C., Li, H., Li, X., Wang, M., Liu, C., Guo, J., & Yang, J. (2018). Temporary hearing threshold shift in healthy volunteers with hearing protection caused by acoustic noise exposure during 3-T multisequence MR neuroimaging. *Radiology, 286*(2), 602-608.

Kalita, U., & Singh, M. (2018). Prediction of transmission loss on a simple expansion chamber muffler. *Journal of Emerging Technologies and innovative research, 5*(12), 1022-1031.

Karthikeyan, M., Sharmila, B., Madhan, M., & Silambarasan, S. (2017). Design of absorptive silencer of drum safety valve. *Advances in Natural and Applied Sciences, 11*(8), 408-416.

Kashikar, A., Suryawanshi, R., Sonone, N., Thorat, R., & Savant, S. (2021). Development of muffler design and its validation. *Applied Acoustics, 180*, 108132.

KNBS. (2012). *Kenya Facts and Figures, 2012.* Nairobi: The Kenya National Bureau of Statistics.

KNBS. (2013). *Statiatical Abstract 2013, Kenya National Bureau of Statistics*. Nairobi: Government Printer.

KPLC. (2011). *Environmental and Social Impact Assessment Report for the Nairobi Transmission Ring Project.* Nairobi: Kenya Power and Lighting Company.

Kuehler, R., Fedtke, T., & Hensel, J. (2015). Infrasonic and low-frequency insert earphone hearing threshold. *The Journal of the Acoustical Society of America, 137*(4), EL347-EL353.

Lacasta, A. M., Penaranda, A., Cantalapiedra, I. R., Auguet, C., Bures, S., & Urrestarazu, M. (2016). Acoustic evaluation of modular grenery noise barrier. *Urban forestry and urban greenery, 20*, 172-179.

Lapka, W. (2018). Numerical study of acoustic-structure interaction of selected helicoidal resonator with flexible helicoidal profile. *Archives of Acoustics, 43*(1), 83-92.

Lapka, W.; Silva, G. J. F. (2012, July). Multi resonant helicoidal resonator for passive noise control in ducted systems. *Experimental Mechanica - New trends and perspectives, Editors JF Silver Gomes, Mario AP Vaz, Proceedings of the 15th International Conference on Experimental Mechanics, ICM15, Porto, Portugalia*, 22-27.

Lie, A., Lie, A., Skogstad, M., Johannessen, H. A., Tynes, T., Mehlum, I. S., . . . Tambs, K. (2016). Occupational noise exposure and hearing: a systematic review. *International archives of occupational and environmental health, 89*(3), 351-372.

Liu, L., Zeng, X., Hao, Z., & Qiu, Y. (2021). A time-domain simulation method to predict insertion loss of a dissipative muffler with exhaust flow. *Physics of Fluids, 33*(6), 067114.

Ljunggren, F., Simmons, C., & Hagberg, K. (2014). Correlation between sound insulation and occupants perception - Proposal of alternative Single Number Rating of impact sound. *Applied Acoustics, 85*, 57-68.

Lubner, R. J., Kondamuri, N. S., Knoll, R. M., Ward, B. K., Littlefield, P. D., Rodgers, D., . . . Kozin, E. D. (2022). Review of audio vestibular symptoms following exposure to acoustic and electromagnetic energy outside conventional human hearing. *Frontiers in neurology, 11*, 234.

Martijn, L., Merve, K., Kim, W., & Jian, K. (2018). Improving the soundscape quality of urban areas exposed to aircraft noise by adding moving water and vegetation. *Acoustical Society of America*, 2906-2917.

Martins, L. R., Guimaraes, G. P., & Fragassa, C. (2018). Acoustical performance of Helmholtz resonators used in vehicular silencers. *FME Transactions, 46*(4), 497-502.

Masa'id, A., Lenggana, B. W., Pratama, D. R., Maharani, E. T., & Sinaga, F. R. (2021). Noise quality and muffler design of a Formula SAE Racecar. *IOP Conference Series: Materials Science and Engineering. 1096*, p. 012057. IOP Publishing.

Mohamad, B., Jalics, K., & Kermani, M. (2019). Exhaust system muffler volume optimization of light commercial passenger car using transfer matrix method. *International Journal of Engineeirng and Management Sciences, 4*(1), 132-138.

Mohamad, B., Jalics, K., & Kermani, M. (2019). Exhaust system muffler volume optimization of light commercial passenger car using transfer matrix method. *International Journal of Engineering Management Sciences, 4*(1), 132-138.

Moyano, D. B., Paraiso, D. A., & Gonzalez-Lezcano, R. A. (2022). Possible effects on health of ultrasound exposure, risk factors in the work environment and occupational safety review. *In Healthcare, 10*(3), 423.

Munjal, M. L. (2014). *Acoustics of Ducts and Mufflers* (2nd ed.). Chichester: John Wiley & Sons.

Murphy, W. J., Themann, C. L., & Murata, T. K. (2016). Hearing protection fit testing with offshore oil-rig inspectors in Louisiana and Texas. *International journal of audiology, 55*(11), 688-698.

Nasim, A., & Talha, G. (2019). Awareness of noise-induced hearing loss and use of hearing protection among young adults in Jordan. *Int. J. Environ Res Public Health, 16*(16), 2961. Retrieved from https://doi.org/10.330/ijerph16162961

Nazirkar, R. D., Meshram, S. N., Namdas, A. D., Navagire, S. U., & Devarshi, S. S. (2014). Design and Optimization of Exhaust Muffler and Design Validation. *Proceedings of 10th IRF International Conference*, (pp. 31-37). Pune.

Olivier, D., Franck, S., Jonathan, T., Nellie, P., Caroline, J., Chantal, G., & Alessia, N. (2019). A critical review of the literature on confort of hearing protection devices: definition of confort and identification of its main attributes for earplug types. *International Journal of Audiology, 58*(12), 824-833.

Onder, S., & Akay, A. (2015). Reduction of traffic noise pollution effects by using vegetation Turkey sample. *Journal of Engineering Economic development, 2*(2), 23.

Onyango, D. O., Kinyua, R., & Mayaka, A. N. (2017). Experimental Investigation of a helicoid as an exhaust noise control element. *3rd DeKUT International Conference on Science, Technology, Innovation and Entrepreneurship.*

Oosterhuis, J. P., Buhler, S., van der Meer, T. H., & Wilcox, D. (2015). A numerical investigation on the vortex formation and flow separation of the oscillatory flow in jet pumps. *Acoustical Society of America, 137*(4), 1722-1731.

Palar, Z., Ari, S., Yilmaz, R., Ozdemir, E., & Kahraman, A. (2013). Acoustic and flow field analysis of a perforated muffler design. *International Journal of Mechanical, Aerospace, Industrial, Mechatrinic, and Manufacturing Engineering, 7*(3), 447-451.

Patel, C., Tiwari, N., & Agarwal, A. (2019). Experimental investigations of soyabean and rapeseed SVO and biodiesels on engine noise, vibrations, and engine characteristics. *Fuels, 238*, 86-97.

Peng, T., Zhu, Q., Tokhi, M. O., & Yao, Y. (2020). Fuzzy logic feedforward active noise control with distance ratio and acoustic feedback using Takagi-Sugeon Kang inference. *Journal of low frequency noise, vibration and active control, 39*(1), 174-189.

Praveen, R., Ramshad, N. M., Sagar, S., & Vakkachan, T. K. (2018). Parametric Design Optimization of a Reactive Muffler. *International Journal of Pure and Applied Mathematics*, 983-988.

Rabinowitz, P., Cantley, L. F., Galusha, D., Trufan, S., Swersey, A., Dixon-Ernst, C., . . . Neitzel, R. (2018). Assessing hearing conservation program effectiveness. *Journal of Occupational and Environmental Medicine, 60*(1), 29-35.

Ranjbar, M., & Kermani, M. (2016). A Comparative Study on Design Optimization of Mufflers by Genetic Algorithm and Random Search Method. *Journal of Robotics and Mechatronic Systems*, 1-6.

Reddy, M. R., & Reddy, K. M. (2012). Design and Optimization of automotive mufflers IN AUTOMOBILES. *International Journal of Engineering Research and ApplicationS,* 395-398.

Reitz, R. D., Ogawa, H., Payri, R., Fausler, T., Kokjohn, S., Moriyoshi, Y., . . . Zao, H. (2020). IJER editorial: the future of the internal combustion engine. *International Journal of Engine Reaearch, 21*(1), 3-10.

Rossi, E., De Salvio, D., D'Orazio, D., & Garai, M. (2019). Measuring and identifying background noise in offices during work hours. *InIOP Conference Series: Materials Science and Engineering, 609*(4), P042005.

Ruiz-Garcia Cosola, V., Olivieri, F., & Ruiz-Garcia, L. (2022). A systematic review of the impact of green walls on urban comfort temperature reduction and noise attenuation. *Renewable and sustainable energy reviews, 162*, 112463.

SGS. (2014). *Environmental Impact Assessment Study Report for the Proposed Installation of a 2T Liquified Petroleum Gas Storage Tank and Filling Olant on L.R. No. 209/7139 off Likoni Road in Industrial Area Nairobi.* Nairobi: SGS Kenya Limited.

Sherekar, V., & Dhamangaonkar, P. K. (2014). Design Principles for an Automotive Muffler. *International Journal of Applied Engineering Research, 9*(4), 483-489.

Stansfeld, S., Haines, M., & Brown, B. (2011). Noise and Health in the Urban Environment. *Reviews on Environmental Health, 15*(1-2), 43-82.

Suganeswaran, K., Parameshwaran, P., Amirthamani, S., & Palanimohan, D. (2014). Design and Optimization of Mufflers for Manufacturing. *International Journal of Innovative Research in Science, Engineering and Technology, 3*, 282-290.

Tan, W., Khor, T. S., & Zunaidi, N. H. (2016). Development of acoustical simulation model for muffler. *International Journal of GEOMATE, 11*(4), 2385-2390.

Themann, C. L., & Masterson, E. A. (2019). Occupational noise exposure: A review of its effects, epidemiology and impact with recommendations for reducing its burden. *The Journal of the Acoustical Society of America*, 3879-3905.

Tutunea, D., Calbureanu, M. X., & Lungu, M. (2013). The computational Fluid Dynamics (CFD) study of fluid dynamics performance of a resistance muffler. *International Journal of Mechanics, 4*, 401-408.

UNCED. (1992). Agenda 21. *United Nations Conference on Environment and Development.* Switzerland: United Nations Conference on Environment and Development.

Vavakou, A., Scherberich, J., Nowotny, M., & van der Heijden, M. (2021). Tuned vibration modes in a miniature hearing organ: Insite from the bushcricket. *Proceedings of the National Academy of Sciences*, *118(39).*

Walker, J. K., Cleveland, L. M., Davis, J. L., & Seales, J. S. (2013). Auditory screening and interpretation. *Am Fam Physician, 87*(1), 41-47.

Wang, H., Luo, P., & Cai, M. (2018). Calculation of Noise barrier insertion loss based on varied vehicle frequencies. *Applied Sciences, 8*(1), 100.

Wang, Y., Song, B. F., Song W. P., & Ren, J. (2017). Numerical computation for the impact of flow rate and rotational speed on the flow-induced noise of the centrifugal pump. *Journal of Vibroengineering, 19*(8), 6455-6470.

Ward, G. N. (2016). *Linearized theory of steady high-speed flow*. United Kingdom: Cambridge University Press.

Waugh, A., & Grant, A. (2014). *Ross & Wilson anatomy and physiology of the ear and hearing: Occupational exposure to noise: Evalustion, prevention and control.* (12, Ed.) London: Elsevier Health Sciences.

Wayna, S., & Mickiewicz, W. (2014). Multi-modal acoustic flow decomposition examined in a hard walled cylindrical duct. *Archives of Acoustics, 39*(2), 289-296.

WHO. (1999). Guidelines for Community Noise. Geneva: World Health Organization.

WHO. (2011). *Burden of Disease from Environmental Noise.* Denmark: World Health Organization.

Xue, F., & Sun, B. (2018). Experimental study on the comprehensive performance of the application of U-shaped corrugated pipes into reactive mufflers. *Applied acoustics, 141*, 362-370.

Yao, Y., Wei, S., Zhao, J., Chen, S., Feng, Z., & Yue, J. (2013). Experimental and CFD analysis of reactive mufflers. *Research Journal of Applied Science, Engineering and Technology, 6*(17), 3282 - 3288.

Zang, B., & Poon C., S. (2018). Sound insulation properties of rubberized lightweight aggregate concrete. *Journal of Cleaner Production*, 3176-3185.

Zhu, D. D., & Ji, Z. L. (2016). Transmission loss prediction of reactive silencers using 3-D time-domain CFD approach and plane wave decomposition technique. *Applied Acoustics, 112*, 25-31.

APPENDICES

Appendix I: Integrating Sound Level Meter Calibration

Integrating sound level meter calibration

The instrument **(**1:1 octave band Pulsar Nova integrating sound level meter Model 45) was calibrated using a 1:1 Octave Band Filter complying to IEC 61260:2001 (Electroacoustics standard) removable preamplifier for Class 1 Instruments before taking measurements. Calibration was also carried out at the end of every measurement session to make sure that nothing has happened to the instrument during the session. The calibration process was as follows;

1. The microphone was first switched on and then carefully pushed into the cavity at the end of the calibrator. Precaution was taken to ensure that the microphone is fully inserted into the cavity and that it is past the 'O' ring seals. Confirmation was made to ensure that the small pressure equalization hole next to the microphone cavity on the calibrator is not blocked, as this could cause damage to the microphone. Care was also taken when pushing the microphone into the calibrator not to use a twisting motion, as this would likely cause damage to the preamplifier.
2. The power button on the end of the calibrator was then switched on. The 'calibrate button' in the instrument Menu was selected and then allowed to measure the sound level from the acoustic calibrator to determine if it was within the required tolerance and level. The calibration level must be stable to within ±0.075dB for 5 consecutive seconds for the calibration to be successful.
3. When the calibration is complete, the instrument displays the level along with the correction or adjustment made. The sound level meter is preset with the correction values needed for Pulsar Instruments microphone capsules, so no manual adjustment was required. The calibration level expected was 93.7dB as specified by the manufacturer. The calibration level together with the correction value were recorded.

Data downloading procedure

Before downloading measurements, the integrating sound level meter was connected to a personal computer with the AnalyzerPlus software installed. The connection was through the supplied mini-B USB cable to the USB connector under the removable rubber connector panel at the bottom of the instrument. When the AnalyzerPlus software is run, it automatically detects the instrument plugged in and searches for completed measurements to download. Downloading takes place for the selected measurements and upon confirmation by the user.

Appendix II: Average Data for Internal Combustion Engine Noise – Without Exhaust System

Average data for the VVT-i gasoline internal combustion engine noise source – without the exhaust system in place

Background noise level: 32.9 dB(A)

Engine speed (rpm)		1,000	1,500	2,000	2,500	3,000	3,500	4,000	4,500
		Noise level dB(A)							
Centre frequency (Hz)	31.5	86.3	84.1	84.1	87.3	85.8	88.3	90.7	94.8
	62.5	89.7	94.6	99.6	103.9	99.9	100.5	100.5	102.8
	125.0	96.8	99.9	101.4	104.0	108.1	110.9	112.5	114.9
	250.0	90.9	94.0	97.6	101.3	103.4	107.9	109.8	111.0
	500.0	73.5	83.2	90.3	95.3	97.8	103.5	107.2	111.4
	1,000.0	73.4	82.3	90.0	94.7	97.7	103.8	108.4	112.6
	2,000.0	73.2	78.8	84.3	91.5	95.6	99.3	101.7	105.0
	4,000.0	69.7	76.6	81.7	87.6	92.8	96.6	100.5	104.4
	8,000.0	72.8	75.3	79.6	84.5	88.9	93.8	98.2	102.6
	16,000.0	69.8	74.2	78.1	81.1	84.4	88.6	92.5	97.6

Appendix III: Average Data for Internal Combustion Engine Noise – With Exhaust System

Raw data for the VVT-i gasoline internal combustion engine noise – with the exhaust system in place

Background noise level: 32.9 dB(A)

Engine speed (rpm)		1,000	1,500	2,000	2,500	3,000	3,500	4,000	4,500
		Noise level [dB(A)]							
Centre frequency (Hz)	31.5	84.4	82.1	81.5	84.6	83.9	85.8	87.7	89.5
	62.5	66.9	76.6	71.8	79.2	82.9	80.3	77.6	77.5
	125.0	65.0	61.4	63.8	67.1	78.6	81.0	83.0	87.1
	250.0	61.0	60.8	60.7	62.9	64.9	65.2	69.8	73.2
	500.0	54.0	59.3	66.0	66.6	67.8	69.2	73.1	73.4
	1,000.0	52.4	55.3	62.2	63.9	67.8	68.6	73.2	76.2
	2,000.0	51.8	56.0	60.6	61.1	65.2	68.9	72.0	75.5
	4,000.0	52.7	56.1	59.8	61.1	64.7	68.0	71.0	73.5
	8,000.0	48.0	52.2	54.3	58.3	62.2	63.5	66.4	69.5
	16,000.0	43.8	49.5	52.2	55.9	57.4	61.5	63.8	65.6